Dissertation

Submitted to the
Combined Faculties for the Natural Sciences and for Mathematics
of the Ruperto-Carola University of Heidelberg, Germany

for the degree of
Doctor of Natural Sciences

presented by

Diplom-Biologin Nathalie Jurisch-Yaksi, geboren Jurisch

born in: Sion, Switzerland

Oral examination: 05.03.09

Positive and negative regulator Junb: impact on chromatin remodeling and stress response

Referees:
Prof. Dr. Peter Angel
Prof. Dr. Uwe Strähle

Table of Contents

Acknowledgments

By the end of my PhD, I would like to thank all the people who were deeply involved and who made my PhD work possible, fruitful and enjoyable.

First, my biggest thank goes to Marina Schorpp-Kistner, my supervisor, for constructive discussions and suggestions, but also for sharing knowledge and teaching me many techniques.

I am very grateful to Peter Angel for giving me the possibility of joining his lab for my PhD thesis, for fruitful discussions and suggestions, and for being my first referee.

I am very thankful to Prof. Uwe Straehle who has accepted the responsibility of being my second referee.

Thanks a lot to all members of the Junb sub-group of A100: particularly to Bjoern for teaching me many things about ER stress, to Melanie and Alex for their excellent technical support, and to Tobias and Maite.

I would like to thank also all members of A100 for constructive remarks and the good time spent in the lab.

Finally a big thank to all my friends and family. By being from everywhere in the world, I have learnt so much from all of you and I hope we will be able to keep in touch in the future.

And thank you so much Emre, my husband, for showing me how beautiful life can be, and how, with love, everything is possible…

Abbreviations

ActD	Actinomycin D
ADP	Adenosine triphosphate
AP-1	Activating protein-1
ATF	Activating transcription factor
Atf6	Activating transcription factor 6
ATP	Adenosine triphosphate
Bcl2	B-cell lymphoma 2
bFGF	Basic fibroblast growth factor
BMH	Bis-maldeimidohexane
bp	Base pair
bZIP	Basic leucine zipper domain
°C	Degrees Celsius
C	Cytosine
cAMP	Cyclic adenosine monophosphate
Cbfb	Core binding factor beta
cDNA	Complementary DNA
CDS	Coding sequence
Chop	CAAT/Enhancer binding protein homologous protein
CML	Chronic myeloid leukemia
COBRA	Combined bisulfite restriction analysis
CpG	Cytosine-guanine dinucleotide
Csf2	Colony stimulating factor 2
Csf2r	Colony stimulating factor 2 receptor
CRE	cAMP response element
DMD	Differentially methylated domain
DMSO	Dimethyl sulfoxide
DNA	Deoxyribonucleic acid

DNase	Deoxyribonuclase
DNMT	DNA methyltransferase
dATP	Deoxyadenosine triphosphate
dCTP	Deoxycytinde triphosphate
dGTP	Deoxyguanosine triphosphate
dNTP	Deoxynucleotide triphosphate
DTT	dithiothreitol
dTTP	Deoxythymidine triphosphate
E. Coli	Eschericha Coli
Eif2a	Eukaryotic initiation factor 2 alpha
ELISA	Enzyme-Linked ImmunoSorbent Assay
EMSA	Electrophoretic mobility shift assay
ER	Endoplasmic reticulum
ERK	Extracellular signal-regulated kinases
EtOH	Ethanol
FACS	Fluorescent-activated cell sorting
FBS	Fetal bovine serum
Fig	Figure
G	Guanine
G-CSF	Granulocyte colony stimulating factor
GFP	Green fluorescent protein
GM-CSF	Granulocyte macrophage colony stimulating factor
GMP	Granulocyte/macrophage progenitors
GPCR	G protein coupled receptor
GR	Glucocorticoid receptor
Grp 78, 94	Glucose related protein 78, 94
h	hour
H2A, H2B, H3, H4	Histone 2A, 2B, 3, 4

HDAC	Histone deacetylase
HEK	Human embryonic kidney cells
HIF	Hypoxia-inducible factor
HRP	Horseradish peroxidase
ICR	Imprinting control region
Igf2	Insulin-like growth factor 2
Ire1	Inositol requiring kinase 1
JNK	Jun N-terminal kinase
kb	kilobase
LT-HSC	Long term hematopoietic stem cell
M	molar
MAPK	Mitogen activated protein kinase
MBD	Methyl CpG binding protein
MEF	Mouse embryonic fibroblast
MetOH	Methanol
min	minute
MMP	Matrix metalloproteinase
MOMP	Mitochondria outer membrane pore
mRNA	Messenger RNA
NaB	Sodium butyrate
NAD	Nicotinamide adenine dinucleotide
NF-κB	Nuclear factor kappa B
p- / phospho-	phosphorylated
PAGE	Polyacrylamide gel electrophoresis
PARP	Poly (ADP-ribose) polymerase
PBS	Phosphate buffered saline
PCR	Polymerase chain reaction
Pdgf	Platelets derived growth factor

Pdgfr	Platelets derived growth factor receptor
PERK	protein kinase RNA-like ER kinase
PI3K	Phosphoinositide 3-Kinase
qRT-PCR	Quantitative RT-PCR
RNA	Ribonucleic acid
RNase	Ribonuclease
RT	Room temperature
RTK	Receptor tyrosine kinase
RT-PCR	Reverse transcription PCR
SAPK	Stress Activated Protein Kinase
SDS	Sodium Dodecyl Sulfate
Ser / S	Serine
shRNA	Short hairpin RNA
siRNA	Small interference RNA
SRE	Serum responsive element
SSV	Simian sarcoma virus
Syt	Synaptotagmin
Taq	Thermus aquaticus
TBE	Tris/Borate/EDTA
TsA	Trichostatin A
Thr / T	Threonine
Tm	Tunicamycin
TNF	Tumor necrosis factor
TPA	12-O-Tetradecanoyl-phorbole-13-acetate
TRE	TPA responsive element
U	Uracil
UPR	Unfolded protein response
UTR	Untranslated terminal region

UV	Ultra violet
%(v/v)	Percentage of volume
Vamp	Vesicle-associated membrane protein
Vegf	Vascular endothelial growth factor
vSMC	Vascular smooth muscle cells
%(w/v)	Weight percentage of volume

1 Summary

The AP-1 transcription factor is a central player in a multitude of biological processes from normal development to neoplastic transformation causing cancer. Junb, a subunit of AP-1, is special by the fact that it has at the same time activator and repressor functions. While positively regulated Junb target genes are principally required for proper vascular development, negative regulation of cytokines is of crucial importance to suppress pro-inflammatory and tumorigenic phenotypes. In this work, I approached this double-edge role of Junb by addressing two scientific questions: the mode of operation of Junb as negative transcription regulator and its impact in the ER stress response and apoptosis. First, I could show that, in addition to the general view of being an inhibitor of AP-1 by absorbing Jun activity, Junb also represses genes by epigenetic mechanisms. Although Junb did regulate neither the levels of histone acetylation nor the expression of HDACs, DNMTs and co-repressor complexes, few genes showed differential induction by HDAC inhibitors in wild-type and Junb-deficient fibroblasts. Presumably, these genes may be regulated through a yet to be identified Junb-dependent mechanism involving HDACs. Moreover, Junb regulated the DNA methylation of the imprinting control region of the gene *H19*. The molecular mechanisms involved in Junb-dependent epigenetic regulation appear to be novel and very unusual for an AP-1 member and remains to be fully solved. Secondly, I investigated the role of Junb in ER stress, a condition that has been described to contribute to hypoxia tolerance and tumor progression. Although Junb deficiency resulted in minor changes in the ER stress-triggered unfolded protein response (UPR), Junb-ablated MEFs were resistant towards apoptosis. Very high levels of activated pro-survival kinases resulted in aberrant post-translational modification of BH3-only proteins Bim and Bad and subsequent failure in mitochondria permeabilization and caspases activation. A soluble factor, most likely Pdgfb, elicited a pro-survival autocrine loop causative for the apoptosis resistance in absence of Junb. In summary, the negative regulation of cytokines and growth factors by Junb accounts for most of the deleterious effects observed in absence of Junb, except for the angiogenesis phenotype. Thus, the understanding of how Junb represses genes and the targeting of this specific mechanism would represent a promising therapeutic approach to treat in the future inflammatory disease and cancer.

.

2 Zusammenfassung

Der Transkriptionsfaktor AP-1 ist ein zentraler Akteur in einer großen Zahl biologischer Prozesse von der normalen Entwicklung bis zur neoplastischen Transformation, die zu Krebs führt. Junb, eine Untereinheit von AP-1, ist dadurch außergewöhnlich, dass Junb gleichzeitig Aktivator- und Repressorfunktionen hat. Während positiv regulierte Junb Zielgene in der Hauptsache für eine geordnete vaskuläre Entwicklung erforderlich sind, ist die negative Regulation von Zytokinen für die Unterdrückung von entzündlichen und tumorgenen Phänotypen von entscheidender Bedeutung. In der vorliegenden Arbeit habe ich diese zweischneidige Rolle von Junb analysiert, indem ich zwei wissenschaftliche Fragen bearbeitete: die Arbeitsweise von Junb als negativer transkriptioneller Regulator und seinen Einfluss in der ER Stressantwort und Apoptose. Als Erstes konnte ich zeigen, dass zusätzlich zur generellen Ansicht, dass JunB AP-1 durch Abfangen der Jun Aktivität hemmt, Junb Gene auch über epigenetische Mechanismen inaktiviert. Obwohl Junb weder die Menge an Histonazetylierung, noch die Expression von HDACs, DNMTs und Ko-Repressorkomplexen regulierte, zeigten einige Gene in Wildtyp und Junb-defizienten Fibroblasten unterschiedliche Induktion nach HDAC Inhibitorgabe. Dies lässt vermuten, dass diese Gene durch einen noch zu identifizierenden Junb-abhängigen Mechanismus via HDACs reguliert sein könnten. Darüber hinaus regulierte Junb die DNA Methylierung der Imprinting Kontrollregion des H19 Gens. Der molekulare Mechanismus dieser Junb-abhängigen epigenetischen Regulation scheint neuartig und sehr ungewöhnlich für ein AP-1 Mitglied und muss noch vollständig geklärt werden. Als Zweites habe ich die Aufgabe von Junb im ER Stress untersucht, einem Zustand der mit Hypoxietoleranz und Tumorprogression im Zusammenhang steht. Obwohl das Fehlen von Junb zu minimalen Veränderungen im ER Stress induzierten Stoffwechselweg UPR führt, waren MEFs ohne Junb Apoptose-resistent. Sehr hohe Level an aktivierten überlebensstimulierenden Kinasen resultierten in veränderter posttranslationaler Modifikation der „BH-3 only“ Proteine Bim und Bad und im nachfolgendem Ausbleiben der Mitochondrienpermeabilisierung und Caspase-Aktivierung. Ein löslicher Faktor, sehr wahrscheinlich Pdgfb, löste einen überlebensfördernden autokrinen geschlossenen Regelkreis aus, der für die Apoptoseresistenz in Abwesenheit von Junb ursächlich ist. Zusammengefasst ist die negative Regulation von Zyktokinen und Wachstumsfaktoren durch Junb für die meisten schädlichen Auswirkungen verantwortlich, die mit Ausnahme des Angiogenesephänotyps, in Abwesenheit von Junb auftreten. Daher würde das Verständnis darüber wie Junb Gene reprimiert und der somit mögliche gezielte Eingriff in diesen

Mechanismus ein viel versprechender therapeutischer Ansatz bieten, um künftig entzündliche Erkrankungen und Krebs zu behandeln.

3 Introduction

The development of multicellular organisms is very complex and, thus, requires a tight regulation. Developmental programs include cell division, growth, migration and differentiation, which are all governed by complex signaling pathways resulting in changes in gene expression. Proper gene expression is absolutely essential for the maintenance of the cellular integrity of higher organisms, while aberrant gene expression results in the development of various diseases such as cancer. Gene expression is regulated on multiple levels, from transcription by transcription factors to translation and post-translational modifications.

Much of our current knowledge about the characteristics of transcription factors comes from the discovery and study of Activating Protein-1 (AP-1). Since the AP-1 transcription factor mediates gene regulation in response to a wide variety of physiological and pathological stimuli, it is a central player in a multitude of cellular processes from normal development to neoplastic transformation causing cancer. Despite the fact that AP-1 has been identified more than two decades ago, it still maintains a lot of its mystery. Deciphering the complexity of the AP-1 genetic network should help to better understand how the cell performs the critically fine tuning of its fate.

3.1 The transcription factor AP-1

The activating protein-1 (AP-1) is a transcription factor principally composed of dimers between the Jun (Jun, Junb and Jund), Fos (Fos, Fosb, Fra-1, Fra-2), ATF (activating transcription factor, Atf2, LRF-1/ATF-3, Batf, Jdp1, Jdp2) and Maf (c-Maf, MafB, MafA, MafG/F/K) protein families. AP-1 is at the receiving end of signaling cacades elicited by a plethora of physiological and pathological stimuli, including cytokines, growth factors and stress signals, bacterial and viral infections as well as oncogenic stimuli and it regulates, upon activation, numerous target genes (Hess et al., 2004).

3.1.1 Biochemical properties of AP-1

A common feature of AP-1 family members is the conserved bZIP domain. The evolutionarily conserved bZIP domain consists of a leucine zipper region, which allows dimerization of the proteins, combined with a basic DNA binding domain that requires dimerization to bind DNA. While the Fos proteins (Fos, Fosb, Fra-1, Fra-2) can only heterodimerize with members of the Jun family, the Jun proteins (Jun, Junb, Jund) can both

homo- and heterodimerize with Fos or ATF members to form transcriptionally active complexes. In addition to the well-characterized bZIP domain, the AP-1 family members comprise a transactivation domain, which differs between the individual Jun and Fos proteins with regard to its potential (Angel and Karin, 1991; Hess et al., 2004). Whereas Jun, Fos and Fosb are considered strong transactivators, Junb, Jund, Fra-1 and Fra-2 exhibit only weak transactivation potential. Under specific circumstances, the latter may even act as repressors of AP-1 activity by competing for binding to AP-1 sites or by forming inactive heterodimers with Jun, Fos or FosB (Angel and Karin, 1991; Chiu et al., 1989; Hess et al., 2004).

AP-1 regulates gene expression through binding to the palindromic TPA Responsive Element (TRE) consensus sequences. The TRE, composed of the 5'-TGA G/C TCA-3' DNA sequence, was originally identified in the human *collagenase* and *metallothionein IIa* genes and was called so because it is strongly induced by the tumor promoter 12-O-tetradecanoylphorbol-13-acetate (TPA). Although the main DNA element bound by AP-1 is the TRE, some dimers have also been described to bind to the related cAMP-Response Element or CRE. The CRE differs from the TRE by a single base insertion and has the DNA consensus sequence 5'-TGA GC TCA-3' (Angel and Karin, 1991).

3.1.2 Transcriptional and post-transcriptional regulation of AP-1

The net AP-1 activity in a given cell is regulated by a broad range of physiological and pathological stimuli. It is achieved at two major levels: extracellular stimuli can modulate both the abundance and the activity of AP-1 proteins.

The abundance of AP-1 proteins is regulated by transcription of genes encoding AP-1 subunits, control of the stability of their mRNAs and turnover of pre-existing or newly synthesized AP-1 subunits (Karin et al., 1997).

Post-translational modifications and interactions with other transcription factors or cofactors modulate AP-1 activity (Hess et al., 2004). Post-translational modification has been extensively studied for the AP-1 member Jun, that becomes phosphorylated and activated by the Stress Activated Protein Kinase (SAPK) cascade (Minden and Karin, 1997). SAPK, which are Jun N-terminal Kinases (JNK) and p38-kinases, are members of the Mitogen-Activated Protein Kinase (MAPK) superfamily. JNK comprise three isoforms: JNK1, JNK2 and JNK3. Activated by stress stimuli through a MAPK cascade, JNK translocates to the nucleus, phosphorylates Jun within its N-terminal transactivation domain (on Ser63 and Ser73 residues) and thereby enhances its transactivation potential. In addition to Jun, JNK can also phosphorylate Junb, Jund and Atf2 and potentiate their activity (Hess et al., 2004).

Furthermore, AP-1 can be regulated by interaction with other transcription factors and cofactors. For instance, the mutual interference between AP-1 and steroid hormone receptors, particularly the Glucocorticoid Receptor (GR), represents an example of protein-protein interaction based crosstalk. In this context, the anti-inflammatory and immunosuppressive activities of glucocorticoids are mediated, at least in part, by GR-mediated repression of AP-1 activity (Herrlich and Ponta 1994). In addition to GR, many transcription factors (e.g. C/EBP, Ets, Gata, NFAT, NF-κB, Runx, Sp1 and others), transcriptional cofactors (e.g. p300/CBP, TAF1, Trip6 and others) and subunits of chromatin remodeling complexes (e.g. SWI/SNF and HDAC3) have been found to physically interact and modulate AP-1 activity, although in most cases, the exact mechanism of interaction between AP-1 and these proteins remains to be determined (Hess et al., 2004).

3.1.3 Role of AP-1 in development

Most of our knowledge on the function of AP-1 proteins in development was obtained from loss of function experiments using gene targeting in mice. These analyses revealed that each AP-1 component has specific functions during embryogenesis and organogenesis. In addition, while Fos, Fosb, Jund are dispensable, Jun, Junb and Fra-1 are essential for embryonic development since complete ablation of these proteins in mice results in embryonic lethality (Jochum et al., 2001).

Mice lacking Fos are viable and fertile but lack osteoclasts resulting in an osteopetrotic phenotype (Johnson et al., 1992; Wang et al., 1992). Mutant mice also show abnormalities of the hematopoietic system including extramedullary hematopoiesis and lymphopenia (Okada et al., 1994).

Mice lacking Fosb develop normally (Brown et al., 1996; Gruda et al., 1996). However, adult *Fosb* $^{-/-}$ females display a profound nurturing defect that correlates with the absence of Fosb expression in a hypothalamic region critical for nurturing behavior (Brown et al., 1996). In addition, Kuroda and colleagues reported broader neurobehavioral dysfunctions in *Fosb* $^{-/-}$ mice, which may share the same underlying molecular mechanisms that are also responsible for the nurturing defect (Kuroda et al., 2008).

Fra-1 inactivation results in embryonic lethality around day 10 of development due to defects in the placenta and the yolk sac (Schreiber et al., 2000). The development of Fra-1-deficient embryos can be rescued up to birth by providing wild-type extra-embryonic tissues upon generation of tetraploid chimeras. These rescued Fra-1 deficient pups display no

morphological abnormalities, suggesting that Fra-1 is dispensable for the development of the embryo (Schreiber et al., 2000).

The mice lacking Fra-2 show severe growth retardation, appear runted, and die within a week after birth. So far it is unknown for which physiological functions Fra-2 is required to ensure post-natal survival (Eferl et al., 2007).

Mice lacking Jun die between day 12.5 and 13.5 of embryonic development (Hilberg et al., 1993; Johnson et al., 1993). Jun-deficient embryos show defects of the interventricular septum in the heart and incomplete separation of the aorta and the pulmonary artery, indicating that Jun is essential for the development of a normal cardiac outflow tract (Eferl et al., 1999). Mutant embryos also show abnormalities in the liver, which include areas of hemorrhaging and generalized edema as well as increased numbers of apoptotic hepatoblasts and hematopoietic cells (Eferl et al., 1999; Hilberg et al., 1993). However, these abnormalities are not intrinsic to the hematopoietic compartment since lethally irradiated mice can be reconstituted with Jun-deficient fetal liver cells (Eferl et al., 1999).

Junb is also essential for embryonic development and Junb-deficient embryos die between day 8.5 and 10.0 of embryonic development due to vascular defects in the extra-embryonic tissues (Schorpp-Kistner et al., 1999). Junb *in vivo* and *in vitro* functions will be discussed in more details in a subsequent paragraph.

Jund, finally, is dispensable for development. Yet, mutant males show impaired growth, hormone imbalance and age-dependant defects in reproduction due to impaired spermatogenesis (Thepot et al., 2000). In addition, Jund has been shown to be involved in muscle cell differentiation and function (Andreucci et al., 2002; Ricci et al., 2005) and to play a crucial role in T lymphocyte proliferation and T helper cell differentiation (Meixner et al., 2004).

3.1.4 Role of AP-1 in stress response and apoptosis

The isolation of genetically modified cells from animals with ablated AP-1 subunits has contributed to the deciphering of individual functions of these subunits in controlling cell proliferation, differentiation, apoptosis and neoplastic transformation.

AP-1 activity is greatly enhanced upon treatment of cells with genotoxic agents, implying that AP-1 target genes are involved in the cellular stress response, including DNA repair, induction of survival and initiation of the apoptotic program. AP-1 has a dual function in stress response: it can induce apoptosis in some cellular systems but is required for cell survival in others. Therefore, the role of AP-1 in apoptosis should be considered within the

context of a complex network of signaling pathways. Here, some findings are described exemplifying the complexity of AP-1 regulated mechanisms of cell death.

Many studies have highlighted an important role for the extrinsic death receptor pathway mediated by JNK, Jun/AP-1 and FasL (also called CD95L), in the control of lymphoid, fibroblast and neuronal cell fate. JNK, activated by the MAPK cascade, phosphorylates Jun and results in enhanced transcription of target genes implicated in cellular stress-induced apoptosis. Whereas Jun is a potent activator of Fas, FasL and TNF-α transcription, Fos abrogates Jun-mediated activation of Fas as well as negatively regulates FasL expression through a transcriptional repressor element within the FasL promoter (Hess et al., 2004).

Some reports demonstrate a fundamental pro-apoptotic role for JNK/Jun signaling in the stress-induced mitochondrial death pathway (Behrens et al., 1999; Palmada et al., 2002; Whitfield et al., 2001). Expression of a dominant-negative Jun mutant reduces expression of Bim, a BH3-only member of the Bcl-2 family of apoptosis regulators and inhibits mitochondrial cytochrome c release (Whitfield et al., 2001). The importance of a putative JNK–Jun/AP-1–Bim pathway in neuronal cell death control is underscored by pathologies associated with deregulated apoptosis, such as Alzheimer's disease. Furthermore, analyses of cell cultures derived from sympathetic and cerebellar granular neurons revealed a clear dependency on JNK/Jun activity for stimulation of apoptosis upon growth factor withdrawal (Palmada et al., 2002; Whitfield et al., 2001). Finally, the subunit Junb appears to act pro-apoptotic in myeloid cells, as shown in mice lacking Junb in the myeloid lineage that develop a myeloproliferative disease (Passegue et al., 2001; Passegue et al., 2004).

In addition to the pro-apoptotic functions of AP-1, numerous experiments have demonstrated that AP-1 is also critically involved in survival signaling. For instance, Fos expression negatively correlates with increased neuronal cell death in the hippocampus during kainic-acid-induced seizure, indicating an anti-apoptotic role for Fos in this scenario (Zhang et al., 2002). Jun expression is needed to prevent apoptosis in fetal hepatocytes during mouse development (Behrens et al., 1999; Eferl et al., 1999; Hilberg et al., 1993). During liver tumor formation, Jun prevents apoptosis by antagonizing p53 activity, and this may contribute to the early stage of human hepatocellular carcinogenesis (Eferl and Wagner, 2003). Moreover, Jun regulates transcription of p53 in mouse fibroblasts and, thus, apoptosis (Schreiber et al., 1999). Furthermore, enhanced apoptosis in the absence of Jun is also observed in keratinocytes and notochordal cells (Behrens et al., 2003; Zenz et al., 2003). In the case of keratinocytes, Jun regulates expression of EGFR and its ligand HB-EGF, which controls

keratinocyte proliferation and survival (Zenz et al., 2003). Finally, JNK activation can also signal pro cell survival. Davis and colleagues demonstrated that Jund promotes JNK-stimulated survival after TNF treatment by collaborating with NF-κB to increase expression of anti-apoptotic genes such as the inhibitor of apoptosis IAP-2 (Lamb et al., 2003).

3.1.5 Junb, a special member of the Jun family

3.1.5.1 Transcriptional and post-translational regulation of Junb

Junb is induced by a plethora of cellular stress signal and its transcriptional regulation is mediated by different regulatory elements located in the 5' and 3' regions flanking its coding sequence. The transcriptional induction of *Junb* in response to various mitogens is mediated by multiple Ets sites (Coffer et al., 1994), an IL-6 response element containing a STAT3 binding site and a CRE-like site (Nakajima et al., 1993), a GC box, an inverted repeat element and a novel myeloid-specific IL-6 response element (IL-6RE) (Sjin et al., 1999) in the proximal promoter region. In addition, the regulation of Junb by v-src involves the CAAT and TATA box region (Apel et al., 1992). Growth factor-initiated signaling pathways induces Junb through a TRE, a SRE and two Ets-linked motifs located in a region around -1000 to -2000 in the mouse Junb promoter (Phinney et al., 1996). By contrast, Pdgfb, serum, bFGF, phorbol ester and forskolin mediate Junb induction by a SRE and a CRE site located in the 3' flanking region of Junb gene (Perez-Albuerne et al., 1993). Finally, recently, four NF-κB binding sites located downstream of the gene have been shown to mediate transcriptional induction of Junb in response to oxygen deprivation (Schmidt et al., 2007).

Although much less is known about the regulation of Junb via post-translational mechanisms, there are some evidences of Junb phosphorylation and SUMOylation. Junb is phosphorylated by JNK in T cells at threonine residues 102 and 104 and this phosphorylation is important for synergy with c-Maf transcription factor and T helper cell differentiation (Li et al., 1999). In addition, three proline-flanked serine or threonine residues (Ser23, Thr150 and Ser186) are specifically phosphorylated by $p34^{cdc2}$-cyclinB kinase in M and early G1 phase of the cell cycle, correlating with a decrease in Junb protein levels. These residues are not conserved in Jun or Jund and the phosphorylation may target the Junb protein for degradation (Bakiri et al., 2000). Recently, Farras et al. observed that Junb becomes phosphorylated by mid-/late G2 phase, that this phosphorylation leads to proteasome-mediated degradation, and that this event is required for proper cell cycle progression (Farras et al., 2008).

Furthermore, Junb conjugation with small ubiquitin-like modifier (SUMO) on lysine 237 plays a critical role in T cell activation. Indeed, SUMO modification regulates the ability of Junb to induce cytokine gene transcription (Garaude et al., 2008).

3.1.5.2 In vitro and in vivo functions of Junb

Junb has been first characterized as an inhibitor of Jun function following the observations that excess of Junb over Jun is sufficient to inhibit transactivation of AP-1 reporter genes by Jun. Furthermore, Junb alone fails to transactivate artificial reporter genes containing a single TRE. So far, the exact mechanism by which Junb represses transcription is unknown but two different models have been proposed. First, Jun and Junb may compete for the DNA binding site, since both proteins have a similar DNA binding affinity. Secondly, Junb may form a heterodimer with Jun that has a lower transactivation potential than a Jun:Jun homodimer, thus, resulting in a lower net AP-1 activity. Most interestingly, Junb appears to be as effective as Jun in transactivating reporter genes containing multiple AP-1 binding sites (Angel and Karin, 1991; Chiu et al., 1989).

Recent analyses carried out with cells and mice deficient for Junb revealed that Junb is not only a repressor of Jun activity but is also required for the transcriptional activation of key target genes involved in cell cycle regulation, proliferation, differentiation, angiogenesis as well as skin and hematopoietic functions. Thus, both activator and repressor functions of Junb are required for proper cell function and proper development and physiology of mice.

Junb deficiency results in embryonic lethality between day 8.5 and 10.0 of embryonic development due to defective feto-maternal interactions. Most importantly, in absence of Junb, gene expression and function in cells of extra-embryonic tissues, such as trophoblast giant cells, as well as endothelial cells of the yolk sac and placental cell types are affected (Schorpp-Kistner et al., 1999).

Analysis of Junb-deficient MEFs revealed that Junb suppresses cell proliferation via its target gene p16/Ink4a during G1 to S phase transition of the cell cycle (Passegue and Wagner, 2000), but also promotes cell cycle progression from G2 to M phase via the transcriptional activation of cyclin A (Andrecht et al., 2002). Furthermore, recent data showed that the Junb breakdown in mid-/late G2 phase is required for down-regulation of cyclin A2 levels and for proper mitosis (Farras et al., 2008).

Loss of Junb in conditional mutants with either a widespread deletion of Junb in various tissues or even a tissue-specific deletion in epidermis results in a myeloproliferative disease resembling human Chronic Myeloid Leukemia (CML) (Meixner et al., 2008; Passegue et al.,

2001; Passegue et al., 2004). Detailed analyses revealed that Junb inactivation results in CML by specifically expanding the number of Long Term Hematopoietic Stem Cells (LT-HSC) and Granulocyte/Macrophage Progenitors (GMP) (Passegue et al., 2004). Also in humans, loss of Junb due to epigenetic promoter silencing could be associated with CML (Yang et al., 2003), while Junb overexpression has been associated with cutaneous CD30-positive T-cell lymphomas (Rassidakis et al., 2005).

In addition, Junb plays a critical role in bone biology by being responsible for the differentiation and proper function of chondrocytes and osteoblasts (Hess et al., 2003; Kenner et al., 2004).

Furthermore, Junb is a critical regulator of the cutaneous response to injury or stress of the skin as shown by *in vitro* organotypic cultures (Szabowski et al., 2000) and conditional mouse mutants. Mice lacking Junb in the skin develop normally, indicating that Junb is neither required for cutaneous organogenesis nor homeostasis (Florin et al., 2006). Yet, in wounded skin, Junb-deficiency results in delayed tissue remodeling, pronounced epidermal hyperproliferation, disturbed differentiation and prolonged inflammation. These phenotypic skin abnormalities were associated with Junb-dependent alterations in expression levels and kinetics of cytokines governing wound repair, such as Csf2, Gro-1, Mip-2 and Lcn-2 in both the dermal and epidermal compartments of the skin, and with a reduced ability of wound contraction of mutant dermal fibroblasts *in vitro* (Florin et al., 2006). Moreover, inducible epidermal deletion of Junb and Jun in adult mice leads to a phenotype resembling the histological and molecular hallmarks of psoriasis, including arthritic lesions (Zenz et al., 2005). Presumably, loss of Junb in keratinocytes triggers chemokine/cytokine expression resulting in the recruitment of inflammatory immune cells contributing to the psoriasis-like phenotype. Finally, epidermal Junb-deficiency causes skin ulcerations, myeloproliferative disease and low bone mass due to high systemic levels of the negatively regulated Junb-target G-CSF (Meixner et al., 2008).

Junb has also an essential role in the differentiation and function of immune cells. Junb is involved in the differentiation of naïve T cells into T helper 1 and T helper 2 cells, which is a hallmark of the T cell-dependent immune response (Hartenstein et al., 2002). In addition, Junb regulates the ability of Natural Killer cells to kill target cells by regulation of NKG2D-ligand Rae-1epsilon (Nausch et al., 2006). Finally, Junb is a critical regulator of mast cell biology. Junb is required for proper mast cell degranulation and for mast cell mediated-

angiogenic processes, by regulating the expression of *Swap70*, *Vamp8*, *Syt1* and *Vegfa* genes, respectively (Textor et al., 2007).

The most dramatic consequences of loss of Junb are seen in the vascular system. Complete as well as endothelial-specific ablation of Junb result in a similar phenotype affecting the remodeling of the primary vascular plexus in the yolk sac of the developing embryo but also affecting angiogenic remodeling in the embryo itself (Licht et al., 2006; Schorpp-Kistner et al., 1999). A mechanistic explanation for the observed phenotypes could be provided: Junb is a target gene of hypoxia-induced signaling mediated by NF-κB and this occurs independently of the known master regulator of hypoxia-induced signaling Hypoxia-Induced Factor (HIF). Most importantly, *in vitro* analyses revealed that Junb is required for the expression and induction of the key regulator of angiogenesis *Vegfa* upon hypoxia and hypoglycemia (Schmidt et al., 2007; Textor et al., 2006). Thus, Junb is a critical independent regulator of the autocrine and paracrine acting Vegfa. In line with these findings, loss of Junb affects tumor angiogenesis due to impaired paracrine acting Vegf. Junb is also required for proper endothelial cell morphogenesis both *in vivo* and *in vitro* in a cell-autonomous manner as shown by endothelial cell-specific ablation of Junb. In endothelial cells, Junb is required for Cbfb induction in response to hypoxia and subsequently for the expression of the Cbfb and AP-1 target Mmp13 (Licht et al., 2006). In summary, positively regulated Junb targets are required for proper vascular development. Yet, negative regulation of cytokines by Junb is also of unequivocal importance to suppress a pro-inflammatory and pro-cancerogenic phenotype.

3.2 Mechanisms of repression

Gene repression, which is the process of keeping genes in an off state until transcription becomes activated as final step in signal transduction pathways, plays a central role in gene regulation. Indeed, it controls proper gene activation throughout development as well in response to extracellular signals (Courey and Jia, 2001). In fact, impaired gene repression due to aberrant expression of repressor proteins results in diseases, such as Rett (mutation of *MeCP2* gene) and ICF syndromes (Immunodeficiency, Centromere instability and Facial anomalies syndrome, mutation of *dnmt3b* gene) as well as some human cancers. These findings underscores that transcriptional repression and gene silencing is essential for the maintenance of the cellular integrity of higher organisms (Thiel et al., 2004).

Eukaryotic transcriptional repression mechanisms are remarkably variable in their modes of action and effects. Some mechanisms are readily reversible, but others establish a heritable state of long-term silencing (Moazed, 2001). Three different mechanisms are described. First, repression can act directly on the transcription initiation complex. It has been shown that blockade of the targeting of TATA-binding proteins to the TATA box on the DNA or inhibition of the formation of the initiation complex of RNA polymerase II result in gene repression (Pugh, 2000). Secondly, a factor can repress gene expression indirectly by inhibiting an activating component located on the promoter. Such repression can be mediated either by protein-protein interaction and subsequent inhibition of the transactivation activity or by competition for a transcription factor binding site at the promoter of the gene (Cowell, 1994). Third, repression can be achieved by active remodeling of the chromatin structure through epigenetic modifications.

As described in the previous section of this work, Junb, due to its weak transactivation domain, is considered as an inhibitor of AP-1, in particular of Jun. Thus, by forming weakly active dimers with Jun, Junb absorbs the activity of AP-1 and acts as a repressor (Chiu et al., 1989). In this work, I wanted to investigate the ability of Junb to repress genes independently of its weak transactivation activity and to determine whether Junb, in addition, acts as an active repressor by modulating the chromatin structure.

3.2.1 Epigenetics

3.2.1.1 Definition

Epigenetics is the study of heritable alterations in phenotype and gene expression acquired during development and cellular differentiation that are not caused by a modification in the DNA sequence. Epigenetic changes are orchestrated by four different mechanisms: chromatin modifications, DNA methylation, non-coding RNAs as well as nucleosome repositioning. Much of epigenetic studies converged on the analyses of covalent and non-covalent modifications of DNA and histones. Therefore, these two mechanisms, chromatin modifications and DNA methylation, will be described in more detail in the following paragraphs.

3.2.1.2 Histone modifications

In the nuclei of all eukaryotic cells, the double stranded DNA is highly folded and tightly compacted by histone and non-histone proteins in a dynamic three dimensional structure

called chromatin. The chromatin organization is dependent on a higher order structure, namely nucleosomes. The nucleosome, which is wrapped by two superhelical turns of DNA and 147 base pairs in length, represents the basic repeating unit of chromatin and is composed of eight histones: one H3-H4 tetramer and two H2A-H2B dimers (Luger et al., 1997). Histones are small basic proteins which consist of a globular domain and a flexible basic N-terminal tail that protrudes from the nucleosome. N-terminal histone tails are subjected to many covalent modifications which control and modify the DNA binding properties of nucleosomes. At least 8 different modifications have been described so far and include acetylation, lysine and arginine methylation, phosphorylation, ubiquitination, sumoylation, ADP ribosylation and others. In addition, histones can be modified on as many as 60 residues. The complexity is further increased by the fact that some modifications such as methylation can occur in different forms. For instance, lysines are mono-, di- and tri-methylated while arginines are mono- and di-methylated, symmetrically or asymmetrically. Thus, this wide amount of possible modifications provides an enormous potential and ensures a very fine tuning of functional responses (Kouzarides, 2007).

Whereas most of the modifications are still poorly understood, much effort has been brought about the understanding of the function and regulation of histone acetylation and methylation. On the one hand, histone acetylation almost always correlates with chromatin accessibility and transcriptional activity. It is achieved by both relaxation of the DNA backbone following the neutralization of positive charge of the N-terminal histone tail and by recruitment of enzymes. For instance, acetylated histones recruit the bromodomains of nucleosome remodeling complexes, which, under ATP expenditure, displace nucleosomes and open the chromatin (Syntichaki et al., 2000).

On the other hand, methylation can have different functions depending on which residue is modified. While histone H3 methylation on lysine 4 (H3K4) and 36 (H3K36) is associated with transcribed chromatin, H3 methylation on lysine 9 (H3K9), 27 (H3K27) and H4 methylation on lysine 20 (H4K20) correlate with repression. In contrast to histone acetylation, transcriptional regulation by lysine methylation is always achieved through recruitment of chromatin modifying enzymes. For example, methylated H3K4 recruits, via the chromodomain of Chd1, transcription activating complexes (Pray-Grant et al., 2005), while methylated H3K9 or H3K27 binds HP1 and Polycomb proteins, respectively, and mediate chromatin compaction (Bannister et al., 2001).

Furthermore, while most of the covalent modifications are associated with changes in transcription, few of them, such as acetylation, methylation, phosphorylation and ubiquitination, have also been involved in other DNA processes such as DNA repair, replication and condensation (Kouzarides, 2007).

3.2.1.3 Histone modifying enzymes and HDACs

In the past years, much effort has been invested to characterize histone modifying enzymes. Enzymes, which catalyze acetylation (Sterner and Berger, 2000), methylation (Zhang and Reinberg, 2001), phosphorylation (Nowak and Corces, 2004), ubiquitination (Shilatifard, 2006), sumoylation (Nathan et al., 2006), ADP-ribosylation (Hassa et al., 2006) and others, have been identified. Since most modifications have been found to be dynamic, in addition, enzymes have been discovered that remove all previously described modifications, except for arginine demethylases.

Among these enzymes, histone deacetylases (HDACs) attracted particular interest. Indeed, HDACs play global roles in the regulation of gene transcription, cell growth, survival and proliferation and alterations in HDACs expression or activity have been intensively correlated to disease state such as cancer (Cress and Seto, 2000).

HDACs consist of three different classes based on their homology to yeast counterparts. While the class I, composed of HDAC1, 2, 3 and 8, are homologue to RbAp48 (Rb-associated protein 48), the class II, HDA-1 like proteins, comprises at least 6 homologues in vertebrates: HDAC4, 5, 6, 7, 9 and 10. The class III, which do not share any homology with the classes I and II, is composed of NAD+ dependent deacetylases called sirtuins (SIR1-7).

HDACs are tightly regulated through a multitude of mechanisms, such as recruitment into co-repressor complexes, modulation of deacetylase activity by protein-protein interactions or post-translational modifications as well as translocation from the cytoplasm to the nucleus (Yang and Seto, 2008b).

All class I members, with the exception of HDAC8, function as catalytic subunits of mSin3, NuRD (nucleosome remodeling deacetylase), SMRT (silencing mediator of retinoic acid and thyroid hormone receptors) and CoREST (corepressor of RE1-silencing transcription factor) co-repressor complexes (Yang and Seto, 2008b). HDACs do not have the ability to bind directly to DNA, but, by being part of co-repressor complexes, they get to interact with DNA sequence specific factors and repress transcription as well as shape epigenetic patterns. In mammals, two mSin3 co-repressor complexes exist: mSin3A and mSin3B. More precisely, mSin3A is composed of many different proteins, including HDAC1, 2, and ING2. By binding

to methylated histone H3 on lysine 4, ING2 targets the whole complex to deacetylate regions of the genome where H3K4 is methylated (Ahringer, 2000).

Class II members are characterized by tissue-specific expression and can exist both in the nucleus and in the cytoplasm. They contain intrinsic nuclear import and export signals for dynamic nucleo-cytoplasmic trafficking. Therefore, association of partners (such as 14-3-3) upon diverse signaling stimuli controls both the subcellular distribution and the repression activity of HDACs (Yang and Seto, 2008b).

Additionally, although implicated in deacetylation of the histone H4 on lysine 16, recently, sirtuins became of great interest in the scientific community, since they have been described to promote longevity both in yeast and mice and, therefore, to be protective against aging and neurodegenerative disease (Saunders and Verdin, 2007; Vaquero et al., 2007).

Finally, protein acetylation became accepted as a post-translational modification capable of regulating protein activity, localization, protein-protein interaction as well as other mechanisms and the list of acetylated proteins increased in the past years (Yang and Seto, 2008a). There is accumulating evidence that HDACs deacetylate those non histone proteins as well. For instance, HDAC6 controls, in addition to gene expression, multiple cellular processes by deacetylating tubulin as well as hsp90 (Kovacs et al., 2005; Zhang et al., 2008; Zhang et al., 2003).

3.2.1.4 DNA methylation

DNA methylation occurs almost exclusively in the context of CpG dinucleotides in vertebrates and most of the CpG dinucleotides in the genome are methylated (Bird, 2002). Non-CpG methylation has an established function in plants (Chan et al., 2005) and may play a yet-to-be defined role in mammals as well.

Mammalian DNA methylation has been implicated in a broad range of cellular functions and diseases, including tissue-specific gene expression, cell differentiation, genomic imprinting, X chromosome inactivation, regulation of chromatin structure, genomic stability, carcinogenesis and aging (Bird, 2002). It is essential for proper development (Li et al., 1992; Okano et al., 1999) and remains indispensable for the survival of differentiated cells (Jackson-Grusby et al., 2001).

Mechanistically, methylated cytosine residues regulate gene expression by the fact that they can promote or exclude the recruitment of regulatory proteins (Bernstein et al., 2007). On the one hand, methyl-CpG binding proteins bind to methylated CpG dinucleotides and mediate transcriptional repression through interactions with co-repressor complexes and HDACs. A

family of five methyl-CpG binding proteins (MBD1, 2, 3, MeCP2 and Kaiso) has been characterized and each member contains a region closely related to the Methyl-CpG Binding Domain (MBD) of MeCP2 (Bird, 2002). On the other hand, the methylation on cytosine residues can exclude DNA binding proteins from their DNA consensus sequence. It has been described, for example, for CTCF binding at the *H19* locus and will be further explained in the next paragraph.

DNA methylation patterns are dynamic during development. Shortly after fertilization, in mammals, the paternal genome is actively demethylated, while the maternal genome presumably undergoes passive demethylation. Genome-wide methylation levels increase rapidly in the blastocyst and eventually result in the formation of methylation patterns found in the adult (Reik et al., 2001). Although the molecular determinants responsible for the patterning of *de novo* methylation in the blastocyst remain mysterious, *de novo* methylation is achieved by the two DNA Methyltransferases DNMT 3a and 3b. Then, once the methylation patterns are set, the DNA methyltransferase 1 (DNMT1) maintains the methylation patterns between cell divisions by residing in the replication fork and having a higher affinity for hemi-methylated DNA.

Finally, alterations in DNA methylation are observed in patho-physiology such as cancer. Indeed, in tumorigenesis, the methylome undergoes characteristic changes with genome-wide loss of methylation and genome instability, as well as aberrant local gain of methylation on promoters of tumor suppressor genes. These findings underscore that genetics and epigenetics cooperate at all stages of cancer development (Jones and Baylin, 2002, 2007).

3.2.1.5 Imprinting

Genomic imprinting is an epigenetic mechanism of transcriptional regulation through which expression of a subset of mammalian genes is restricted to one parental allele. While either the maternal or paternal allele is expressed, the other is silenced. Imprinting has been found only in mammals and not in other vertebrates.

The importance of imprinting in development and growth have been underscored by the fact that embryos generated from a monoparental genome fail to develop (Solter, 1988), as well as by development of cancers and disease syndromes following loss of imprinting (Prader-Willi, Angelman and Beckwith-Wiedemann syndromes) (Nicholls and Knepper, 2001; Weksberg et al., 2005). A common feature of imprinted genes is the control of fetal development by paternally expressed genes, such as Igf2, and maternally expressed genes, such as H19 and Igf2r, that positively and negatively regulate growth, respectively.

To date, around 70 genes have been shown to be controlled by imprinting. A majority of them are arranged in clusters in the genome and this organization appears to be required for appropriate gene regulation (Verona et al., 2003). Such clusters are often composed of multiple protein coding genes and at least one non-coding region RNA and they are regulated by a major *cis*-acting element, called Imprinting Control Region (ICR). The ICR acquires differential epigenetic modifications such as DNA methylation and histone modifications during gametogenesis, which are subsequently retained during development (Reik et al., 2001).

3.2.1.5.1 H19

H19 and *Igf2* (*insulin-like growth factor 2*) genes were among the first imprinted genes identified in the mouse. Both genes are also imprinted in humans and many aspects of the regulation identified in mice also apply to humans.

The *H19* gene encodes a 2.3 kb non-coding mRNA which is strongly expressed during embryogenesis. So far, the function of *H19* has not been deciphered. Mice carrying deletions of the H*19* gene are viable and fertile. Although such mutations lead to an overgrowth phenotype, the molecular cause has been linked to a loss of imprinting of the adjacent *Igf2* gene. Furthermore, recent work from Cai X and Cullen B identified *H19* as a micro RNA precursor (miR-675) but further analyses are still required to uncover miR-675 target genes and functions (Cai and Cullen, 2007).

The *H19-igf2* locus, located within a conserved imprinted cluster on mouse chromosome 7 and human chromosome 11p15, contains the maternally expressed *H19* and the paternally expressed *Igf2* gene. The imprinting mechanism of *H19* has been widely studied. First, both genes, *H19* and *Igf2*, share a common enhancer located 10 kb downstream of *H19* transcriptional start (Yoo-Warren et al., 1988). Second, the 90 kb segment located between *H19* and *Igf2* genes defines a region where many different regulatory elements have been identified using targeted germ line deletion and transgenic approaches in the mouse (Sasaki et al., 2000). More precisely, the analyses of this cluster revealed an essential 2kb ICR that is differentially methylated. The paternally methylated region, also called Differentially Methylated Domain (DMD), is located 4kb upstream of the *H19* gene. This region is, indeed, essential since its deletion by genetic manipulation leads to a loss of expression of H19 (Brannan and Bartolomei, 1999; Sasaki et al., 2000). The ICR domain contains four binding sites for the CCCTC binding factor (CTCF) included in CpG rich elements.

CTCF binding is crucial for the control of differential expression of *H19* between maternal and paternal alleles as well as for the establishment and the maintenance of differential methylation and imprinting of *H19*. First, CTCF is involved in insulator activity, meaning CTCF can block the interaction between enhancers and promoters. On the maternally inherited allele, CTCF binds to the unmethylated DMD, creating a chromatin insulator which prevents the *Igf2* promoter from gaining access to the downstream enhancers. On the paternally inherited allele, the DMD is methylated, which blocks CTCF binding. This lack of CTCF binding inactivates the insulator, allowing the promoter of the paternal *Igf2* allele to interact with the downstream enhancers and, thus, to be transcribed (Bell and Felsenfeld, 2000; Hark et al., 2000). Secondly, in addition to the fact that CTCF binding is sensitive towards methylation, the DNA methylation itself is dependent on CTCF binding. Indeed, mutation of the CTCF binding site in the DMD results in increased methylation of the maternally inherited gene in post-implantation development (Pant et al., 2003; Schoenherr et al., 2003). Similar results have been obtained upon use of siRNA-mediated knock down of CTCF in the oocyte, which results in increased *H19* DMD methylation (Fedoriw et al., 2004).

3.3 Stress responses

As described above, AP-1 plays multiple roles in stress responses and stress-induced apoptosis being either pro-apoptotic or anti-apoptotic, depending on the balance of AP-1 members in the given cell, the cell lineage, the differentiation stage, the microenvironment and the type of stimulus (Hess et al., 2004). Previous work based on *in vivo* mouse models as well as *in vitro* tissue culture models derived thereof defined a crucial role for Junb in cellular hypoxia and hypoglycemia responses (Schmidt et al., 2007; Textor et al., 2006). Recent evidence has emerged that hypoxia and hypoglycemia may trigger ER stress that may act as an important contributor to hypoxia tolerance and tumor progression. Due to the facts that AP-1 is a key player in many stress responses and that so far a link between AP-1 and ER stress response is still missing, I aimed to decipher the implication of Junb in the ER stress response but also in stress-induced apoptosis.

3.3.1 Unfolded protein response (UPR)

In eukaryotic cells, secreted and transmembrane proteins fold and mature in the lumen of the endoplasmic reticulum (ER). The flux of proteins entering into the ER depends on multiple factors such as cell differentiation, environmental conditions and physiological state of the cell. Cells adjust the protein-folding capacity of the ER according to their requirements in

order to maintain the high quality of transmembrane and secreted proteins. An imbalance between the load of protein entering the ER and the folding capacity of the ER induces a condition of stress, called ER stress. ER stress activates an adaptive response, namely unfolded protein response or UPR, which will act in three steps. First, the cell reduces the protein load entering the ER by lowering protein synthesis and translocation into the ER. Second, in order to increase the capacity of the ER to handle unfolded proteins, the cell transcriptionally activates UPR target genes implicated in the protein folding machinery. Third, if the cell does not re-establish homoeostasis, programmed cell death is triggered (Ron and Walter, 2007).

ER stress has been defined as an initiating and/or contributing factor in a broad range of age-related diseases, including neurodegeneration (Ryu et al., 2002), tumor development (Bi et al., 2005; Koumenis, 2006) and type 2 diabetes (Ozcan et al., 2004; Ozcan et al., 2006).

As shown in Figure 1, ER stress is controlled by a unique ER-located chaperone, namely Grp78 (78kDa glucose-related protein, also BiP or Hspa5). While, under resting state, Grp78 binds to and, therefore, inhibits the downstream initiators of the UPR, misfolded protein accumulation displaces Grp78 and activates UPR (Bertolotti et al., 2000). Three ER stress transducers have been identified and each of them regulates a distinct arm of the UPR: PERK (protein kinase RNA (PKR)-like ER kinase), IRE1 (inositol requiring kinase 1) and ATF6 (activating transcription factor-6) (Szegezdi et al., 2006). Active PERK phosphorylates the eukaryotic Initiating Factor 2 α (eIF2α or Eif2a) and triggers global attenuation of protein synthesis as well as cell cycle arrest (Harding et al., 2000b). In addition, phosphorylated eIF2α selectively translates mRNAs transcripts, such as Atf4 (activating transcription factor 4), which has been described to induce the expression of the pro-apoptotic transcription factor CHOP (CAAT/Enhancer binding protein homologous protein, Gadd153 or Ddit3) (Harding et al., 2000a). IRE1 (or Ern2), which is a serine, threonine protein kinase and an endonuclease, initiates the unconventional splicing of the transcription factor Xbp1 mRNA transcript (X-box binding protein 1). Spliced Xbp1 is subsequently translated and gives rise to a transcription factor activating the expression of numerous genes involved in the UPR, such as *grp78*, *grp94* and *chop* (Calfon et al., 2002). Finally, upon dissociation of Grp78, ATF6 is processed by the site-1 and -2 proteases S1P and S2P (or Mbtps1 and Mbtps2, respectively) in the Golgi and subsequently translocates to the nucleus, where it activates the expression of key players of the UPR (Ye et al., 2000).

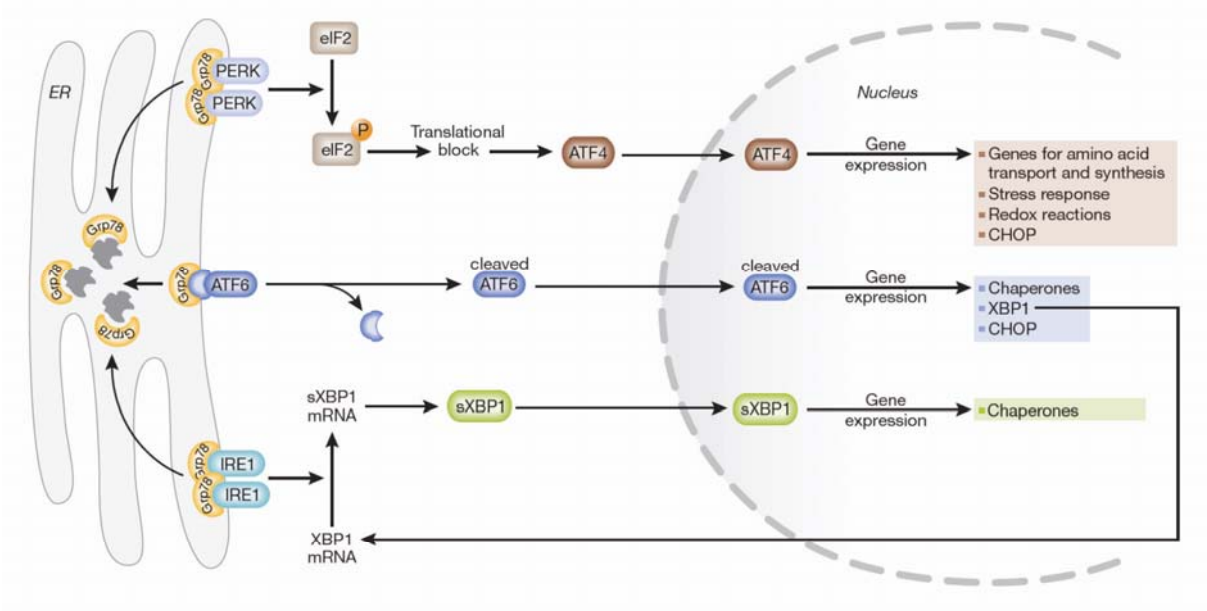

Figure 1: The unfolded protein response. Upon aggregation of unfolded proteins, Grp78 dissociates from the three endoplasmic reticulum (ER) stress sensors, PERK, ATF6 and IRE1, and thus, allows their activation. Activated PERK blocks general protein synthesis by phosphorylating eukaryotic translation initiation factor 2 (eIF2, or eif2s2). Yet, this phosphorylation also enables translation of ATF4. ATF4, a transcription factor, translocates to the nucleus and induces the transcription of *Chop (Ddit3)* as well as genes required to restore ER homeostasis. ATF6 translocates from the ER to the Golgi apparatus, where it gets cleaved and activated. Active ATF6, also a transcription factor, regulates the expression of ER chaperones and XBP1. To be translated, *XBP1* must undergo mRNA splicing (sXBP1), which is carried out by IRE1. XBP1 protein translocates to the nucleus and controls the transcription of chaperones. This adaptive response aims to restore ER function by blocking further build-up of client proteins, enhancing the folding capacity and initiating degradation of protein aggregates. Adapted from Szegezdi et al. 2006.

3.3.2 Prolonged ER stress will result in mitochondria-mediated apoptosis

Upon prolonged misfolded protein load in the ER, PERK, ATF6 and IRE1 signaling will induce cell death. These signaling pathways do not directly cause apoptosis but rather initiate the activation of downstream molecules, which subsequently trigger the cell to the path of death.

As shown in Figure 2, all pathways inducing apoptosis converge on the activation of caspases. Caspases are cysteine-aspartic acid proteases that coordinate the efficient destruction of the cell by cleavage of multiple substrates and activation of DNases. Two pathways of programmed cell death can be distinguished (Fig. 2). The so-called extrinsic or death-receptor mediated pathway is triggered by the death receptors (members of the Tumor Necrosis Factor (TNF) receptor family such as Fas, also named CD95, or TNF receptor-1). Upon binding of the ligand, the receptor recruits and activates caspase-8, which results in the

subsequent activation of downstream effector caspases without any involvement of the mitochondria and the Bcl-2 family members. The second pathway, targeting mitochondrial functionality is called intrinsic pathway. Since prolonged ER stress has been described to induce apoptosis through the intrinsic pathway (Szegezdi et al., 2006), this mechanism will be described in more detail in the following section (Fig. 2).

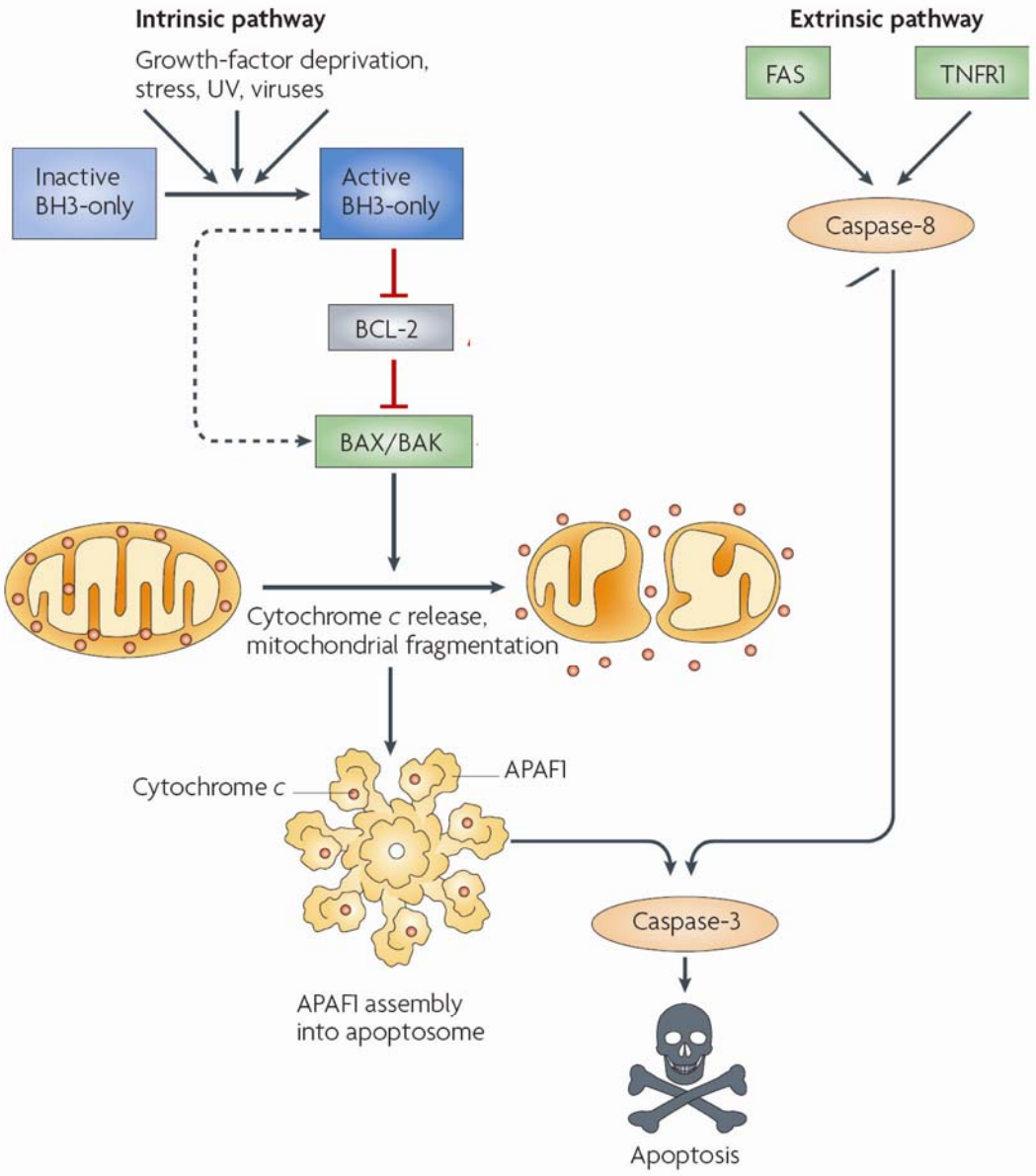

Figure 2: Scheme depicting intrinsic and extrinsic pathways of apoptosis. Apoptosis can be induced by cell surface death receptors, such as Fas and tumor necrosis factor receptor 1 (TNFR1; extrinsic pathway, on the right), or by various genotoxic agents, metabolic insults or transcriptional cues (intrinsic pathway, on the left). The intrinsic pathway starts with the induction or post-translational activation of BH3-only proteins. This results in the inactivation of anti-apoptotic Bcl-2 family members, which relieves inhibition of Bax and Bak and promotes apoptosis. Some BH3-only proteins, such as Bim, may also be able to activate Bax and/or Bak (as shown by the dotted line). Once activated, Bax and Bak promote Cytochrome c release, which leads to the formation of the apoptosome with APAF1 and the activation of caspase-9 and subsequently caspase-3. Caspases in turn cleave a series of substrates, activate DNases and orchestrate the disintegration of the cell. The extrinsic pathway can bypass the mitochondrial step and activate caspase-8 directly, which leads to caspase-3 activation and cell degradation. Adapted from Youle and Strasser, 2008.

In addition to supply energy to the whole cell by generation of adenosine triphosphate (ATP), the mitochondria play a central role in many processes such as cell signaling, differentiation, growth and apoptosis. Most apoptosis-inducing conditions involve the disruption of the mitochondrial transmembrane potential which results in a sudden increase of mitochondria membrane permeability. Thus, osmotic swelling will eventually lead to the rupture of the outer membrane and to the release of pro-apoptotic proteins, such as cytochrome C, from the mitochondria into the cytoplasm (Loeffler and Kroemer, 2000). Those mitochondrial events are kept under strict control by the Bcl-2 family members, which will be further discussed in the next paragraph.

Bcl-2 family members, which are key regulators of the intrinsic apoptosis pathway, have been described by homology to the structure of the original Bcl-2 (B-cell lymphoma-2) protein. The family comprises, in mammals, at least 12 members that have been grouped into three classes. One class inhibits apoptosis (Bcl-2, Bcl-xL, Mcl1 and others), whereas a second class promotes apoptosis (Bax, Bak and others). The third class, composed of BH3-only proteins (Bad, Bid, Bim, Bmf, Noxa, Puma and others), have a conserved BH3 domain that binds and regulates the anti-apoptotic Bcl-2 family members, thereby promoting apoptosis (Youle and Strasser, 2008; Zha et al., 1996). There are clear evidences that the pro-apoptotic members Bax and Bak are crucial for inducing permeabilization of the outer mitochondrial membrane, by forming oligomeres which resemble pores (Saito et al., 2000; Schlesinger et al., 1997). Yet, the biochemical nature of these pores remains unknown and controversial. Anti-apoptotic members, such as Bcl-2 and Bcl-xL, inhibit the formation of oligomeres by direct binding to Bax and Bak and, thus, hinder the formation of pores in the outer mitochondrial membrane and subsequent caspase activation (Sedlak et al., 1995).

Once the outer mitochondrial membrane is permeabilized, proteins including cytochrome c are released into the cytosol. Then, cytochrome c forms with APAF-1 a heptameric protein ring called apoptosome, which binds to pro-caspase-9 and induces its activation through a conformational change (Shi, 2006). Active caspase-9 will eventually result in activation of the effector caspase-3 and subsequent cell death (Hakem et al., 1998).

The molecular mechanisms involved in the death of ER stressed cells remain poorly understood and many different models have been proposed, which involve diverse essential molecules, such as Bcl-2 family members, CHOP, SAPK/JNK, and caspase-12.

Bcl-2 family members have been shown to be essential for ER stress-mediated apoptosis. Indeed, Bax and Bak ablation in MEFs result in resistance towards ER stress and treatment

with other stress stimuli known to activate the intrinsic apoptosis pathway, including growth factor retrieval, ultraviolet (UV) irradiation, staurosporine and etoposide (Wei et al., 2001). In addition, an imbalance in expression of pro-apoptotic and anti-apoptotic Bcl-2 family members with excess of anti-apoptotic protein levels results in decreased cell death following ER stress induction (Szegezdi et al., 2006). Although the involvement of Bcl-2 proteins in ER stress-mediated apoptosis is well known, their regulation by UPR is less understood. So far two different mechanisms have been described. First, CHOP, a pro-apoptotic transcription factor induced upon PERK activation, has been shown to negatively regulate Bcl-2 gene expression. Indeed, overexpression of CHOP results in induction of apoptosis due to low Bcl-2 expression and re-expression of Bcl-2 in these cells could efficiently block CHOP-induced apoptosis (McCullough et al., 2001). Secondly, induction and post-translational modifications of BH3-only proteins by JNK has been reported as key event in the ER stress-mediated apoptosis cascade. JNK is activated by a protein complex formed by activated IRE1 which contains the adaptor protein TRAF2 and the MAPK Kinase ASK1 (Urano et al., 2000). JNK-triggered phosphorylation of Bim releases Bim from an inhibitory association with the dynein motor complex and, thus, allows Bim to exert its pro-apoptotic effects (Lei and Davis, 2003). In addition, JNK promotes Bax translocation to the mitochondria through phosphorylation of 14-3-3, a cytoplasmic anchor of Bax (Tsuruta et al., 2004).

Finally, caspase-12 has been proposed as a key mediator of ER stress-induced apoptosis. *Caspase12* $^{-/-}$ MEFs have been reported to exhibit partial resistance specifically against ER-stress inducing agents (Nakagawa et al., 2000). However, in a recent work published by Saleh and colleagues, *Caspase12* $^{-/-}$ MEFs, originated from another source, displayed no resistance to ER stress mediating agents (Saleh et al., 2006). In addition, only a few consistent data linking caspase-12 to downstream caspase activation is available, thus, it is difficult to state an essential role for this caspase in ER-stress induced apoptosis (Szegezdi et al., 2006).

4 Aims

During my thesis work, I addressed two scientific problems associated with the *in vivo* functions of Junb that are still not yet solved but that may be of fundamental importance with regard to the double-edge role of Junb in cancer: the function of Junb as a negative transcriptional regulator and its impact in the ER stress response and apoptosis.

The analysis of global gene expression between wild-type and Junb knock-out mouse embryonic fibroblasts revealed a big set of genes derepressed in absence of Junb. It was claimed that Junb, by being a weak transactivator, on its own may act as a repressor by forming less active heterodimers with other AP-1 subunits and, thus, absorbing the Jun and other AP-1 members' activity. In this work, I investigated the repressor activity of Junb and wanted to decipher other possible repression mechanisms. Therefore, during my PhD work, I aimed to answer these two questions.

1. Does Junb modulate the acetylation-deacetylation status of genes by regulating the expression of HDACs and/or members of co-repressor complexes?

2. Does Junb regulate methylation of promoters and/or imprinted domains?

Previous work based on *in vivo* mouse models as well as *in vitro* tissue culture models derived thereof defined a crucial role for Junb in cellular hypoxia and hypoglycemia responses. Recent evidence has emerged that hypoxia and hypoglycemia may trigger ER stress and UPR. Since UPR controls protein synthesis, cell metabolism, cell cycle progression and cell death, it may act as an important contributor to hypoxia tolerance and tumor progression. Although AP-1 is a key player in many stress responses and stress-induced apoptosis, so far a link between AP-1 and ER stress response is still missing. Therefore, I studied the implication of Junb in the ER stress response but also in stress-induced apoptosis in order to answer the following questions:

1. Is Junb induced upon ER stress? And is the UPR deregulated in absence of Junb?

2. Does loss of Junb affect ER stress-mediated apoptosis? And if so what are the molecular mechanisms responsible for the observed phenotype?

5 Material and methods

5.1 Material

5.1.1 Chemicals

Acrylamid/Bisacrylamid (30:0,8)	Roth, Karlsruhe
Agarose	Sigma, Deisenhofen
Ammoniumperoxodisulfat (APS)	Janssen Chimica
Ampicillin	Sigma, Deisenhofen
Bacto agar	Roth, Karlsruhe
Bacto tryptone	Gerbu Biotechnik, Gaiberg
Bacto yeast extracts	Gerbu Biotechnik, Gaiberg
β-Mercaptoethanol	Merck, Darmstadt
Bismaleimidohexane (BMH)	Pierce
Bovine serum albumine, fraction V	Sigma, Deisenhofen
Bromphenol blue	Serva, Heidelberg
Calcium chloride	Merck, Darmstadt
DC protein measurment kit	Biorad, Munich
Dithiothreitol (DTT)	AppliChem, Darmstadt
DMSO (Dimethylsulfoxide)	Merck, Darmstadt
EDTA (Ethylenediamine-tetraacetate)	Roth, Karlsruhe
EGTA	Roth, Karlsruhe
Entellan	Merck, Darmstadt
Eosin B	Sigma, Deisenhofen
Enhanced chemiluminescent system	Perkin Elmer, Waltham, USA
Ethanol	Sigma, Deisenhofen
Ethanolamine	Merck, Darmstadt
Ethidium bromide	AppliChem, Darmstadt
Fugene	Roche, Mannheim
HEPES	Gerbu Biotechnik, Gaiberg
Hoechst H33342	Calbiochem, Darmstadt
Isopropanol	Sigma, Deisenhofen
Kanamycin	Sigma , Deisenhofen
Mayer’s hematoxylin	Roth, Karlsruhe

Methanol	Sigma , Deisenhofen
Milk powder	Roth, Karlsruhe
MitoTracker® CMXRos	Invitrogen, Karlsruhe
Mowiol	Calbiochem, Darmstadt
Nitrocellulose-Membran	Schleicher und Schuell, Dassel
Positively charged nylon membrane	GE healthcare, Munich
Paraformaldehyde	Roth, Karlsruhe
Polybrene	Sigma, Deisenhofen
Proteinase K	Merck, Darmstadt
Puromycin	Sigma, Deisenhofen
Saccharose	Merck, Darmstadt
SDS	Gerbu Biotechnik, Gaiberg
TEMED	Roth, Karlsruhe
Triton X-100	AppliChem, Darmstadt
Tween 20	Sigma, Deisenhofen
Xylol	Merck, Darmstadt
Xylencyanol	Serva, Heidelberg

All other chemicals not listed here were either from Merck, Sigma or Roth.

5.1.2 Enzymes and molecular biology reagents

AnnexinV APC	BD Biosciences, Heidelberg
dNTP	Promega, Mannheim
OligodT	Fermentas, St-Leon-Rot
Restriction enzymes	Promega, Fermentas, New England Biolabs
Revertaid M-MuLV Reverse Transcriptase	Fermentas, St-Leon-Rot
Riboblock RNase inhibitor	Fermentas, St-Leon-Rot
RQ1 DNase RNase-free	Promega, Mannheim
SYBR green fluorescein	Thermo Scientific
T4 DNA ligase	Promega, Mannheim
Taq polymerase	Genaxxon, Steinbrenner
Thermosensitive Alcaline Phosphatase	Promega, Mannheim

Gene ruler 100bp DNA ladder	Fermentas, St-Leon-Rot
Gene ruler DNA ladder mix	Fermentas, St-Leon-Rot
Protein marker IV	Peqlab Biotechnology, Erlangen

5.1.3 Equipment

Bacterial petri dishes	Greiner, Frickenhausen
Cell culture articles	TPP, Trasadingen, Switzerland
Cell incubator	Heraeus, Hanau
Centrifuge	Heraeus, Hanau
Centrifuge J2-HS with rotors JS-13.1 and JA-1	Beckman, Munich
Electrophoresis chambers	Cosmo bio, Carlsbad, USA
ELISA reader	Biorad, Munich
Gel documentation	Peqlab Biotechnology, Erlangen
FACS Calibur	Becton Dickinson, Heidelberg
Leica microscope	Leica, Bensheim
Microtome RM 2155	Leica, Bensheim
PCR Cycler	BioRad, Munich
Plastic tubes	TPP, Trasadingen, Switzerland
Reaction Tubes	Steinbrenner Laborsystem, Wiesenbach
SDS-PAGE chambers	Sigma, Deisenhofen
Slides	Bender and Hohbein, Karlsruhe
Nanodrop Spectrophotometer	PeqLab Biotechnology, Erlangen
UV-Stratalinker 2400	Stratagene, Heidelberg
Wet blotting transfer system	Sigma, Deisenhofen
Whatman 3MM paper	Schleicher und Schuell, Dassel

5.1.4 Oligonucleotides

5.1.4.1 RT-PCR oligonucleotides

Junb

primers for qRT-PCR

- RT2 qPCR primer assay – SYBR Green Mouse Junb: PPM03821A, SuperArray

HPRT

Name	Sequence 5'-3'
hprt-F	GCATTTAAAAGGAACTGTTGACAACG
hprt-R	TTGTTGGATTTGAAATTCCAGACAAG

ER-located chaperones

Name	Sequence 5'-3'
grp78-F	AGGACATCAAGTTCTTGCCATT
grp78-R	AATAGTGCCAGCATCTTTGGTT
grp94-F	TCAGAGACATGTTGCGGCGGATTA
grp94-R	TTCTGCGTCTTCTGAGGTGTCTTC
calnexin-F	AGGGGAGGTTTATTTTGCTGAC
calnexin-R	CATGATGCTTGGCCCGAGACA

XBP1 splicing

Name	Sequence 5'-3'
mXBP1.19S	GGCCTTGTGGTTGAGAACCAGGAG
mXBP1.14AS	GAATGCCCAAAAGGATATCAGACT

Mitochondria-mediated apoptosis

Name	Sequence 5'-3'
clusterin-F	GAAGTTCTATGCACGTGTCTGC
clusterin-R	TCCTGAAAGAGCGTGTCTATGA

Growth factors

Name	Sequence 5'-3'
Pdgfa-F	AGCCGGCCGCCCCTCTCC
Pdgfa-R	TTTTGTGGTTTTGTTTTCGCTCTC
Pdgfb-F	AGCAGAGCCTGCTGTAATCG
Pdgfb-R	GGCTTCTTTCGCACAATCTC

Pdgfralpha-F	CTGGGAAAGTGGCCTGGACGAAC
Pdgfralpha-R	ACGCCGCTGAGATGCTACTGACG
Pdgfrbeta-F	CTGCGCTGGACCTGCTATGAGAC
Pdgfrbeta-R	TGGTGACAGTGGCCCGAGGTAAC
gmcsf-F	ATCAAAGAAGCCCTAAACCTCCTG
gmcsf-R	CTGGCCTGGGCTTCCTCATT
csf2ra-F	ATGTTTAACGACATTGATGTCACC
csf2ra-R	GGGTTAGGGTTTGTTAAGAACTGA
csf2rb-F	GTCAAGCCCATCTCTAACTACGAT
csf2rb-R	GATCTTTTCCTTCCACTTCCTGTA
csf2rb2-R	ATTGCATCATTTCTCCACCTATTT
csf2rb2-R	CAGTGAACATAGACCAAGGAACAC
kgf-F	CTGGCCTTGTCACGACCTGTTTCT
kgf-R	-CCCTTTCACTTTGCCTCGTTTGTC

Epigenetics

Name	**Sequence 5'-3'**
dnmt1-F	CCACTGCATTTGCTGAATACAT
dnmt1-R	TGGTAGAAGGAGGAACAGTGGT
dnmt3b-F	GATGGCTTTCTTTTACCCTCCT
dnmt3b-R	AATAGCATCCTCCAGCAAATGT
ctcf-F	ACTTGCGAAAGCAGCATTCC
ctcf -R	TGTCTTGCCATTGTGTTCCG

Junb target genes

Name	**Sequence 5'-3'**
lpl-F	TTGAAAGTGGGTTTTCCTGAGT
lpl-R	CTCCTGCCTGCTGTCTTCTAAT
decorin-F	GAACCTGAAGGACTTGCATACC
decorin-R	CAAGCACATTGTTCAGTCCATT

gsta4-F	GAGAAGATGCAAAAGGATGGAC
gsta4-R	TCCTGACTCTCTCCTTCAGGTC
cyba-F	CGATGTGGACAGAAGTACCTGA
cyba-R	CTGCCAGCAGATAGATCACACT
wdr79-F	CCTGATGGCAATCTCTTCTTCT
wdr79-R	TCCACTGATATCCCACACAGAG
epb4.1l4b-F	GACGGACGGAATATCAAGCTAC
epb4.1l4b-R	ATTGTGGACTTCAGGATTTGCT
slc35e3-F	AAGACACACCCCTAGGTCTCAA
slc35e3-R	ACATTTAGTGAGGCCAGGAAAA
fas-F	AAAGTGCTGGAAAAGGAGACAG
fas-R	TCTTGCCCTCCTTGATGTTATT
h19-F	GGGGACTTCTTTAAGTCCGTCT
h19-R	GGGTGCTATGAGTCTGCTCTTT
mkp1-F	AACTCGGCACATTCGGGACCAA
mkp1-R	CAAGCGAAGAAACTGCCTCAAACA
id1-F	GCCCCAGAACCGCAAAGTGA
id1-R	TTAACCCCCTCCCCAAAGTCTCTG
id3-F	GGTGCGGCTGCTACGAG
id3-R	TTCAGGCCACCCAAGTTCAGTCC

5.1.4.2 Non radioactive EMSA oligonucleotides

Name	**transcription factor site**	**Origin of binding site**	**sequence 5'-3'**
PDGF-wt-F	AP-1, ets1. NFAT	PDGFb	AGCTGCGCTGACTCCGGGC CAGGAGAGGAAAGGCTGA GCT
PDGF-wt-R	AP-1, ets1. NFAT	PDGFb	AGCTCAGCCTTTCCTCTCCT GGCCCGGAGTCAGCGCAGC T

MMP13-TRE-F	AP-1	MMP13	AGCTAAAGTGGTGACTCATCACTATAGCT
MMP13-TRE-R	AP-1	MMP13	AGCTATAGTGATGAGTCACCACTTTAGCT
consensus-SP-1-F	SP-1		ATTCGATCGGGGCGGGGCGAGC
consensus -SP-1-R	SP-1		GCTCGCCCCGCCCCGATCGAAT
PDGF-SP1-F	SP-1	PDGFb	AGCTTGTCTCCACCCACCTCTCAGCT
PDGF-SP1-R	SP-1	PDGFb	AGCTGAGAGGTGGGTGGAGACAAGCT
PDGF-TRE-F	AP-1	PDGFb	AGCTTAGGGTGAATCACAGAAGGAAGCT
PDGF-TRE-R	AP-1	PDGFb	AGCTTCCTTCTGTGATTCACCCTAAGCT
PDGFbwt-Ets1-F	ets1	PDGFb	AGCTCCAGGAGAGGAAAGGCTGAGCT
PDGFbwt-Ets1-R	ets1	PDGFb	AGCTCAGCCTTTCCTCTCCTGGAGCT
Ets-F	ets1	stromyelosin1	AGCTGCAGGAAGCATTTCCTGGAGCT
Ets-R	ets1	stromyelosin1	AGCTCCAGGAAATGCTTCCTGCAGCT

5.1.5 shRNA

shRNA against mouse clusterin cloned into the lentivirus vector pLK0.1-puro were purchased from Sigma-Aldrich.

Name	Sequence 5'-3' and region targeted by the shRNA
shRNA1	CCGGCCGGTTTATATGATCTTCATACTCGAGTATGAAGATCATATAAACCGGTTTTTG Region: CDS

shRNA2	CCGGCCTGAAACAGACCTGCATGAACTCGAGTTCATGCAG GTCTGTTTCAGGTTTTTG Region: CDS
shRNA4	CCGGGCTAAAGTCCTACCAGTGGAACTCGAGTTCCACTGGT AGGACTTTAGCTTTTTG Region: CDS
shRNA5	CCGGAGGGAAGTAAGTACGTCAATACTCGAGTATTGACGT ACTTACTTCCCTTTTTTG Region: CDS
Non-targeting shRNA	Catalogue number: SHC002

5.1.6 Antibodies

Name	Company	Catalogue number
Junb (N17)	Santa Cruz Biotechnology	Sc-46

ER-stress proteins

Name	Company	Catalogue number
Grp78	Cell Signaling Technology	3177
CHOP	Santa Cruz Biotechnology	Sc-575
p-eIF2a	Cell Signaling Technology	9725
eIF2a	Upstate	ab5369

Mitochondria-mediated apoptosis

Name	Company	Catalogue number
Caspase 3	Cell Signaling Technology	9662
Caspase 6	Cell Signaling Technology	9762
Caspase 9	Cell Signaling Technology	9504
Cleaved PARP (Asp214)	Cell Signaling Technology	9544
Bax	Cell Signaling Technology	2772

Bak	Cell Signaling Technology	3814
Bcl2	Cell Signaling Technology	2870
Bcl-XL	Cell Signaling Technology	2762
Bad	Cell Signaling Technology	9292
p-Bad S112	Cell Signaling Technology	9296
p-Bad S136	Cell Signaling Technology	9295
Clusterin	Santa Cruz Biotechnology	Sc-6419
Cytochrome c	Promega	G7421

MAPK pathway and growth factor signaling

Name	**Company**	**Catalogue number**
p-ERK1,2	Cell Signaling Technology	9101
ERK1,2	Cell Signaling Technology	4696
p-JNK (T183/Y185)	Cell Signaling Technology	9251
JNK1	Santa Cruz Biotechnology	Sc-1648
JNK2	Santa Cruz Biotechnology	Sc-7345
p-Akt S473	Cell Signaling Technology	4051
Akt	Cell Signaling Technology	9272
p-PDGFRa Y754	Cell Signaling Technology	2992
PDGFRa	Cell Signaling Technology	3164
p-PDGFRb Y751	Cell Signaling Technology	3166
PDGFRb	Cell Signaling Technology	3169

Epigenetic mediators

Name	**Company**	**Catalogue number**
HDAC 1	Cell Signaling Technology	2062
HDAC 2	Upstate	05-814
HDAC 3	Cell Signaling Technology	2632
HDAC 5	Cell Signaling Technology	2082
HDAC 6	Cell Signaling Technology	2162
HDAC 7	Cell Signaling Technology	2882

MeCP2	Upstate	07-013
mSin3A	Santa Cruz Biotechnology	Sc-994
CTCF	Upstate	07-729

Name	**Company**	**Catalogue number**
HSC70	Stressgen	SPA-816
Actin	Santa Cruz Biotechnology	Sc-1615
RCC1	BD biosciences	610377

Secondary antibodies

Name	**Company**	**Catalogue number**
Anti-mouse HRP-conjugated	Cell Signaling Technology	7076
Anti-rabbit HRP-conjugated	Cell Signaling Technology	7074
Anti-goat HRP-conjugated	Santa Cruz Biotechnology	Sc-2020

5.1.7 Inhibitors

- N-glycosylation inhibitor
  - Tunicamycin, Sigma
- PI3-Kinase inhibitor
  - Wortmannin, Sigma
  - LY294002, Calbiochem
- Proteasome inhibitor
  - MG132, Sigma
- RNA polymerase II inhibitor
  - Actinomycin D, Sigma
- HDAC inhibitors
  - Trichostatin A, Sigma
  - Sodium Butyrate, Sigma
- Protease inhibitor
  - Sigma

- Phosphatase inhibitors
    - Phosphatase inhibitor cocktail I, Sigma
    - Phosphatase inhibitor cocktail II, Sigma

5.1.8 Kits

- RNA extraction kit: RNeasy, Qiagen
- Genomic DNA extraction kit: blood and tissue extraction kit, Qiagen
- Plasmid purification kit: PureLink HiPure plasmid maxi kit, Invitrogen
- PCR purification kit, Qiagen
- Gel extraction kit, Qiagen
- Bisulfite treatment of genomic DNA: EpiTect Bisulfite kit, Qiagen
- LightShift Chemiluminescent EMSA kit, Pierce
- Dual luciferase assay system, Promega
- Mycoplasma PCR detection kit, PromoKine

5.1.9 Bacterial culture

- Bacteria strains used :
    - E.Coli DH5 alpha,
    - TOPO-10 (Invitrogen)
- TY medium composition: 1% Bacto-tryptone, 1% Bacto yeast extract, 0,1% Casamino acids, 5% NaCl
- Solid medium contains 2% (w/v) Agar
- Ampicillin: 100µg/ml,
- Kanamycin: 50µg/ml

5.1.10 General buffer and solutions

- PBS**:** 137 mM NaCl, 2.7 mM KCl, 6.5 mM Na2HPO4, 1.5 mM KH2PO4, pH 7.6
- TBE: 90 mM Tris-HCl, 90 mM Boric acid, 2.5 mM EDTA
- SDS running buffer: 25mM TrisBase, 250mM Glycine, 0.1% SDS
- TE**:** 10 mM Tris-HCl pH 8.0, 1 mM EDTA
- 10x DNA loading buffer: 0.25% (w/v) bromophenol blue, 0.25% (w/v) xylene cyanol FF, 30% (v/v) glycerol
- Laemmli sample buffer: SDS 2%, glycerol 10%, 50mM Tris pH 6.8, 5% b-mercaptoethanol, bromophenol blue

5.1.11 Cell culture

5.1.11.1 Cell types

- Mouse embryonic fibroblasts (MEFs) were isolated at embryonic day 8.5 and immortalized using the 3T3 protocol
  - Wild-type: clones 1, 7, 47
  - *Junb* $^{-/-}$ MEFs: clones 6, 10, 49
- HEK293T cells
- Phoenix ecotropic packaging cells: Orbigen, San Diego, USA

5.1.11.2 Cell culture material

DMEM (Dulbecco Modified Earle's Medium) high glucose	PAA, Pasching, Austria
Trypsin 2.5% (10x)	Lonza, Wuppertal
Fetal bovine serum	Sigma, Deisenhofen
Penicillin/streptomycin	PAA, Pasching, Austria
L-Glutamine 200mM (100x)	PAA, Pasching, Austria
Cell culture petri dishes	TPP, Trasadingen, CH

5.1.12 Animals

Mice were housed in specific pathogen free and light, temperature (21°C), and humidity (50%-60% relative humidity) controlled conditions. Food and water were available ad libitum. The procedures for performing animal experiments were in accordance with the principles and guidelines of the ATBW (officials for animal welfare) and were approved by the Regierungspräsidium Karlsruhe.

5.2 Methods

5.2.1 Bacterial methods

5.2.1.1 Transformation

Competent bacteria were incubated on ice with plasmid DNA (50-100ng) for 30 min, heat shocked at 42°C for 90 seconds and then replaced on ice for 2 min. After adding 1 ml of TY medium, the bacteria were incubated 1h at 37°C with shaking. Transformed bacteria were then further selected on a TY-Agar plate containing the appropriate antibiotics.

5.2.2 DNA methods

5.2.2.1 Plasmid mini-preparation and maxi-preparation

Transformed bacteria were grown overnight in 3 ml (mini-preparation) or 200 ml (maxi-preparation) of TY-medium supplemented with the appropriate antibiotics. For plasmid mini-preparation, bacteria were resuspended and lysed in the solution provided with the purification kit from Invitrogen. The DNA was further precipitated with 2.5 volumes of 100% EtOH (-20°C), washed with 1 volume 70% EtOH and resuspended in H_2O. For maxi-preparation, plasmid DNA was extracted with the purification kit from Invitrogen following the instruction of the manufacturer. DNA was resuspended in H_2O. Purity and concentration were measured with a NanoDrop spectrophotometer.

5.2.2.2 Isolation of genomic DNA

Genomic DNA from tissues was extracted using the following procedure. The tissue was digested in 500µl tail buffer (50mM Tris-HCl pH 8.0, 100mM NaCl, 100mM EDTA, 1% SDS) supplemented with 250µg of Proteinase K overnight at 56°C. Proteins were precipitated with 250µl 5M NaCl. Then, the DNA in the supernatant was precipitated with 0.67 volume of isopropanol, washed with 70% EtOH and resuspended in TE buffer.
For the analysis of DNA methylation, genomic DNA was extracted using the DNA blood and tissue extraction kit from Qiagen following the instructions of the manufacturer.

5.2.2.3 Cloning and sub-cloning

In order to clone a promoter region or a coding sequence, primers containing the restriction site of interest were designed. The PCR fragment was subsequently sub-cloned into the pGEMT-easy (Promega) or TOPO-pCR4 (Invitrogen) vectors and its sequence was confirmed by sequencing (MWG Biotech). 1 µg of the vector was digested with 3 units of the adequate restriction enzyme in the recommended buffer and further isolated by electrophoresis. The separated fragment of DNA was then isolated with the Gel extraction and Purification Kit from Qiagen following the instructions. Equimolar amounts of insert and vector (minimum 100ng) were ligated overnight at 4°C with 3 unit of T4 ligase following the instruction of the company.

5.2.2.4 PCR

A standard PCR reaction was performed as follows:

- 10-500 ng template DNA
- 2.5 µl 10 x PCR buffer recommended by the Taq provider
- 1 µl 25mM dNTP solution (containing dATP; dCTP; dGTP; dTTP; pH 7.0)
- 0.2 µl of each primer (0.1 µg/µl or 10µM)
- 1 U Taq polymerase
- H_20 to 25 µl

DNA was initially denatured for 5 min at 95°C. PCR was carried out with 20-40 cycles for each 30 sec at 95°C; 30 sec at the appropriate annealing temperature and 0.5-1.5 min extension at 72°C, depending on the length of DNA fragment to amplify.

5.2.3 RNA methods

5.2.3.1 RNA isolation

RNA was isolated from cultured cells with the RNeasy kit from Qiagen following the instruction of the manufacturer. RNA from tissues was extracted in PeqLab Gold RNA pure followed by a second purification over the columns of the RNeasy easy kit from Qiagen. Purity and concentration were measured with a NanoDrop spectrophotometer.

5.2.3.2 DNase digestion of RNA

In order to avoid genomic DNA contamination, 5 µg of RNA were digested with 1 unit of RQ1 RNase-free DNase for 30 min at 37°C in a final volume of 20 µl. RQ1 digested RNA was then purified following a phenol-chloroform extraction. In brief, 1/10 volume of 3M NaOAc (pH 5.2), one volume of phenol and one volume of chloroform:isoamyl alcohol (49:1) were added and mixed well. The mixture was centrifugated at 13 000 rpm at room temperature for 5 min. The upper phase containing the DNA was carefully taken and precipitated with 2.5 volumes of 100% ice-cold ethanol. After 2 h incubation at -20°C, the mixture was centrifugated at 4°C at 13 000 rpm for 30min. The supernatant was removed and the pellet washed with 70% ethanol. After another centrifugation, the pellet was dried and resuspended in RNase-free H_2O.

5.2.3.3 Reverse Transcriptase PCR (RT-PCR)

5 µg of RQ1-digested RNA was reverse transcribed into cDNA as follows

- 5 µg of RQ1-digested RNA denatured at 70°C for 5 min
- 1 µl of oligo-dT primers

- 10 µl of 5x reverse transcriptase buffer
- 2 µl of 25mM dNTP solution
- 2 µl of RNase inhibitors (Riboblock)
- 1 µl of reverse transcriptase
- In a final volume of 50 µl

The reaction was incubated at 42°C for 1 h followed by 10 min at 70°C in order to inactivate the reverse transcriptase. cDNA was further diluted and used for semi-quantitative or quantitative PCR. The amplified products were then analyzed on an agarose gel.

5.2.3.4 Quantitative RT-PCR

Relative quantification of PCR products was assessed as follows: PCR amplification was done in triplicates in a final volume of 25 µl by using a SYBR green mix. Primer efficiency was measured for each PCR run, by including dilution series of a reference cDNA. The primer efficiency was incorporated into the calculation of the fold induction as indicated hereafter.

$$\frac{Eff_{GOI}^{\,Ref(GOI) - Sample(GOI)}}{Eff_{HKG}^{\,Ref(HKG) - Sample(HKG)}} = \text{Fold Induction}$$

Eff = efficiency
GOI = gene of interest
HKG = house keeping gene
Ref = sample you set to 1
Sample = sample to be measured in reference to Ref

5.2.4 Protein methods

5.2.4.1 Cell extracts

5.2.4.1.1 Whole cell extracts

Cells were washed twice with PBS and lysed in RIPA (50mM Tris pH 8.0, 150mM NaCl, 0.1% SDS, 0.5% deoxycolic acid, 1% Nonidet P-40, 2mM DTT) or Cell Lysis buffer (Cell Signaling Technology). After 30 min incubation on ice, the extracts were briefly sonicated (2.5 min in a Bioruptor sonicator with an ON/OFF cycle of 30 sec / 20 sec) and centrifugated 20 min at 13'000 rpm at 4°C. The supernatant was collected and kept at -80°C.

5.2.4.1.2 Nuclear extracts

Cells were washed twice with PBS and collected in hypotonic buffer (20mM HEPES, 10mM KCl, 1mM MgCl2, 0.5mM DTT, 0.1% Triton X-100, 20% glycerol supplemented with proteases and phosphatases inhibitors). The cell membranes were destroyed by 18 strokes with a douncer. After centrifugation at 2'000 g for 5 min at 4°C, the supernatant containing the cytoplasmic fraction was collected. The pelleted nuclei were further lysed in extraction buffer (20mM HEPES, 10mM KCl, 1mM MgCl2, 0.5mM DTT, 0.1% Triton X-100, 20% glycerol, 420mM NaCl supplemented with proteases and phosphatases inhibitors) and nuclear membranes were destroyed by performing 5 freeze and thaw cycles. Debris were then removed by another centrifugation step at 13'000 rpm. The supernatant was collected and kept at -80°C.

In order to obtain nuclear extracts from animal tissues, the samples were pulverized by using a dismembrator. The powder was then resuspended in hypotonic buffer and the samples were processed as described before.

5.2.4.1.3 CHAPS extracts

Cells were washed twice with PBS and lysed in CHAPS buffer (Cell Signaling Technology). After 30 min incubation on ice, three freeze and thaw cycles were performed. The extracts were centrifugated 20 min at 13'000 rpm at 4C. The supernatant was collected and kept at -80°C.

5.2.4.1.4 Mitochondria extracts and Bax oligomerization

Cells were washed twice with PBS and lysed in hypotonic buffer (250mM sucrose, 20mM HEPES pH7.5, 10mM KCl, 1.5mM $MgCl_2$, 1mM EDTA, 1mM EGTA, supplemented with proteases and phosphatases inhibitors). The cytoplasmic fraction was incubated with 5mM Bismaleimidohexane (BMH) for 30min at RT or with DMSO. The cytoplasmic fraction was further centrifuged and the pellet, containing the mitochondrial fraction, was lysed into Laemmli buffer and boiled at 95°C for 5 minutes.

5.2.4.1.5 Protein concentration determination

The protein concentration of the samples was measured with the DC protein measurement kit from Biorad.

5.2.4.2 Western Blotting

20 to 50 µg of proteins were denatured into Laemmli sample buffer and boiled at 95°C for 5 min. Denatured protein were separated on a SDS-polyacrylamide gel (SDS-PAGE). Proteins

were transferred onto a nitrocellulose membrane overnight in a wet blotting system (25mM Glycine, 0.15% Ethanolamine, 25% MetOH) by application of 69 V. The membrane was then blocked against unspecific signal by incubation in 5% milk or BSA in PBS/0.1% Tween-20. The first antibody was incubated overnight at 4°C, and then the membrane was washed 3 times with PBS/0.1% Tween-20 and incubated for an hour with the secondary antibody. After 3 additional washes with PBS/0.1% Tween-20, the signal was revealed with an enhanced chemiluminescence system.

5.2.4.3 Luciferase

48 h after transfection cells were lysed in luciferase extraction buffer (100mM K-phosphate pH 7.6, 0.2% Triton X-100, and 1mM DTT) and incubated 15 min at room temperature. Measurement of luciferase activity was performed with the dual luciferase reporter assay system from Promega following the instructions of the manufacturer.

5.2.4.4 Electrophoretic Mobility Shift Assay (EMSA)

Non radioactive EMSA were performed according to the LightShift Chemiluminescent kit from Pierce. In brief, 5µg of nuclear extracts were incubated in binding buffer with 50ng polydI.dC and competitor DNA (unlabelled oligonucleotides) for 10 min at RT. 20 fmoles of 5' biotinylated primers encompassing the transcription binding site of interest were then added to the mixture and incubated 20 further min at RT. Each transcription factor requires a special binding buffer related to its biochemical properties. For AP-1, the binding buffer is composed of 10mM Tris pH 7.5, 50mM KCl, 10% glycerol, 5mM MgCl2, 0.5mM EDTA, 2mM DTT. For SP-1, the binding buffer is composed of 10mM Tris pH 7.5, 150mM KCl, 15% glycerol, 0.1 % NP-40, 15mM MgCl2, 0.1µM ZnCl2, 1mM DTT.

After incubation 20 min at RT, the complex was loaded on a 4% polyacrylamide gel previously pre-run for 1h. Migration was performed at 200V for 1h30 in 0.25% TBE buffer. Then, the probes were transferred in a wet blotting system in 0.5% TBE buffer at 500mA for 1h30 at 4°C. The DNA was further cross linked on the membrane by application of 1200µJoules in a UV cross linker. Detection of shifted probes was made by using a chemiluminescent system with streptavidin-HRP according to the manufacturer's instructions.

5.2.5 Epigenetics methods

5.2.5.1 Isolation of histones

Cells were washed twice with PBS and lysed in hypotonic buffer (20mM HEPES, 10mM KCl, 1mM $MgCl_2$, 0.5mM DTT, 0.1% Triton X-100, 20% glycerol supplemented with proteases, phosphates and HDAC inhibitors). Cells were disrupted by 18 strokes in a dounce homogenizer. The lysate was centrifugated at 2'000g for 5 min at 4°C and the supernatant transferred to another tube. The nuclear pellet was washed twice with hypotonic buffer and resuspended in 100 µl ice-cold H_2O. Sulfhydric acid (H_2SO_4) was added to a final concentration of 0.4N. After 1 hour incubation on ice, the sample was centrifugated at 13'000 rpm for 15 min at 4°C. The proteins of the supernatant including the histones were precipitated with 10 volumes acetone by overnight incubation at -20°C. After centrifugation at 13'000 rpm for 15 min at 4°C, the pellet was air dried and resuspended in H_2O. The purity of the histone preparation was assessed by SDS-PAGE followed by a Coomassie staining.

5.2.5.2 DNA methylation analysis: Combined Bisulphite Restriction Analysis (COBRA) and bisulphite sequencing

The bisulfite treatment of 2 µg of genomic DNA was performed with the EpiTect Bisulfite Kit from Qiagen following the instructions of the manufacturer. PCR amplification of the regions of interest was performed with PCR primers recognizing bisulfite converted DNA sequences. The primers were designed with the Methprimer software.

For COBRA analysis, the PCR fragments were digested with the restriction enzyme BstUI following the instruction of the provider. The fragments were separated by gel electrophoresis.

For bisulfite sequencing, the PCR fragments were cloned into the TOPO-pCR4 vector and sequencing of 5 to 10 mini-preparations of DNA were analyzed.

5.2.6 Immunoflorescence methods

5.2.6.1 Mitotracker / Cytochrome c staining

Cells, seeded on glass coverslips, were labeled *in vivo* 30 min with 200nM MitoTracker®, washed with PBS and fixed with 4% formaldehyde for 15 min. All steps were performed in the dark in order to avoid quenching of the fluorescent MitoTracker® dye. After 2 washes with PBS, cell membrane were permeabilized by incubation with 100% ice-cold Methanol at -

20°C for 20 min. Cells were further washed three times with PBS and unspecific signal was blocked with 1%BSA/PBS supplemented with 0.2% Tween 20 for 1 h. Coverslips were washed with PBS and incubated with cytochrome c antibody (diluted 1:1000 in PBS supplemented with 0.3% Triton X-100) overnight at 4°C. After 3 washes with PBS, cells were incubated with the secondary antibody (Alexa488-conjugated goat anti mouse diluted 1:500) and with Hoechst 33342 (diluted 1:1000) 1h at RT. After 3 additional washes, coverslip were mounted with mowiol on microscope slides.

5.2.7 Cell culture

5.2.7.1 Culture conditions

Mouse embryonic fibroblasts (MEFs) cells were cultivated in high glucose DMEM supplemented with 4mM glutamine and 10% FBS and were maintained at 37°C and 8% CO_2. Cells were trypsinised (0.25% Trypsin) three times a week. Mycoplasma tests (PromoKine mycoplasma PCR detection kit) were performed routinely.

5.2.7.2 Co-culture conditions

Cells were co-cultivated in a 0.4 µM filter insert (Falcon) placed above a six-well dish. Cells were seeded in equal density and were allowed to grow for 48h. Dishes were carefully shacked every 6 to 10h to obtain a homogenous growth factor distribution.

5.2.7.3 Transfection

5.2.7.3.1 Calcium phosphate transfection

50 µl of a solution of 1M of $CaCl_2$ was added to the appropriate amount of plasmid DNA diluted into 500 µl of H_2O. HBS 2x (50mM HEPES, 280mM NaCl, 1.5mM Na2HPO4, pH 7.05) was added drop by drop to the mixture while vortexing. The mixture was incubated 15 min in order to allow the calcium phosphate precipitate to form and subsequently added to a 10 cm diameter dish with semi-confluent cells. The precipitate was left on the cells for 24 hours, then the medium was replaced.

5.2.7.3.2 Transfection with Fugene

Plasmid DNA and Fugene were added to DMEM in a ratio of 1: 2.5. The mixture was incubated for 15 min at RT and added to semi-confluent cells. 24 h later, the medium was replaced with fresh medium.

5.2.7.4 Retroviral and lentiviral Transduction

In order to produce retrovirus, a 10cm diameter dish of ecotropic Phoenix packaging cells was transfected with 25 µg of the vector of interest. One day after transfection, the medium was replaced by 6 ml of fresh medium. After 48h, the supernatant containing the virus particles was filtrated through a 0.45 µm filter and supplemented with 8µg/µl polybrene, before being added to the transduced cells. After 24h incubation, the cells were passaged and further analyzed. For lentivirus production, the same procedure was applied in HEK293T cells by co-transfection of plasmids encoding gag-pol (pMDLgrpRRE), VSV-g (pMD2-G) and Rev (pRSVrev).

5.2.8 FACS analysis

5.2.8.1 AnnexinV staining

Cells, treated with different drugs for the appropriate time, were trypsinised and resuspended in 100 µl of AnnexinV buffer (10mM Hepes/NaOH pH 7.4, 150mM NaCl, 5mM KCl, 1mM MgCl2, 1.8 mM CaCl2). Cells were incubated with 2 µl AnnexinV APC for 30 min on ice in the dark, then washed and AnnexinV incorporation was measured by fluorescent activated cell sorting (FACS) with a FACS Calibur.

6 Results

6.1 Junb as a positive and negative transcription regulator

6.1.1 Analysis of histone H3 acetylation marks

Gene activation has been correlated with an increased acetylation of the promoter region (Marushige, 1976). In order to investigate whether the observed gene de-repression in the absence of Junb is due to an increase in global histone acetylation, I analyzed the levels of acetylated histone H3 in wild-type and Junb-deficient cells. Therefore, I isolated histones from cells treated with Trichostatin A (TsA), a large spectrum HDAC inhibitor, or with vehicle (DMSO) and subsequently determined levels of acetylation on 3 different lysines (K9, K18 and K27) of the N terminal tail of histone H3 by immunoblot. As shown in Figure 3, no significant increase in acetylation could be observed in unchallenged Junb-deficient MEFs when compared to wild-type cell. Treatment with TsA for 4 and 12h lead to similar increased levels of acetylation of histone H3 on the lysines 9, 18 and 27 for both wild-type and *Junb* $^{-/-}$ MEFs. Thus, loss of Junb does not result in a global hyperacetylation of histone H3.

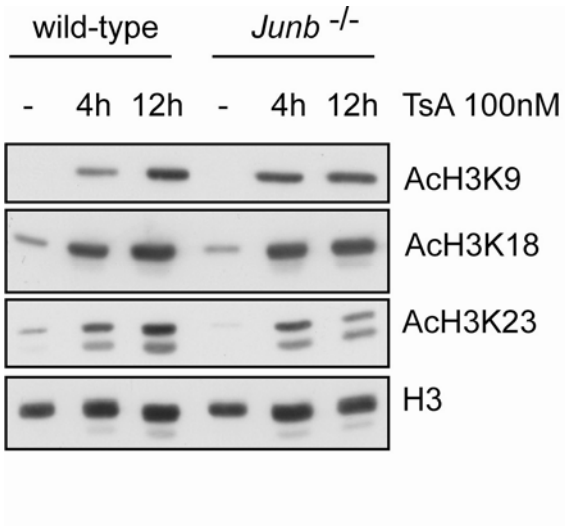

Figure 3: Histone 3 acetylation status is not altered in MEFs lacking Junb. Wild-type and Junb-deficient MEFs were treated with 100nM TsA for 4 and 12h or with vehicle (-). Histones were isolated and acetylation status of Histone 3 (H3) was monitored by immunoblot analysis using antibodies recognizing acetylated Histone 3 on Lysine 9 (AcH3K9), on Lysine 18 (AcH3K18) and on Lysine 23 (AcH3K23). Immunoblot with antibody against total H3 served as control for equal loading and quality of extracts.

6.1.2 Analysis of HDACs expression

Within the last years, it became clear that histone acetylation is also located outside of coding sequences and is very important for the stability of the genome (Kouzarides, 2007). Thus, promoter hyperacetylation of a subset of genes, namely the Junb targets, could not be detected on total histone extracts. Further analyses, such as the determination of expression levels of enzymes that remove histone acetylation, HDACs, would be required to monitor

global differences in acetylation distribution. In order to analyze whether an impaired expression of HDACs would be causative of the observed gene de-repression, we determined HDACs protein levels in wild-type and Junb-deficient MEFs. Immunoblot analysis of nuclear protein fractions revealed no difference in the expression and localization of HDACs 1, 2, 3, 5, 6 and 7 between wild-type and Junb-deficient MEFs (Fig. 4).

Since HDACs require co-repressor complexes to be targeted to promoter regions, I also measured protein levels and localization of the co-repressor complexes mSin3A and MeCP2 by immunoblotting. Similar mSin3A levels were observed for wild-type and Junb-deficient MEFs (Fig. 4). Protein expression and localization of MeCP2, that binds to methylated CpGs and targets HDACs to DNA methylated promoter regions, was also not altered in Junb-deficient MEFs when compared to wild-type cells (Fig. 4).

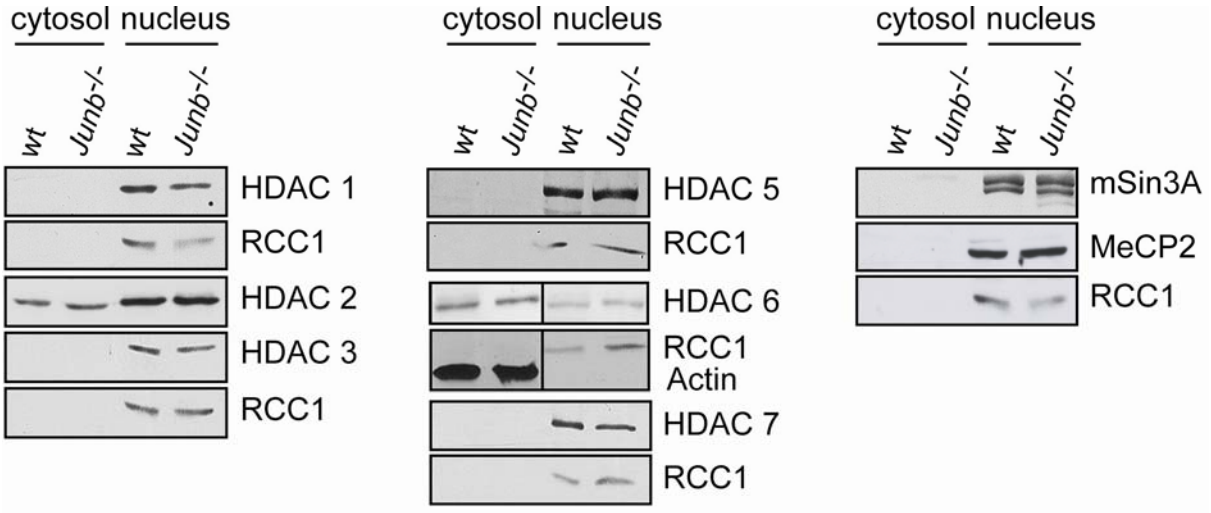

Figure 4: Wild-type and Junb-deficient MEFs show no difference in protein expression of HDACs and co-repressor molecules. Immunoblot analysis of 50 μg of nuclear and cytoplasmic extracts using specific antibodies against HDAC 1, 2, 3, 5, 6, 7, mSin3A and MeCP2, respectively. RCC1 and Actin served as control for equal quality and quantity of loaded nuclear and cytoplasmic proteins, respectively.

In conclusion, levels of HDACs, mSin3A and MeCP2 are unaffected in Junb-deficient MEFs.

6.1.3 Analysis of transcription induction by HDAC inhibition

Although, no apparent differences in HDACs, mSin3A and MeCP2 levels were detected, it still may be feasible that the promoters of previously identified Junb repressed genes were regulated by HDACs. In order to prove that, I measured by qRT-PCR the induction of Junb-repressed mRNA transcripts in response to HDAC inhibition. In order to avoid any unspecific

effects of HDAC inhibitors, MEFs were treated with two different inhibitors covering a broad spectrum of HDACs: TsA and Sodium Butyrate (NaB).

MEFs were treated for 24h with TsA (100nM) and NaB (10mM) applying doses that induce similar levels of H3 acetylation (H3K9Ac; Fig. 5A). Immunoblot analysis of nuclear extracts revealed that Junb is not induced upon 24h treatment with TsA and NaB (Fig. 5B).

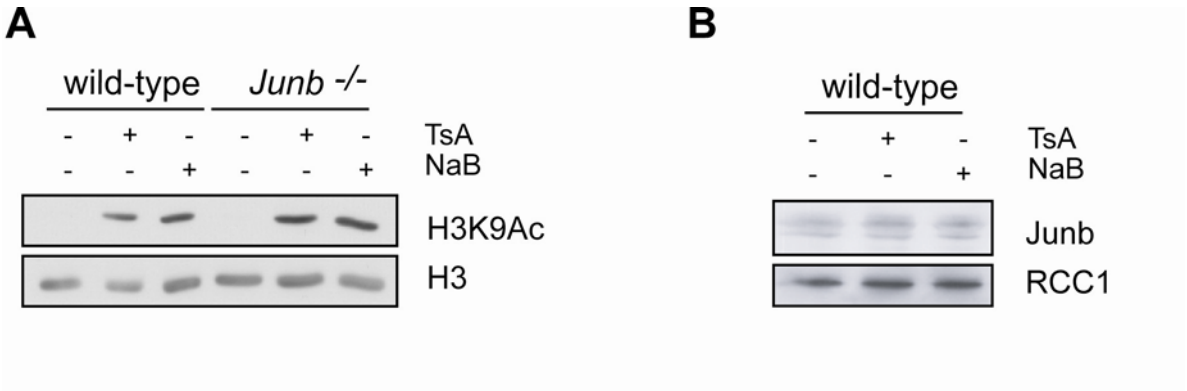

Figure 5: Treatment of wild-type and Junb-deficient MEFs with the HDAC inhibitors TsA and NaB efficiently induces acetylation of Histone 3 most likely independently of Junb. (A). MEFs were treated with the HDAC inhibitors TsA (100nM) and NaB (10mM) or with vehicle (-) for 24h. Histones were isolated and acetylation of Histone 3 on Lysine 9 (H3K9Ac) was monitored by immunoblotting (B). Nuclear extracts were prepared and Junb levels were analyzed by immunoblotting. Histone 3 (H3) and RCC1 served as control for equal quality and quantity of loaded histone and nuclear extracts, respectively.

Then, MEFs were subjected to the HDAC inhibitor treatments as described and RNA was extracted. qRT-PCR was performed for all Junb-repressed target genes which have been identified in previous transcription profiling arrays (Florin et al., 2004). Four different classes of genes could be identified. First, I could identify genes induced by both HDAC inhibitors in wild-type as well as in Junb-deficient MEFs (Fig. 6). This class comprised the following genes: *lipoprotein lipase* (*lpl*), *clusterin* (*clu*), *mapk phosphatase 1* (*mkp1*), *SUMO1 activating enzyme subunit 2* (*sae2*) as well as *solute carrier family 35 member E3* (*slc35e3*).

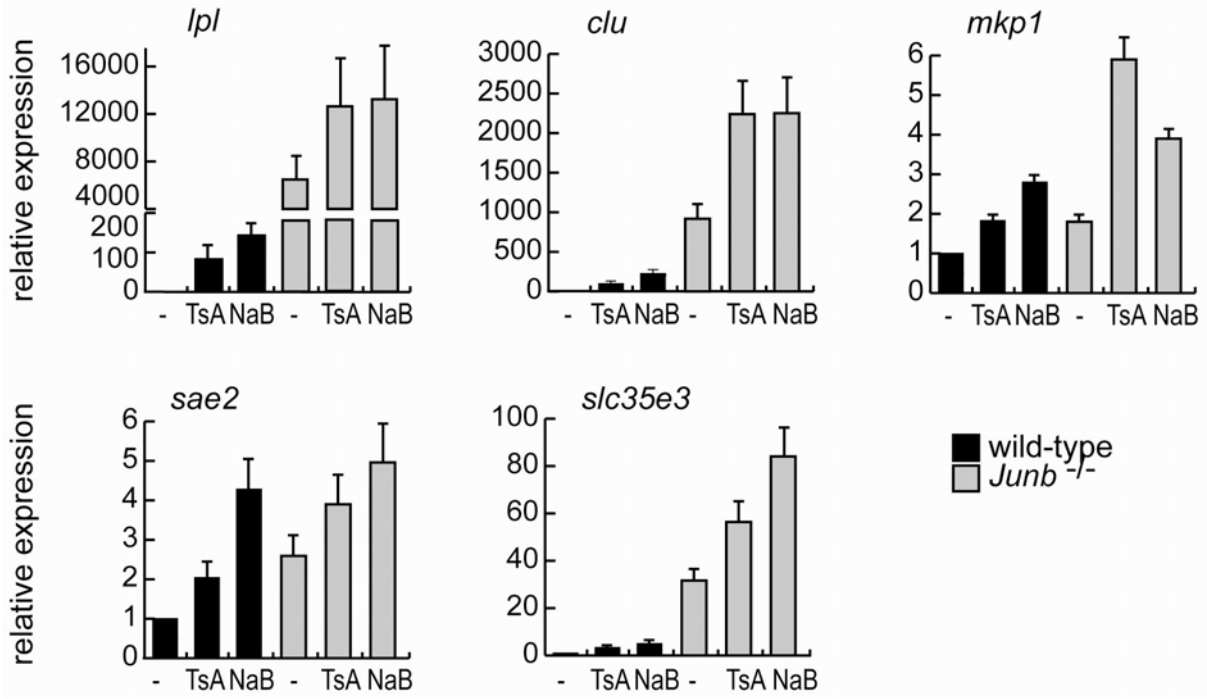

Figure 6: Genes upregulated in both wild-type and *Junb* $^{-/-}$ MEFs upon treatment with HDAC inhibitors. MEFs were treated with the HDAC inhibitors TsA (100nM), NaB (10mM) or with vehicle (-) for 24h and RNAs were extracted. qRT-PCR was performed with specific primers recognizing *lipoprotein lipase* (*lpl*), *clusterin* (*clu*), *mapk phosphatase 1* (*mkp1*), *SUMO1 activating enzyme subunit 2* (*sae2*) and *solute carrier family 35, member E3* (*slc35e3*), as indicated on top of graphs. Relative expressions of three independent experiments are given. *Hprt* was used as housekeeping gene for normalization.

Secondly, I could define genes that were only induced in wild-type MEFs (Fig. 7). These genes were encoding for *glutathione S-transferase alpha 4* (*gsta4*), *erythrocyte protein band 4.1-like 4b* (*epb4.1l4b*) and *inhibitor of DNA binding 1* (*id1*).

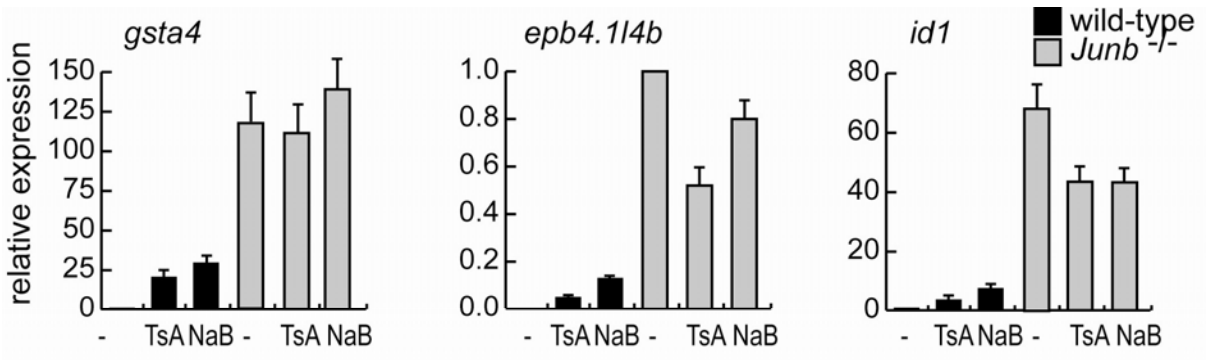

Figure 7: Genes solely upregulated in wild-type MEFs upon treatment with HDAC inhibitors. MEFs were treated with the HDAC inhibitors TsA (100nM), NaB (10mM) or with vehicle (-) for 24h and RNAs were extracted. qRT-PCR was performed with primers recognizing *glutathione S-transferase alpha 4* (*gsta4*), *erythrocyte protein band 4.1-like 4b* (*epb4.1l4b*) and *inhibitor of DNA binding 1* (*id1*), as indicated on top of graphs. Relative expressions of three independent experiments are given. *Hprt* was used as housekeeping gene for normalization.

Furthermore, expression of many genes did not change upon treatment with TsA or NaB (Fig. 8A). These genes were *78 kDa glucose-regulated protein* (*grp78*), *decorin*, *cytochrome b-245 alpha polypeptide* (*cyba*), *WD repeat domain 79* (*wdr79*) as well as *Fas*. Finally, the expression of few genes such as *inhibitor of DNA binding 3* (*id3*) and *keratinocyte growth factor* (*kgf*) was decreased due to TsA and NaB treatments (Fig. 8B).

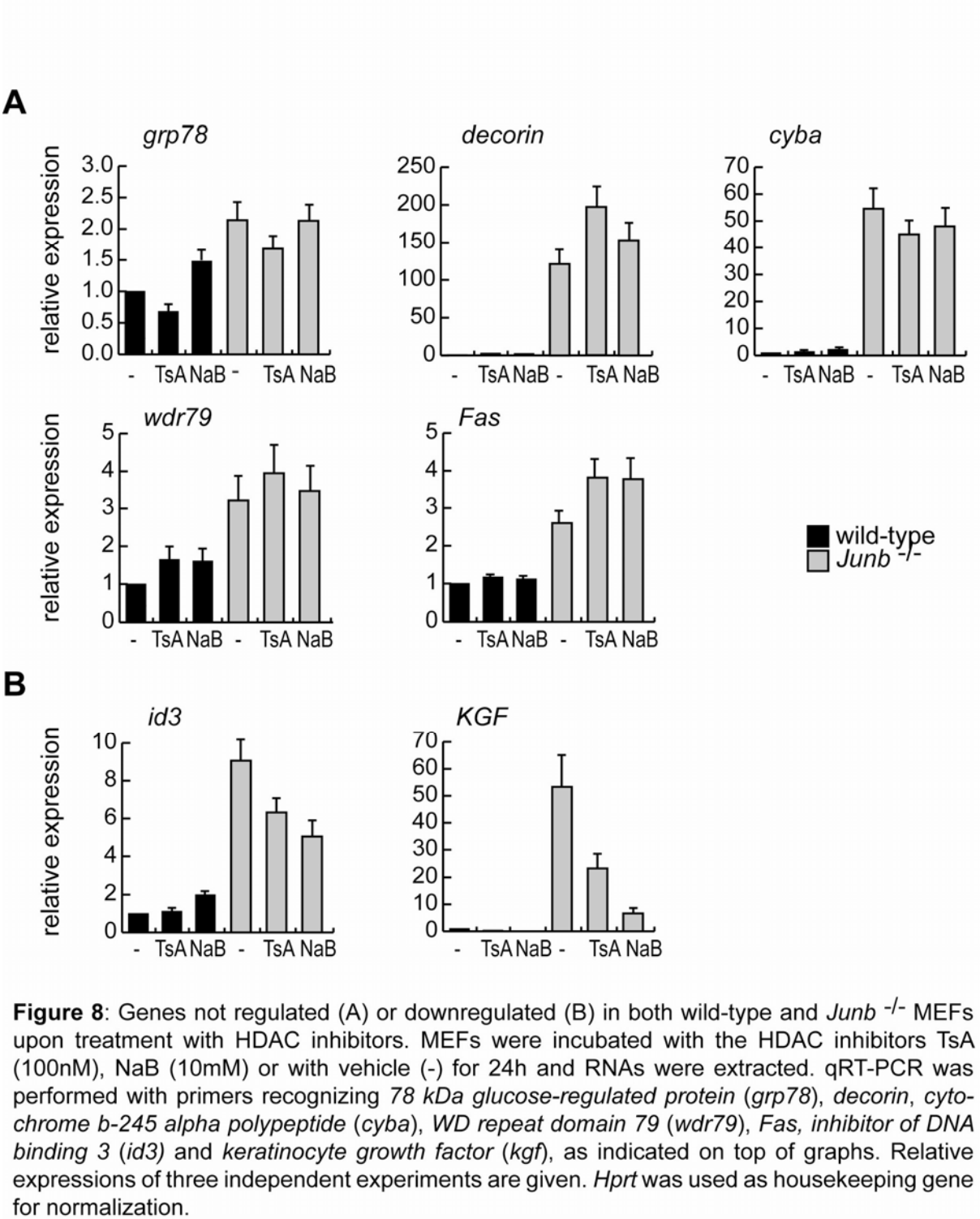

Figure 8: Genes not regulated (A) or downregulated (B) in both wild-type and *Junb* $^{-/-}$ MEFs upon treatment with HDAC inhibitors. MEFs were incubated with the HDAC inhibitors TsA (100nM), NaB (10mM) or with vehicle (-) for 24h and RNAs were extracted. qRT-PCR was performed with primers recognizing *78 kDa glucose-regulated protein* (*grp78*), *decorin*, *cytochrome b-245 alpha polypeptide* (*cyba*), *WD repeat domain 79* (*wdr79*), *Fas, inhibitor of DNA binding 3* (*id3)* and *keratinocyte growth factor* (*kgf*), as indicated on top of graphs. Relative expressions of three independent experiments are given. *Hprt* was used as housekeeping gene for normalization.

Taken together, this approach identified a subset of Junb-target genes that are regulated by HDACs in wild-type and Junb knock-out MEFs. Among those genes, *gsta4*, *epb4.1l4b and id1* are of particular interest since they are induced by HDAC inhibitors only in wild-type cells, suggesting that these genes may be regulated through yet to be identified Junb-dependent HDACs mechanism.

6.1.4 H19, a novel Junb target gene

The *H19* transcript has been identified as the most highly up-regulated gene in Junb-deficient MEFs by previous transcription profiling array (Florin et al., 2004). This could be validated by semi-quantitative RT-PCR (Fig. 9A) demonstrating that *H19* transcripts were highly increased in *Junb* $^{-/-}$ cells. De-repression was truly Junb-dependent as re-expression of Junb in null cell upon retroviral transduction reduced *H19* transcripts to levels observed in wild-type cells. This confirms that *H19* is a novel Junb-target gene.

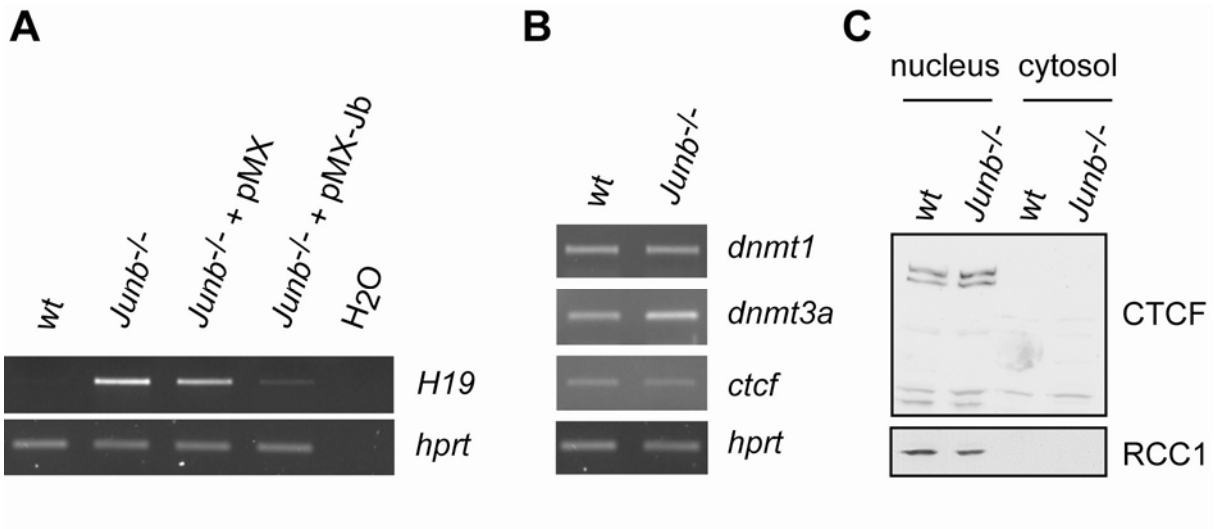

Figure 9: Junb represses *H19* expression independently of dnmt1, dnmt3a and CTCF. (A) Increased *H19* expression in Junb-deficient MEFs that can be suppressed again by re-expression of Junb as assessed by semi-quantitative RT-PCR. In order to re-express Junb, -/- cells were stably transduced with a retrovirus encoding Junb. (B) *Junb*$^{-/-}$ show no difference in the expression of *dnmt1*, *dnmt3a* and *ctcf* when compared to wild-type MEFs as analyzed by RT-PCR. *hprt* was used to monitor equal cDNA concentration. (C) CTCF protein levels are similar between wt and *Junb*$^{-/-}$ MEFs as measured by immunoblot of nuclear extracts. RCC1 served as control to ensure equal quality and loading of nuclear proteins.

In order to investigate whether an impaired expression of *H19* regulators may be causative for the enhanced transcript levels of *H19* in Junb-deficient MEFs, I analyzed the expression of *dnmt1*, *dnmt3a* and *ctcf* by RT-PCR. Yet, wild-type and Junb-deficient MEFs expressed *dnmt1*, *dnmt3a* and *ctcf* transcripts at similar levels (Fig. 9B). In line with these findings,

CTCF protein levels were also unaffected in Junb-deficient MEFs as shown by immunoblot of nuclear extracts (Fig. 9C), while the expression of DNMT1 and DNMT3a proteins could not be detected by immunoblot, most likely due to very low expression levels (data not shown). Thus, Junb regulates *H19* transcription but not the expression of factors involved in the setting and maintenance of the imprinting status of this gene.

6.1.5 Junb regulates the methylation of the H19 imprinting domain

Since CTCF binds only to its unmethylated DNA recognition sequence, loss of methylation of the imprinting domain of *H19* would increase the binding of CTCF, enhance the activity of the downstream enhancer on *H19* promoter and result in increased gene expression.

I, therefore, analyzed the methylation status of the CTCF binding sites within the *H19* imprinting domain in wild-type and Junb-deficient MEFs. For this propose, I isolated genomic DNA from wild-type and *Junb*$^{-/-}$ MEFs and subsequently treated the DNA with bisulfite. Treatment of DNA with bisulfite converts cytosine to uracil residues, but leaves 5-methylcytosine residues unaffected, thus allowing us to discriminate between methylated and unmethylated cytosines.

First, I analyzed the methylation status of the imprinted region encompassing the CTCF recognition sites by Combined Bisulfite Restriction Analysis (COBRA). During the course of this method, the regions of interest were amplified by PCR and the amplicons were digested with BstUI, a restriction enzyme containing the dinucleotide CG within its restriction site. By the bisulfite treatment, unmethylated cytosines were converted to uracil, leading to the loss of the BstUI restriction site. Thus, observation of an undigested PCR product is reminiscent of absence of DNA methylation and a digested PCR product is a sign for the presence of DNA methylation. Only the 1st, 3rd and 4th CTCF sites could be analyzed by COBRA since the 2nd CTCF site did not fulfill the necessary prerequisite of containing a BstUI restriction site (Fig. 10A). While wild-type MEFs displayed approximately a 1:1 ratio of unmethylated and methylated CTCF sites (Fig. 10B), *Junb* $^{-/-}$ MEFs showed significantly elevated amounts of unmethylated amplicons for all three CTCF sites (Fig. 10B).

Secondly, in order to analyze the methylation status of each individual cytosine located in the region of interest, bisulfite sequencing experiments were carried out for the 2nd and 4th CTCF site. The bisulfite sequencing revealed for the wild-type cells that 100% of the PCR amplicons covering both CTCF sites were methylated (Fig. 10C). By contrast, a significant increase of unmethylated cytosines (represented by empty circles) was observed in Junb-deficient MEFs. Interestingly, the CTCF site number 2 displayed loss of methylation only in

the CTCF consensus sequence, while the 4th CTCF binding site displayed loss of methylation on a wide region encompassing the consensus sequence (Fig. 10C).

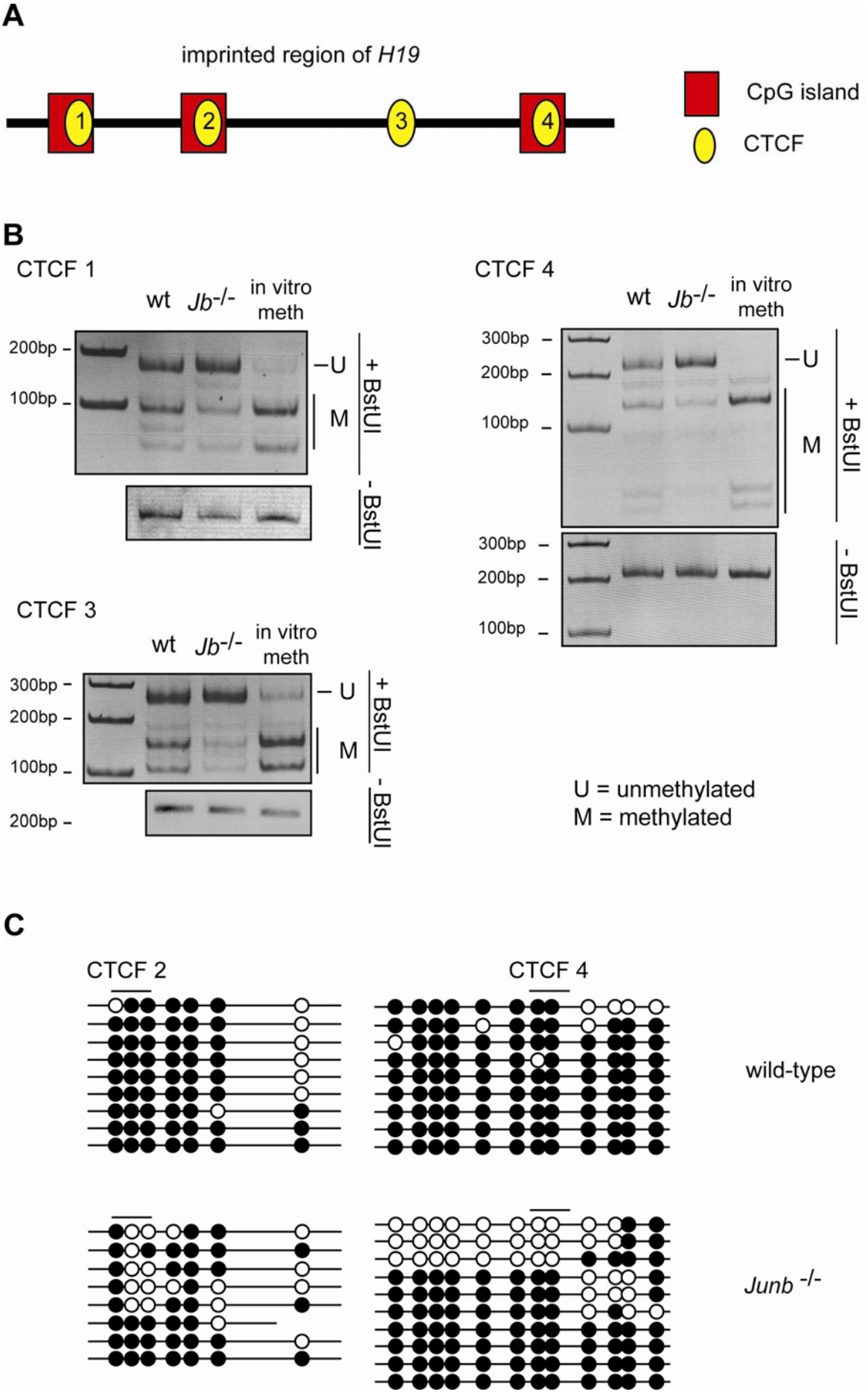
A
imprinted region of H19
1
2
3
4
CpG island
CTCF
B
CTCF 1
wt
Jb-/-
in vitro meth
200bp
100bp
U
M
+ BstUI
- BstUI
CTCF 4
300bp
200bp
100bp
CTCF 3
U = unmethylated
M = methylated
C
CTCF 2
CTCF 4
wild-type
Junb -/-

Figure 10: Methylation of CTCF binding sites within the imprinted region of *H19* is lost in Junb-deficient MEFs. (A) Schematic representation of the imprinted domain of *H19*. Red blocks represent CpG islands and yellow circles the four CTCF binding sites. (B) Genomic DNA of wild-type and *Junb* $^{-/-}$ MEFs was isolated and treated with bisulfite. PCR amplification of the 1st, 3rd and 4th CTCF sites was performed using primers that recognize bisulfite treated DNA. The PCR fragments were digested with the restriction enzyme BstUI and analyzed on a polyacrylamide gel. The PCR fragments incubated without BstUI served as control for equal PCR amplification and loading. An *in vitro* methylated sample was included as positive control in all analyses. Treatment of DNA with bisulfite converts cytosine residues to uracil, but leaves 5-methylcytosine residues unaffected. Thus, a BstUI recognition site containing meythlated cytosines remains while one harboring unmethlyated cytosines is upon bisulfite treatment no longer restricted. U: unmethylated, M: methylated. (C) Loss of methylation at the 2nd and 4th CTCF binding site within the imprinted region of *H19*. Genomic DNA of wild-type and *Junb* $^{-/-}$ MEFs was isolated and treated with bisulfite. PCR amplification of the 2nd and 4th CTCF site as described in B. PCR fragments were subcloned, DNA of 8-10 individual clones was prepared and subsequently sequenced. Methylated CpG islands remain upon bisulfite sequencing as CG sequence and are represented by a black circle. Unmethylated CpG are converted by bisulfite treatment to UpGs and are given in the graph as open circles.

Taken together, these analyses revealed that methylation at the four CTCF binding sites is impaired or lost in Junb-deficient MEFs and that the molecular mechanisms regulating the methylation status of each CTCF site may be different.

6.2 Junb is a novel decision maker for death or survival

6.2.1 Junb is induced in response to ER stress

To investigate whether Junb is causally implicated in the ER stress response, I analyzed the expression of Junb in wild-type and Junb-deficient MEFs following Tunicamycin application. Tunicamycin (Tm), a nucleoside antibiotic that inhibits the enzyme N-acetylglucosamine phosphotransferase blocks the synthesis of all N-linked glycoproteins and, thereby, causes ER stress. Tm treatment of wild-type cells resulted in a significant induction of *Junb* mRNA transcripts already 15, 30, and 45 minutes (data not shown) but with a maximum at 1 and 4 h post Tm application as measured by qRT-PCR (Fig. 11A). Analysis of Junb protein levels revealed a rapid upregulation of Junb starting 10 min post treatment, with a peak at 4 to 8 h and a decline to basal levels 24 h post treatment. No Junb protein was detectable in Junb-deficient MEFs (Fig. 11B).

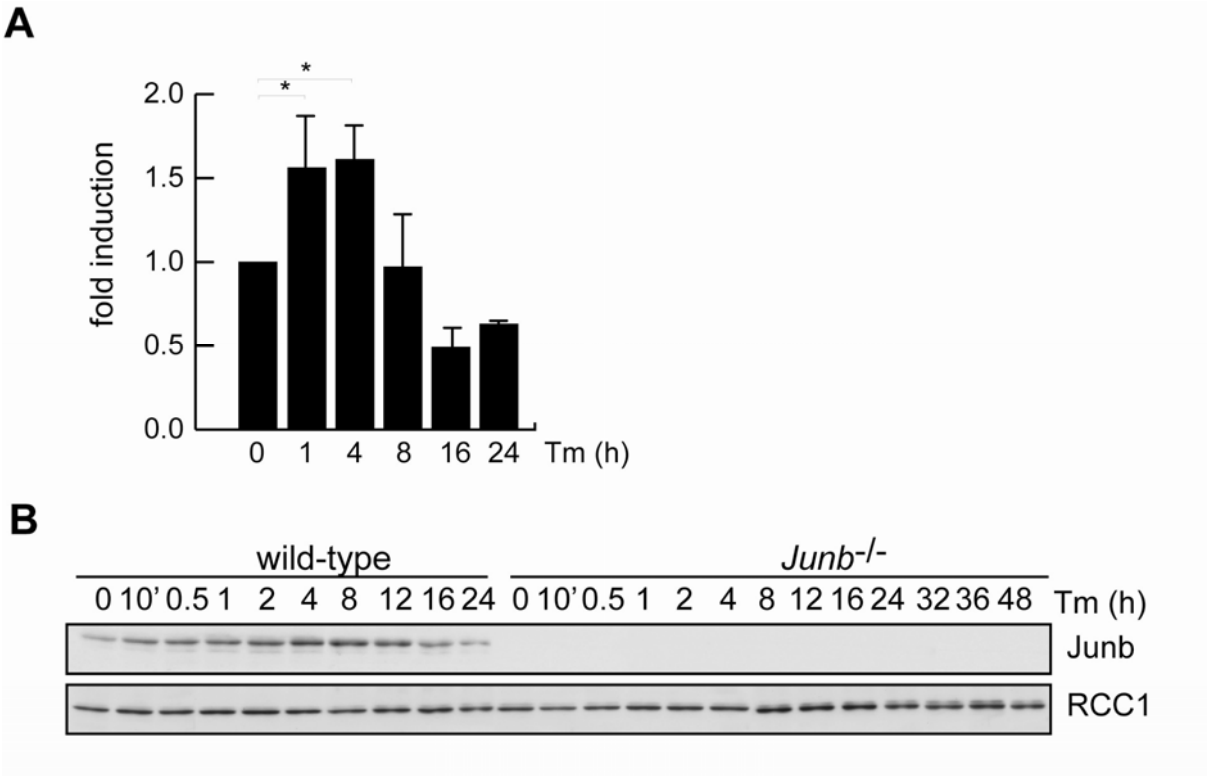

Figure 11: Junb is induced in response to Tm. (A) qRT-PCR analysis of wild-type and *Junb* $^{-/-}$ MEF treated with Tm (5μg/ml) for the indicated time points. *Hprt* was used as housekeeping gene. Relative gene expression is given. *: $p<0.05$ according to Student's t-test. (B) Immunoblot analysis of nuclear extracts of wild-type and *Junb* $^{-/-}$ MEFs treated with Tm (5μg/ml) for the indicated time points. RCC1 was used to ensure equal quality and loading of nuclear extracts.

6.2.2 Loss of Junb results in increased expression of ER-located chaperones and to minor changes in UPR

To investigate the role of Junb in ER stress, we monitored the expression of ER-located chaperones and UPR signaling molecules in Tm-treated wild-type and Junb-deficient MEFs. ER-located chaperones and enzymes, such as Grp78, Grp94 and Oxidoreductin-like 1, are essential for protein folding in the ER and are good markers of ER steady state and ER stress. Thus, I analyzed their mRNA expression in unchallenged as well as in Tm-treated MEFs (Fig. 12). qRT-PCR analyses revealed that untreated Junb-deficient MEFs harbored significantly increased endogenous levels of *grp78*, *grp94* and *oxidoreductin-like 1*. Furthermore, treatment with Tm induced expression of all three chaperone mRNAs both in wild-type and *Junb*$^{-/-}$ MEFs. While mRNA transcripts levels were comparable between wild-type and *Junb*$^{-/-}$ cells 4 and 8 h post Tm application, transcripts levels of all three chaperones were significantly increased in Junb-deficient MEFs 16 h post treatment (Fig. 12).

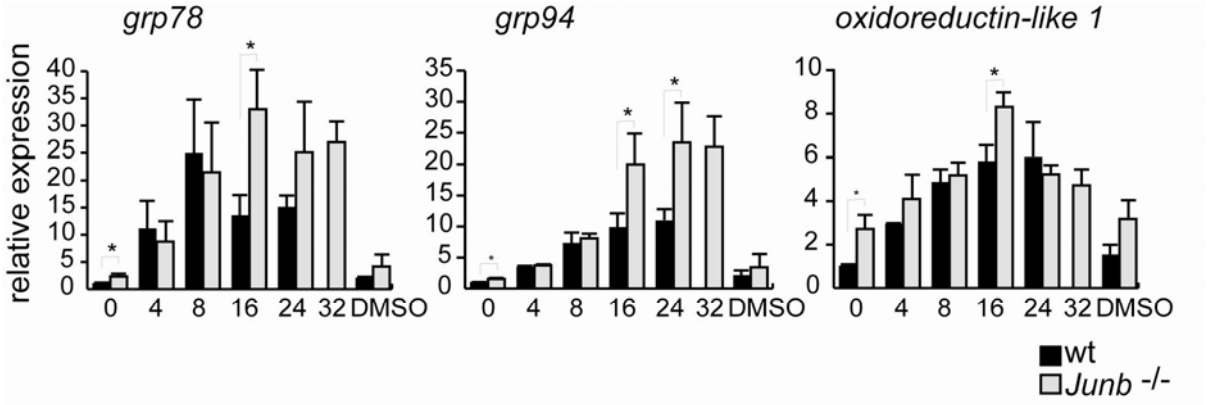

Figure 12: Increased transcript levels of ER-located chaperones in Junb-deficient MEFs: Wild-type (wt) and Junb-deficient MEFs were treated with Tm for the indicated time points (h) or with vehicle (dmso, 32h) and total RNA was extracted. qRT-PCR was performed with primers specific for *grp78*, *grp94* and *oxidoreductin-like 1*, as indicated on top of graphs. Relative expression is given. * : p <0.05 according to Student's t-test.

Furthermore, analysis of Grp78 protein revealed for Junb-deficient MEFs a delayed induction kinetics. While, in wild-type cells, Grp78 protein was already induced 4 h post treatment and reached its maximum levels at 8 h lasting until 24 h post induction, Grp78 protein in Junb-deficient cells was only induced at 8 h with its maximum at 16 to 48 h post Tm application (Fig. 13A). A major event in the Grp78-triggered signaling of the UPR is the processing of Xbp1. In both wild-type and Junb-deficient MEFs, processed Xbp1 (Xbp1s) was detected 4 h post Tm treatment (Fig. 13B). Yet, kinetics and extent of Xbp1 processing appeared to be slightly different for *Junb*$^{-/-}$ MEFs with enhanced levels of spliced Xbp1s found 4 and 8 h post Tm treatment. To monitor PERK signaling, phosphorylation of eIF2α was determined. Phosphorylated eIF2α was already detected in unchallenged Junb-deficient MEFs (Fig. 13C). In response to Tm application, a further increase in phospho-eIF2α was found in Junb-deficient MEFs, yet, the kinetics of induction was slightly delayed in comparison to wild-type cells. Finally, expression of the UPR-induced pro-apoptotic transcription factor CHOP was monitored. CHOP protein was induced in both wild-type and Junb-deficient MEFs with a maximal induction 16 h post Tm treatment (Fig. 13D). While the kinetics of CHOP induction was similar, total amount of CHOP protein was slightly diminished in *Junb*$^{-/-}$ cells.

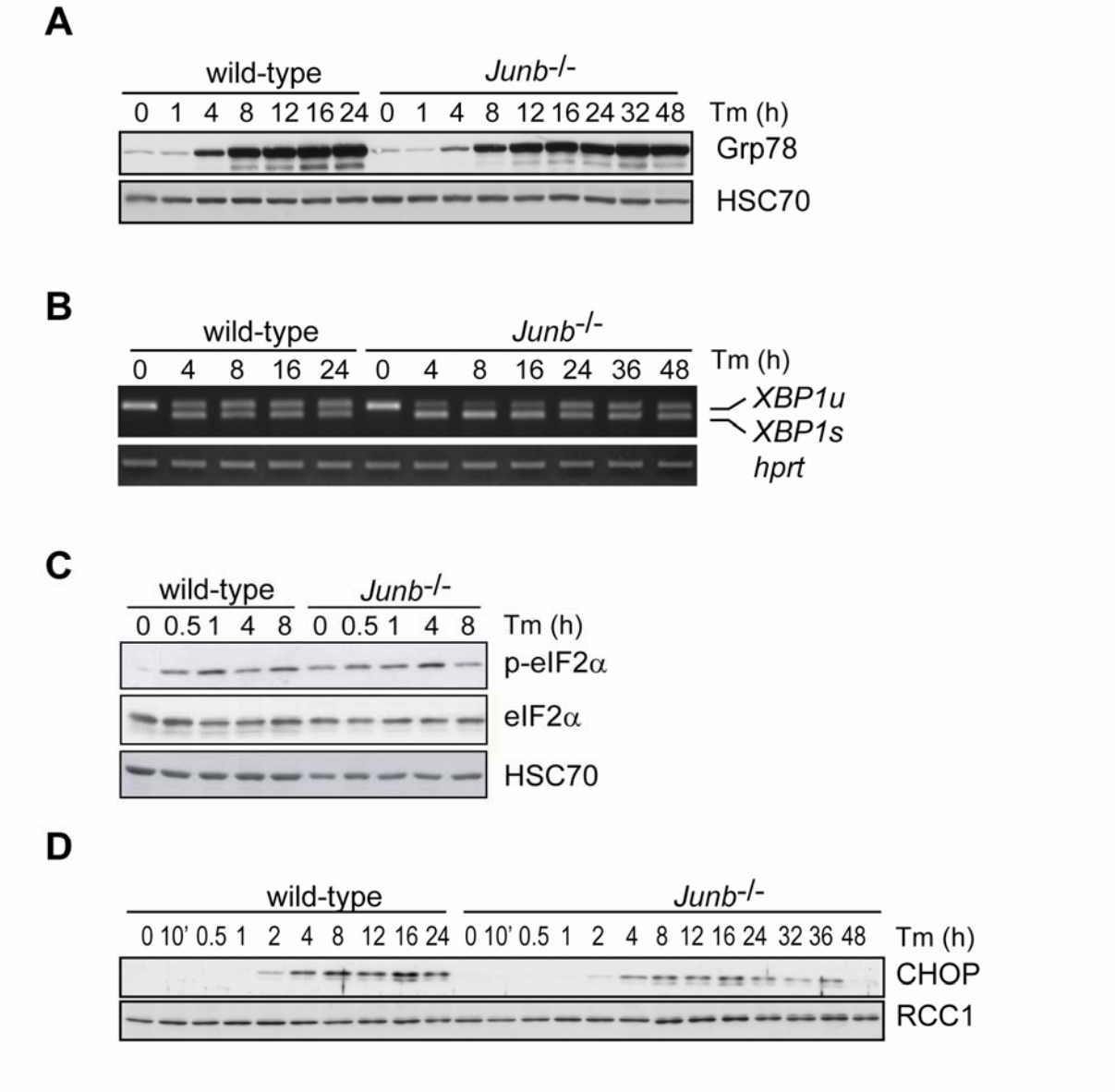

Figure 13: Junb-deficient MEFs show UPR upon Tm treatment but display minor differences when compared to wild-type. (A) Slightly delayed induction of Grp78 was seen by immunoblot using 20µg of whole cell extracts. (B) Increased splicing of XBP1 was assessed by RT-PCR using primers that discriminate between unspliced (*XBP1u*) and spliced (*XBP1s*) XBP1 variants. *hprt* was used to control equal cDNA concentration. (C) Induction of phosphorylation of eIF2α was assessed by immunoblotting of whole cell extracts (20µg) with an antibody recognizing phosphorylated eIF2α. (D) Kinetics of CHOP induction was monitored by immunoblot using 50 µg of nuclear extracts. HSC70 and RCC1 served as control for equal quality and quantity of loaded proteins.

In summary, unchallenged Junb-deficient cells show somewhat elevated chaperone expression being reminiscent of endogenous ER stress, however, *Junb*$^{-/-}$ cells are still able respond to the ER stress inducing agent Tm by initiating UPR signaling.

6.2.3 Junb deficiency renders cells resistant toward stress-induced apoptosis

Sustained ER stress leads to the induction of cell death (Szegezdi et al., 2006). To determine the apoptosis rate in response to prolonged Tm treatment, wild-type and Junb-deficient MEFs were stained by AnnexinV and subsequently analyzed by flow cytometry (Fig. 14). No obvious differences in the rate of spontaneous apoptosis could be observed in cells left untreated. 40% of wild-type cells were AnnexinV-positive 24 h post treatment with Tm. By contrast, only 12% of Junb-deficient MEFs were positively stained for Annexin V. In order to determine whether MEFs were resistant towards ER stress-mediated apoptosis or whether they harbored a general apoptosis defect, MEFs were treated with stress stimuli such as proteasomal inhibitor (MG132) and UV. While MG132 and UV treatment induced 60% and 40% AnnexinV positive cells, respectively, in wild-type MEFs, Junb knock-out cells were resistant towards both stresses displaying only 15% cells positively stained for AnnexinV. Importantly, treatment of both wild-type and *Junb*$^{-/-}$ with vehicle (DMSO) did not induce any significant cell death. Moreover, Junb-deficient MEFs were hypersensitive in response to a low dose of CD95L that efficiently induced apoptosis in these cells as evidenced by more than 40% AnnexinV positive cells, while wild-type cells were not responsive (10% positive cells).

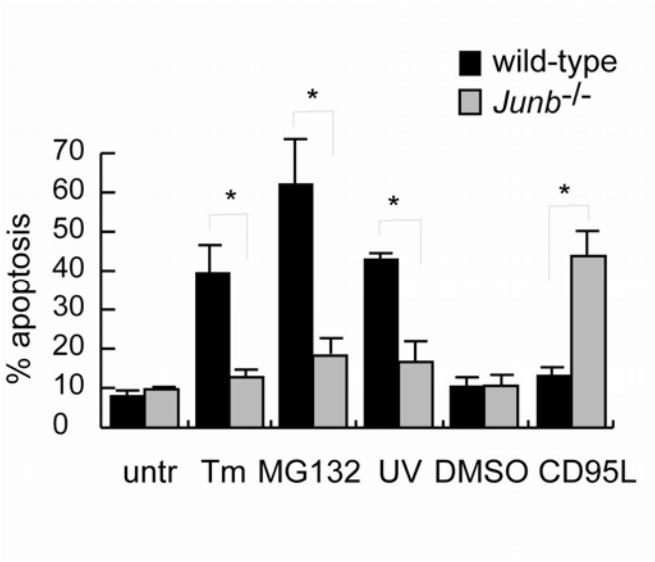

Figure 14: Loss of Junb confers resistance toward stress stimuli-induced apoptosis. Wild-type and Junb-deficient MEFs were treated with Tm (5µg/ml, 24h), proteasome inhibitor MG132 (5µM, 16h), UV (40J/cm^2, 24h), CD95L or vehicle (DMSO, 24h) and apoptosis was measured by AnnexinV staining and subsequent flow cytometry analysis. While *Junb*$^{-/-}$ MEFs were resistant toward stress stimuli, CD95L efficiently induced apoptosis. Error bars of at least 3 different measurements show s.e.m. values. *: $p<0.05$ according to Student's t-test.

In conclusion, loss of Junb confers resistance toward stress stimuli-induced cell death, but Junb-deficient cells have the capacity of undergoing apoptosis upon death receptor activation. As the activation of caspases is a prerequisite for the induction of apoptosis, we assessed the processing of caspases upon Tm treatment by immunoblotting. In wild-type cells, the effector

caspase 3, and the initiator caspases 6 and 9 were activated 24 h post Tm treatment (Fig. 15), while in Junb-deficient MEFs, no (caspases 6 and 9) or only very marginal caspase processing (caspase 3) was detectable. To exclude a potential delay in caspase processing in *Junb*$^{-/-}$ cells, we also determined levels of cleaved caspases at later time points. Even at 32, 36 and 48 h post Tm application no caspase processing was detected. As a read-out for caspase activity, the cleavage of the caspase-3 target PARP was determined. Whereas PARP was efficiently cleaved in wild-type MEFs, Junb-deficient MEFs exhibited no PARP cleavage (Fig. 15). Thus, Junb-deficient MEFs fail to undergo apoptosis in response to ER stress due to a failure of caspase activation.

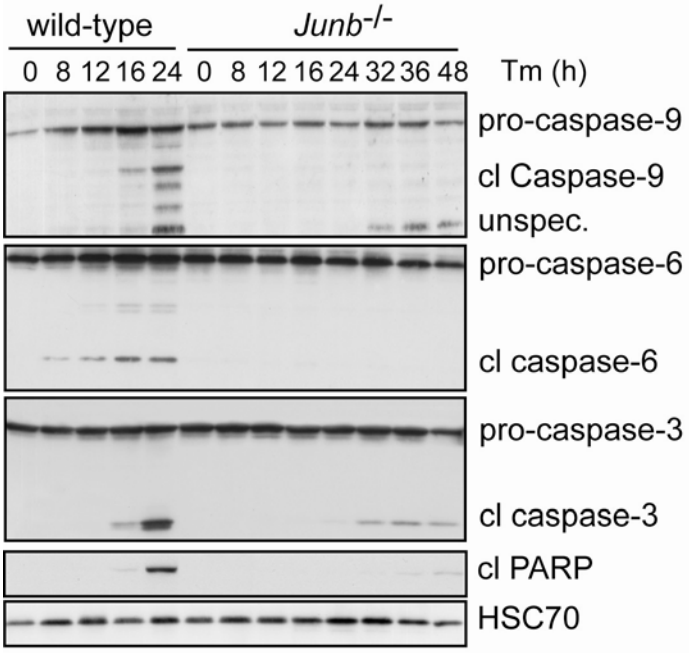

Figure 15: Impaired caspase activation upon prolonged Tm treatment in Junb-deficient MEFs. Wild-type and *Junb*$^{-/-}$ cells were lysed in CHAPS buffer at indicated time points post Tm treatment. Activation of caspases was monitored by immunoblotting. Appearance of a smaller cleavage product is indicative for activation. PARP cleavage, which is induced by active caspase-3, was detected by immunoblot using an antibody recognizing specifically the cleaved form. HSC70 was used to ensure equal quality and loading of whole cell extracts.

6.2.4 Junb-deficient MEFs exhibit a defective intrinsic apoptosis pathway

Recently, Masud et al (Masud et al., 2007) have shown that ER stress induced apoptosis primarily depends on the mitochondrial intrinsic pathway. Activation of this intrinsic pathway results in cytochrome c release from the mitochondria. Cytochrome c subsequently triggers the formation of the apoptosome and eventually leads to the processing of caspase 9. As no caspase 9 processing was observed in Junb-deficient MEFs, I analyzed the release of cytochrome c from the mitochondria of wild-type and Junb-deficient MEFs in response to Tm treatment (Fig. 16). In wild-type MEFs, 18 h post Tm application, all cytochrome c had been released from the mitochondria as demonstrated by loss of co-staining with the mitochondrial marker Mito Tracker® by immunofluorescence analysis. By contrast, in Junb-deficient cells, cytochrome c did not translocate to the cytoplasm at 18 h or even 48 h post

Tm treatment since cytochrome c staining was still overlapping with the mitochondrial marker at these time points (Fig.16, right panel).

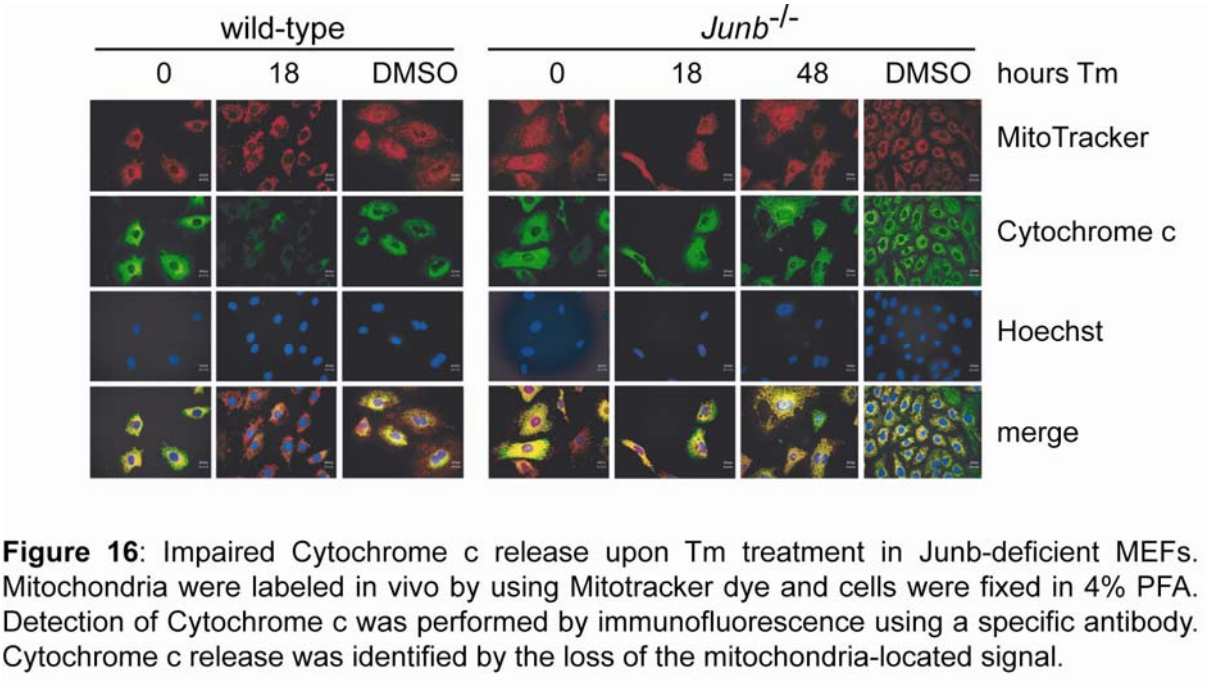

Figure 16: Impaired Cytochrome c release upon Tm treatment in Junb-deficient MEFs. Mitochondria were labeled in vivo by using Mitotracker dye and cells were fixed in 4% PFA. Detection of Cytochrome c was performed by immunofluorescence using a specific antibody. Cytochrome c release was identified by the loss of the mitochondria-located signal.

A prerequisite for cytochrome c release upon apoptosis induction is the oligomerization of Bax at the mitochondrial membrane that facilitates the formation of the MOMP (mitochondrial outer membrane pore). Bax oligomerization was measured by immunodetection of the crosslinked mitochondrial fraction. Oligomerization was detected 21 h post Tm application in wild-type cells, while no Bax oligomerization was found in Junb-deficient MEFs at this time point but could be detected 48 h post Tm treatment (Fig. 17A).

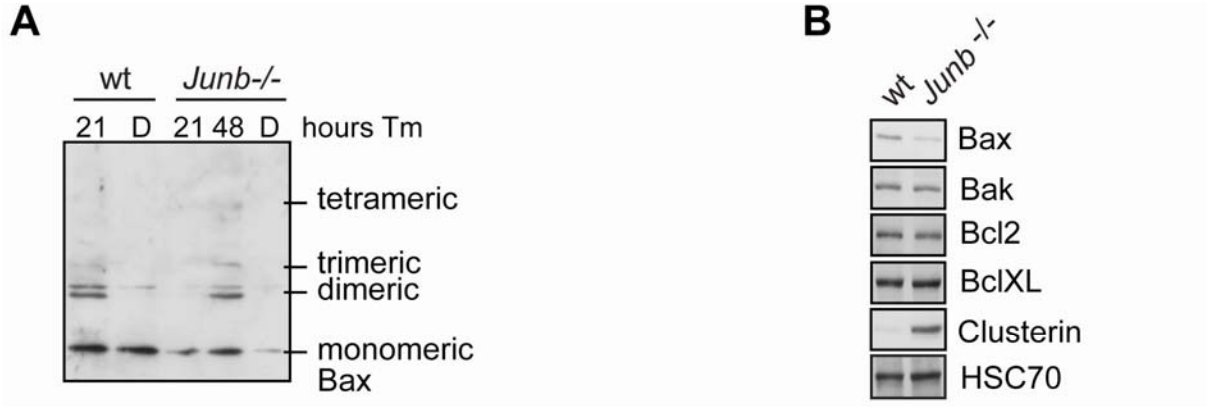

Figure 17: Loss of Junb results in impaired Bax expression and oligomerization on mitochondrial membranes as well as in elevated clusterin levels. (A) Mitochondrial membranes were isolated and incubated with the cross-linking agent BMH. Bax oligomerization was assessed the appearance of bands corresponding to multimeric forms of Bax on a gradient SDS-PAGE upon immunoblot analysis. (B) Expression of the BH3 proteins family members Bax, Bak, Bcl-2 and Bcl-XL and of clusterin was assessed by immunoblotting of whole cell extracts. HSC70 was used to ensure equal protein loading. D, DMSO control.

Thus, loss of Junb results in delayed Bax oligomerization upon prolonged ER stress which is causative of the absence of cytochrome c release from the mitochondria.

6.2.5 Aberrant expression and post-translational modification of pro- and anti-apoptotic Bcl2 family members in *Junb*$^{-/-}$ MEFs

Mitochondrial outer membrane pore formation is governed by the net balance of pro-apoptotic Bcl-2 members such as Bax, Bad, Bak and Bim and anti-apoptotic Bcl-2 family members including Bcl-2, Bcl-xL. The net activity is determined via expression levels but also post-translational modification of Bcl-2 members.

Thus, I investigated the expression and post-translational modification of key Bcl-2 members. Junb-deficient MEFs displays diminished protein levels of Bax both on whole cell extracts (Fig. 17B) and mitochondrial membranes (Fig. 17A). However, *bax* mRNA transcripts were not diminished in Junb-deficient MEFs (data not shown). Furthermore, levels of Bak, Bcl2, Bcl-xL were not affected in Junb-deficient MEFs (Fig. 17A).

Recently, Zhang and colleagues revealed a crucial role of clusterin in the regulation of apoptosis by inhibiting Bax oligomerization (Zhang et al., 2005). Clusterin levels were elevated both on mRNA (Fig. 6) and protein levels (Fig. 17B) in Junb-deficient MEFs. In order to decipher the impact of increased clusterin expression on the cell death phenotype, *clusterin* mRNA levels were suppressed by siRNA technology in *Junb*$^{-/-}$ MEFs. Junb-null MEFs were infected with lentiviral particles encoding 4 different shRNAs against clusterin and one non-targeting shRNA. One week post infection and subsequent puromycin selection,

clusterin expression was measured by RT-PCR and immunoblot. Clusterin mRNA and protein levels could be efficiently suppressed upon infection with shRNAs number 1, 2 and 5 (Fig. 18A and 18B), while cells infected with non-targeting control shRNA and shRNA 4 showed clusterin levels similar to the ones measured in uninfected *Junb*$^{-/-}$ MEFs. To determine whether clusterin suppression may rescue the apoptosis failure, shRNA-infected Junb-deficient MEFs were treated with Tm and cell death was monitored morphologically. In contrast to wild-type cells, no cell death was observed in *Junb*$^{-/-}$ MEFs (Fig. 18C) in whose clusterin was efficiently knocked-down. Thus, increased clusterin levels are not responsible for the apoptosis resistance of Junb-deficient MEFs.

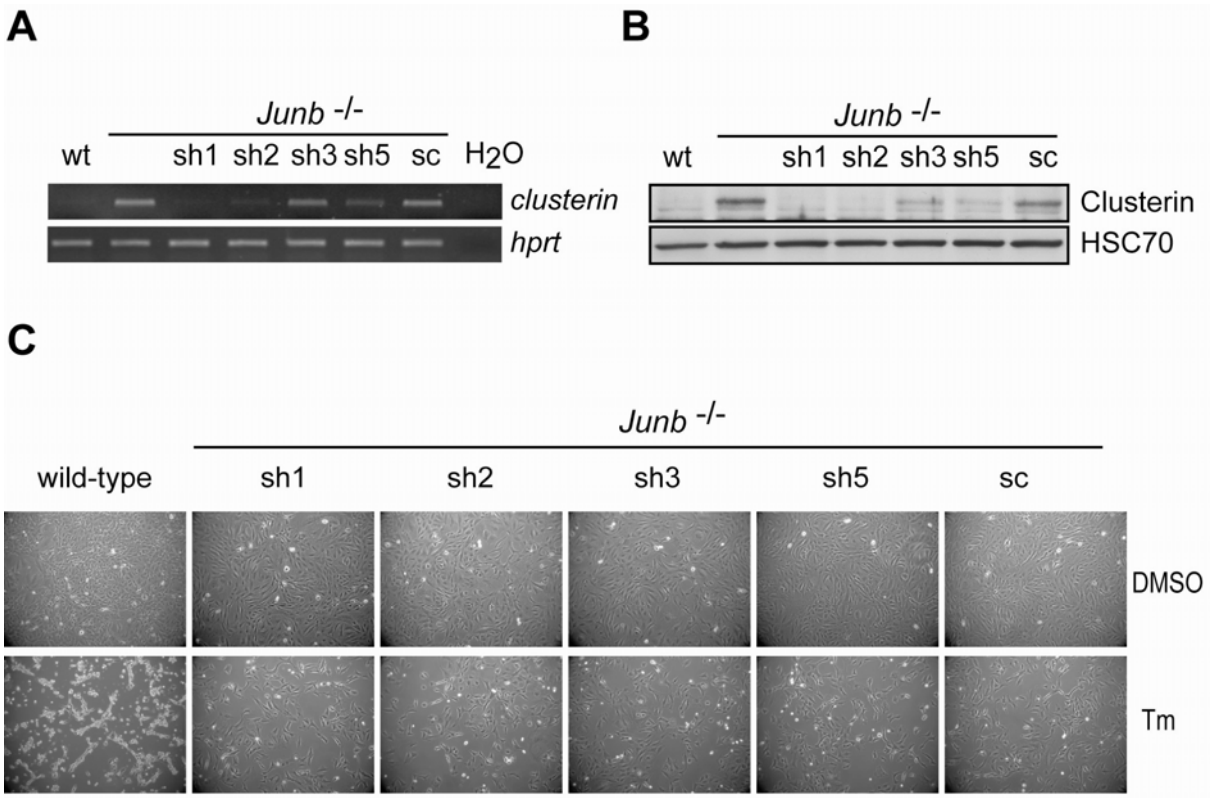

Figure 18: ShRNA-mediated clusterin suppression does not rescue the apoptosis failure of *Junb* $^{-/-}$ MEFs. Cells were transduced with lentiviruses containing 4 different shRNAs as well as a non targeting control shRNA (sc = scrambled). One week post transduction and puromycin selection, total RNA and whole cell extracts were prepared. (A) RT-PCR was performed with specific primers recognizing clusterin. *Hprt* was used to monitor equal cDNA concentration. (B) Clusterin protein expression was analyzed by immunoblot. HSC70 was used to ensure equal protein loading. (C) Wild-type and shRNA transduced cells were incubated with vehicle (DMSO) or Tm (5µg/µl) for 32h, cell death was monitored microscopically and photographs were taken.

In order to decipher whether an imbalance of pro- and anti-apoptotic Bcl-2 members in favor for anti-apoptotic proteins may be causative for apoptosis resistance of Junb-deficient cells, I determined the post-translational modifications of the Bcl-2 family members Bim and Bad. Bim is phosphorylated on multiple serine and threonine residues by both pro-survival and pro-apoptotic kinases. While phosphorylation of Bim by the MAPK Extracellular signal Regulated Kinase (ERK) leads to its degradation by the proteasome (Hubner et al., 2008), pro-apoptotic Bim phosphorylation by JNK induces formation of the MOMP (Lei and Davis, 2003), and subsequent cell death. Thus, I analyzed the Bim levels by immunoblot analysis. In wild-type cells, Bim protein levels were strongly induced between 1 and 4 h and again 24 h post Tm treatment. The Bim specific antibody detected a protein smear most likely due to a significant portion of slower migrating phosphorylated Bim. While no induction of Bim protein could be observed in Junb-deficient cells in response to Tm application, a slower migrating Bim, which is indicative for phosphorylated Bim, was very prominent in untreated Junb-deficient cells as well as in -/- cells harvested shortly post Tm treatment (Fig. 19, 0 up to 1 h post Tm treatment). At later time points Bim levels were induced with a maximum at 24 h but in contrast to wild-type cells, no Bim phosphorylation even at late time points, 32 and 48 h could be detected (Fig. 19).

Bad is phosphorylated on the serine residues 112 by ERK and 136 by Akt, respectively, and subsequently sequestered in the cytoplasm by 14-3-3. Upon stress stimuli, Bad is dephosphorylated, translocates to the mitochondrial membrane and induces the formation of the MOMP, and subsequent cell death (Youle and Strasser, 2008). Thus, I analyzed the levels of Bad phosphorylation at S-112 and S-136 following Tm application in wild-type and Junb-deficient MEFs. In wild-type cells, some Bad phosphorylation on both serine residues was detected from 30 min to 8 h post Tm treatment, whereas no Bad phosphorylation could be detected at 16 to 24 h post treatment when the cells undergo apoptosis (Fig. 19 compared to Fig. 14). By contrast, high levels of phosphorylated Bad were measured in unchallenged *Junb*$^{-/-}$ MEFs and phospho-Bad protein persisted up to 24 and 32 h post Tm treatment, the time point when wild-type cells undergo apoptosis.

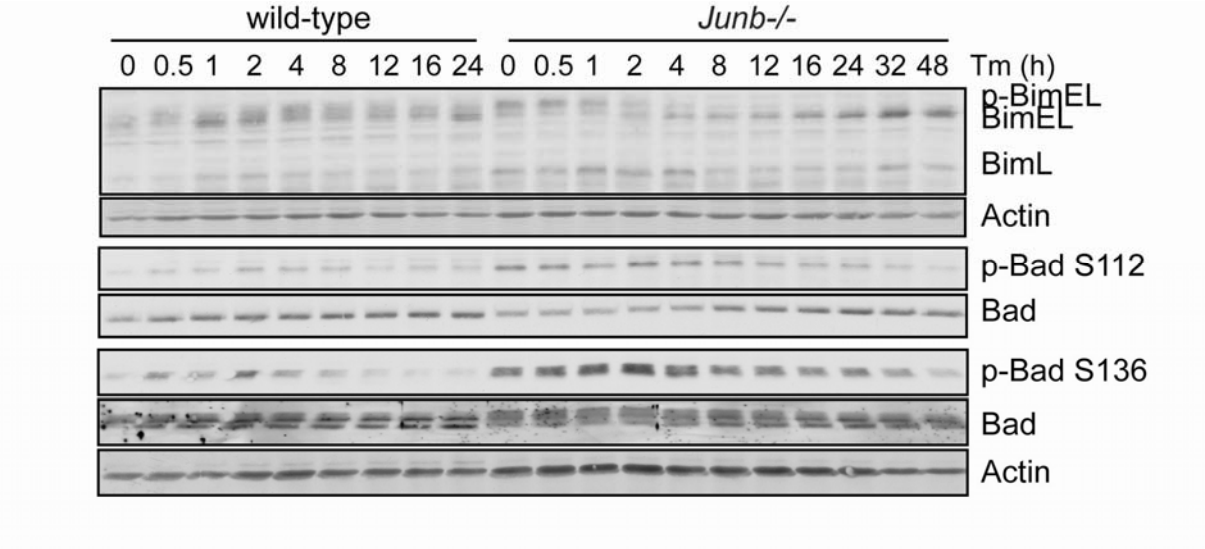

Figure 19: Increased post-translational modifications of the BH3 members Bim and Bad in *Junb*$^{-/-}$ MEFs. Phosphorylation of Bim was assessed by the appearance of a super-shifted band upon immunoblot analysis using an antibody recognizing all Bim protein isoforms. Phosphorylation of Bad was assessed by immunoblot using antibodies recognizing specifically Bad that has been phosphorylated at serine residues S112 and S136. Actin was used to monitor equal protein loading.

Thus, Junb-deficient MEFs are different from wild-type cells by diminished protein levels of Bax and increased levels of clusterin. Yet, these alterations are not solely responsible for the cell death resistance of Junb-deficient MEFs. Most importantly, aberrant phosphorylation of Bcl-2 family members Bim and Bad observed in *Junb*$^{-/-}$ MEFs confers anti-apoptotic behavior.

6.2.6 Imbalance in favor of anti-apoptotic Bcl2 family members is due to enhanced pro-survival signaling

Bim and Bad are phosphorylated by the kinase Akt and the MAP kinases ERK and JNK. As altered and even more abundant p-Bim and p-Bad levels were observed in *Junb*$^{-/-}$ cells, I analyzed the activation of these upstream kinases in wild-type and Junb-deficient MEFs following Tm application. Strikingly, untreated Junb-deficient MEFs displayed elevated levels of phosphorylated Akt (Fig. 20A) and ERK (Fig. 20B). Although phosphorylation of Akt was further induced 1 h post Tm treatment in *Junb*$^{-/-}$ MEFs similarly to wild-type cells (Fig. 20A), levels of phosphorylated ERK only marginally increased upon Tm treatment in wild-type and dramatically decreased upon Tm treatment in Junb-deficient MEFs (Fig. 20B). Tm-induced phosphorylation of JNK was identified as a major inducer of ER stress mediated apoptosis (Urano et al., 2000). In wild-type cells, JNK phosphorylation was only slightly induced at early time points following Tm application and prominent p-JNK levels were

detected 24 h post Tm treatment, at a time point when wild-type cells were apoptotic. By contrast, no p-JNK was found at any time point post Tm treatment in *Junb*$^{-/-}$ MEFs. Thus, Junb-deficiency results in an aberrant balance of pro-survival and pro-apoptotic signaling as apparent by major differences in p-Akt, p-ERK and p-JNK levels.

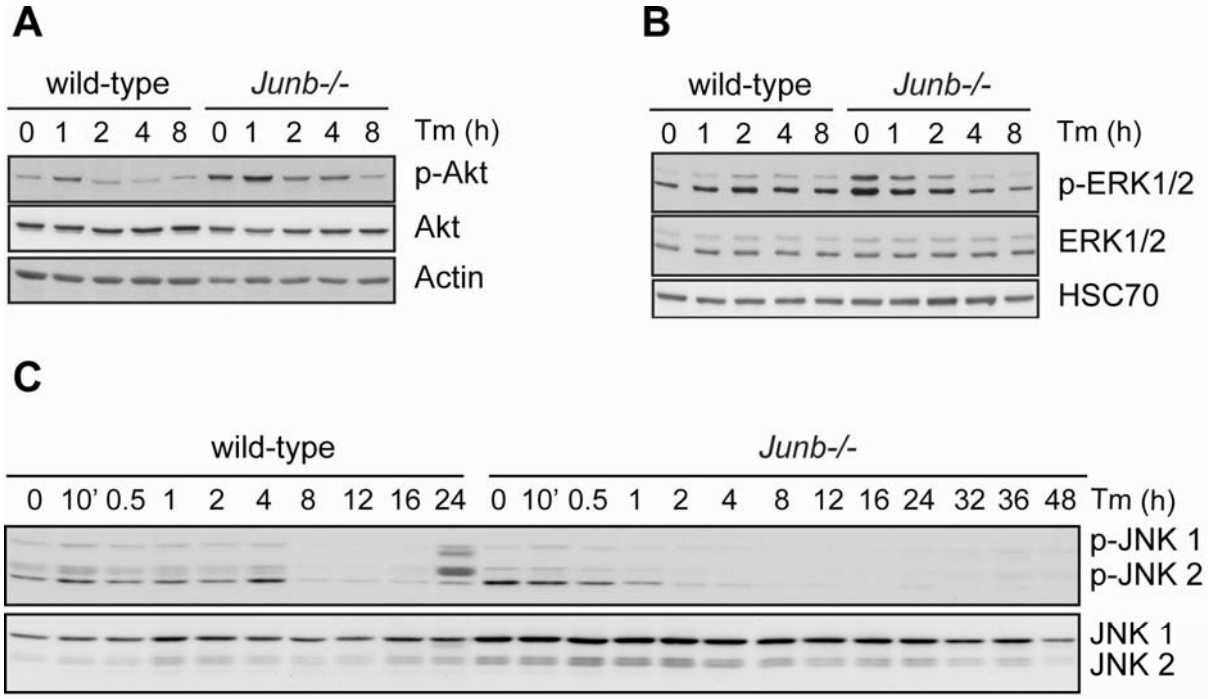

Figure 20: Junb-deficient MEFs exhibit aberrant Akt , ERK1/2 and JNK1/2 signaling. Control and Junb-deficient MEFs were treated for the indicated time points with Tm and levels of Akt (A), ERK1/2 (B), JNK1/2 (C) and their respective phosphorylated isoforms were determined by immunoblot analysis using specific antibodies. Actin and HSC70 served as control for equal protein quality and loading.

The kinases Akt and ERK respond to activation of Phosphoinositide-3 Kinase (PI3K) and Ras elicited by extracellular stimuli. In order to decipher whether an increased PI3K activity in *Junb*$^{-/-}$ cells is causative for phosphorylated Akt and ERK signaling, wild-type and Junb-deficient MEFs were treated with PI3K inhibitors. In order to ensure specific action of the inhibitors, two different PI3K inhibitors, Wortmannin and LY294002, were used. Treatment of wild-type and Junb-deficient MEFs with either inhibitor resulted in a decrease of p-Akt, p-ERK and p-Bad on S136 (Fig. 21). Wortmannin, which has a very short half-life (Vanhaesebroeck and Waterfield, 1999), inhibited phosphorylation of Akt and ERK 1 h post application and lost its activity by 4 h (ERK) and 8 h (Akt) post treatment (Fig. 21A). By contrast, LY294002 required a minimum time span of 16 h in order to inhibit Akt and ERK phosphorylation (data not shown). 24 h post application, levels of phosphorylated Akt, ERK

and Bad on S136 were reduced to basal levels both in wild-type and Junb-deficient MEFs (Fig. 21B).

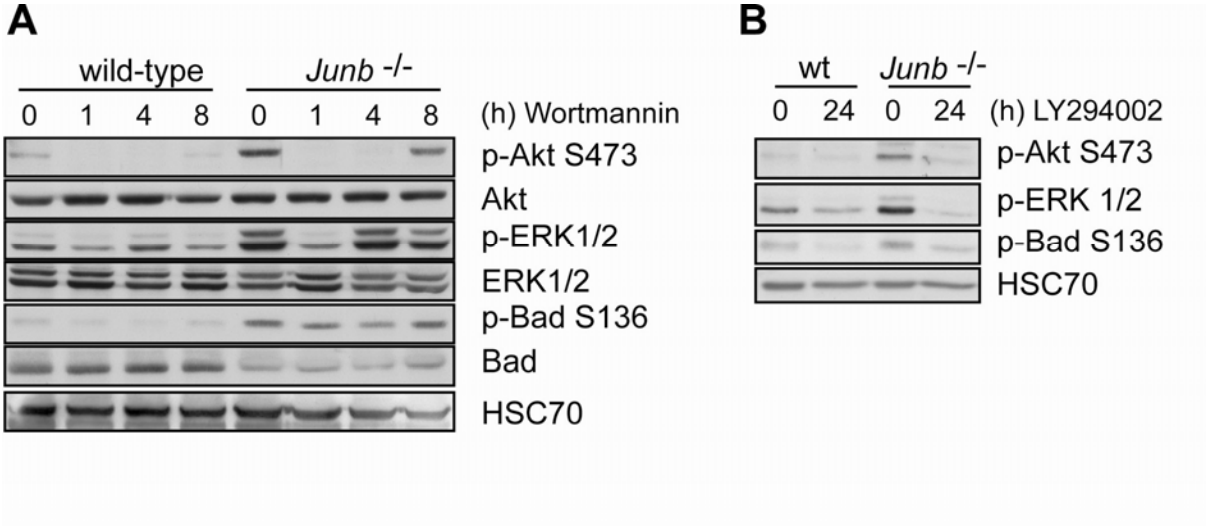

Figure 21: Inhibition of PI3-Kinase signaling in Junb-deficient cells results in normalization of p-Akt, p-ERK1/2 and p-Bad levels. MEFs were treated with two different PI3K inhibitors, 1µM wortmannin (A) or 20µM LY294002 (B) for the indicated time points; whole cell extracts were prepared and analyzed by immunoblot using specific antibodies. HSC70 was used to monitor equal protein quality and loading.

Taken together, increased PI3K activity is causative of the enhanced pro-survival signaling and subsequent apoptosis resistance observed in Junb-deficient MEFs.

6.2.7 Presence of (a) soluble factor(s) responsible for autocrine pro-survival signaling in Junb-deficient MEFs.

PI3K is activated downstream of numerous Receptor Tyrosine Kinases (RTKs) and G Protein Coupled Receptors (GPCRs) that directly or through adaptor proteins bind and activate PI3K. PI3K activity is, thus, carefully regulated by growth factor-receptor interactions (Stokoe, 2005). In order to determine whether Junb-deficient MEFs express increased levels of soluble factors which would enhance PI3K activity, wild-type cells were cultured in presence of Junb-deficient MEFs in a transwell co-culture system as described in Figure 22A. Wild-type and *Junb*$^{-/-}$ MEFs were seeded at equal density in a porous insert positioned above a six-well and were allowed to grow for 48 h. Dishes were carefully shacked every 6 to10 h in order to avoid any growth factor deposition. Since the substrate on which cells grow can influence PI3K signaling, wild-type and Junb-deficient cells were co-cultured in both directions, meaning wild-type in the insert and Junb-null in the six-well as well as vice versa. After 48 h of incubation, whole cell extracts were prepared and analyzed by immunoblot. Levels of p-Akt and p-ERK were independent of the substrate on which the cells were grown (Fig. 22B).

Importantly, co-culture of wild-type MEFs with *Junb*$^{-/-}$ resulted, in wild-type cells, in marginally increased levels of p-Akt, and prominent levels of p-ERK similar to those observed for unchallenged *Junb*$^{-/-}$ MEFs (Fig. 22B). In addition, co-culture did not reduce the levels of p-Akt and p-ERK in Junb-null MEFs, revealing that the soluble factor(s) is (are) present in excess and sufficient to sustain autocrine and paracrine signaling in both cell types at the same time.

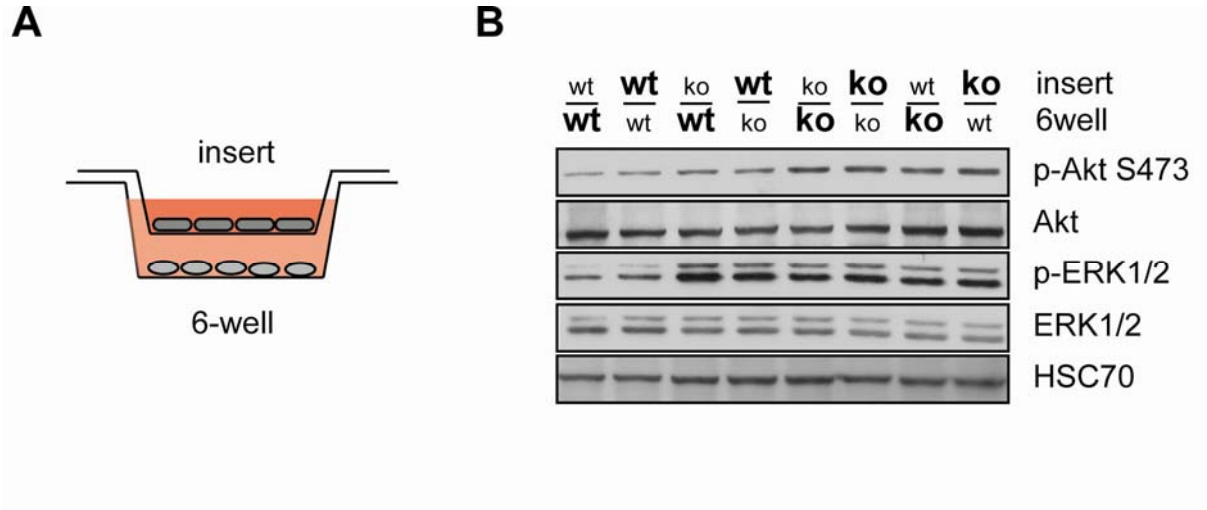

Figure 22: Presence of (a) soluble factor(s) produced by Junb-deficient fibroblasts which is/are responsible for the enhanced prosurvival signaling. (A) Schematic representation of the transwell co-culture experimental approach. An insert with pores of 0.4µM was disposed above a 6-well dish. Cells were seeded in equal density and were allowed to grow for 48 h. Dishes were carefully shacked every 6 to 10 h to obtain a homogenous growth factor distribution.(B) Whole cell extracts were prepared and analyzed by immunoblot. Bold lettering indicates the source of cell extracts used. HSC70 was used to monitor equal protein loading.

Previous experiments identified Junb as a repressor of many cytokines such as G-CSF and Csf2 (also called GM-CSF) in fibroblasts (Meixner et al., 2008; Saito et al., 2000; Szabowski et al., 2000). Since Csf2 has been described to induce phosphorylation of Akt and ERK in myeloid cells (Klein et al., 2000), I analyzed the impact of Csf2 overexpression in MEFs. As shown by RT-PCR in Figure 23A, Junb-deficient MEFs express large amount of *Csf2* mRNA. To decipher whether fibroblasts can respond to Csf2, we determined the levels of Csf2 receptor expressed in wild-type and *Junb*$^{-/-}$ MEFs. Csf2 receptor consists of 2 subunits: a cytokine specific alpha-chain (Csf2ra), which binds the ligand with low affinity, and a beta-chain (Csf2rb), which forms only upon association with the alpha-chain a high affinity receptor. So far, two isoforms of the beta-chain have been described Csf2rb and Csf2rb2 (Geijsen et al., 2001). RT-PCR analyses of two different pairs of wild-type and Junb-deficient clones revealed that *Junb*$^{-/-}$ MEFs expressed neither *Csf2ra* nor *Csf2rb* and only marginal

amounts of *Csf2rb2* transcripts (Fig. 23B). By contrast, wild-type cells expressed the alpha chain *Csf2ra* but none of the *Cs2rb* isoforms.

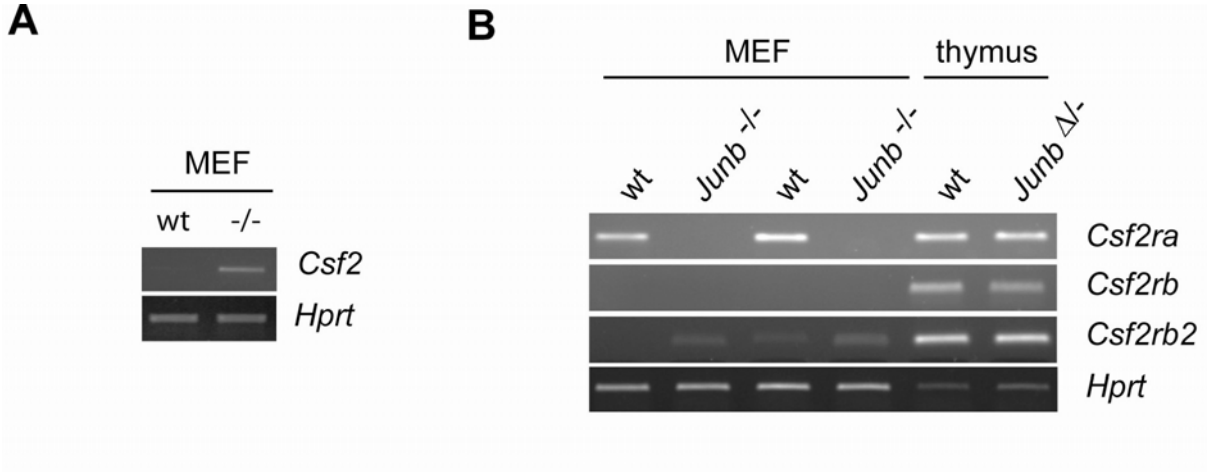

Figure 23: Junb-deficient MEFs produce more Csf2 but do not express the receptor subunits, *Csf2ra* and *Csf2rb*/*Csf2rb2* that compose the functional Csf2 receptor. (A) Semi-quantitative RT-PCR analysis shows enhanced *Csf2* mRNA levels in Junb-deficient MEFs. (B) *Junb* $^{-/-}$ MEFs do not express the Csf2 receptor subunits *Csf2ra* and *Csf2rb*, as assessed by RT-PCR. on cDNA derived from two different cell clone pairs. RNA isolated from the thymus of wild-type and *Junb* Δ/- Collalpha2-cre mice was used as positive control for *Csf2ra*, *Csf2rb*, *Csf2rb2* expression. *Hprt* was used to monitor equal cDNA concentration.

Moreover, RT-PCR performed on cDNA prepared from wild-type and Junb-null thymus as positive control for *Csf2ra*, *Csf2rb* and *Csf2rb2* expression, revealed no difference of Csf2 receptor expression between wild-type and Junb-null thymus. Thus, since MEFs do not express the functional Csf2 receptor, Csf2 can be excluded as the factor being responsible for increased p-Akt and p-ERK

6.2.8 Pdgfb is a novel negatively regulated Junb target gene

Platelet-derived Growth Factor (Pdgf) is a potent mitogenic growth factor acting on mesenchymal cells such as fibroblasts via Akt signaling (Heldin and Westermark, 1999). Pdgf family consists of Pdgf-a, -b, -c and -d which form either homo- or hetero-dimers. The Pdgfs bind to the protein kinase receptor Pdgfra and Pdgfrb, which also form dimers. Extensive studies have shown that, while Pdgf-aa homodimer binds only to Pdgfr-aa dimer, Pdgf-bb binds preferentially Pdgfr-bb dimer (Andrae et al., 2008). Thus, we measured mRNA transcript levels of *Pdgfa*, *Pdgfb*, *Pdgfra* and *Pdgfrb* by qRT-PCR. As described in Figure 24A, levels of *Pdgfa*, *Pdgfb*, *Pdgfra* were significantly increased in Junb-deficient MEFs, while levels of *Pdgfrb* were slightly increased (1.8x, non significant). Although Junb null MEFs harbored increased levels of *Pdgfa* and Pdgfra mRNA and protein, no endogenous

phosphorylation of the Pdgfra could be detected by immunoblot (Fig. 24B). By contrast, elevated levels of Pdgfrb protein and endogenous phosphorylation of the Pdgfrb could be detected by immunoblot of Junb-deficient whole cell extracts (Fig. 24B). Thus, Pdgfb appears as a very good candidate being responsible for the enhanced endogenous levels of p-Akt and p-ERK.

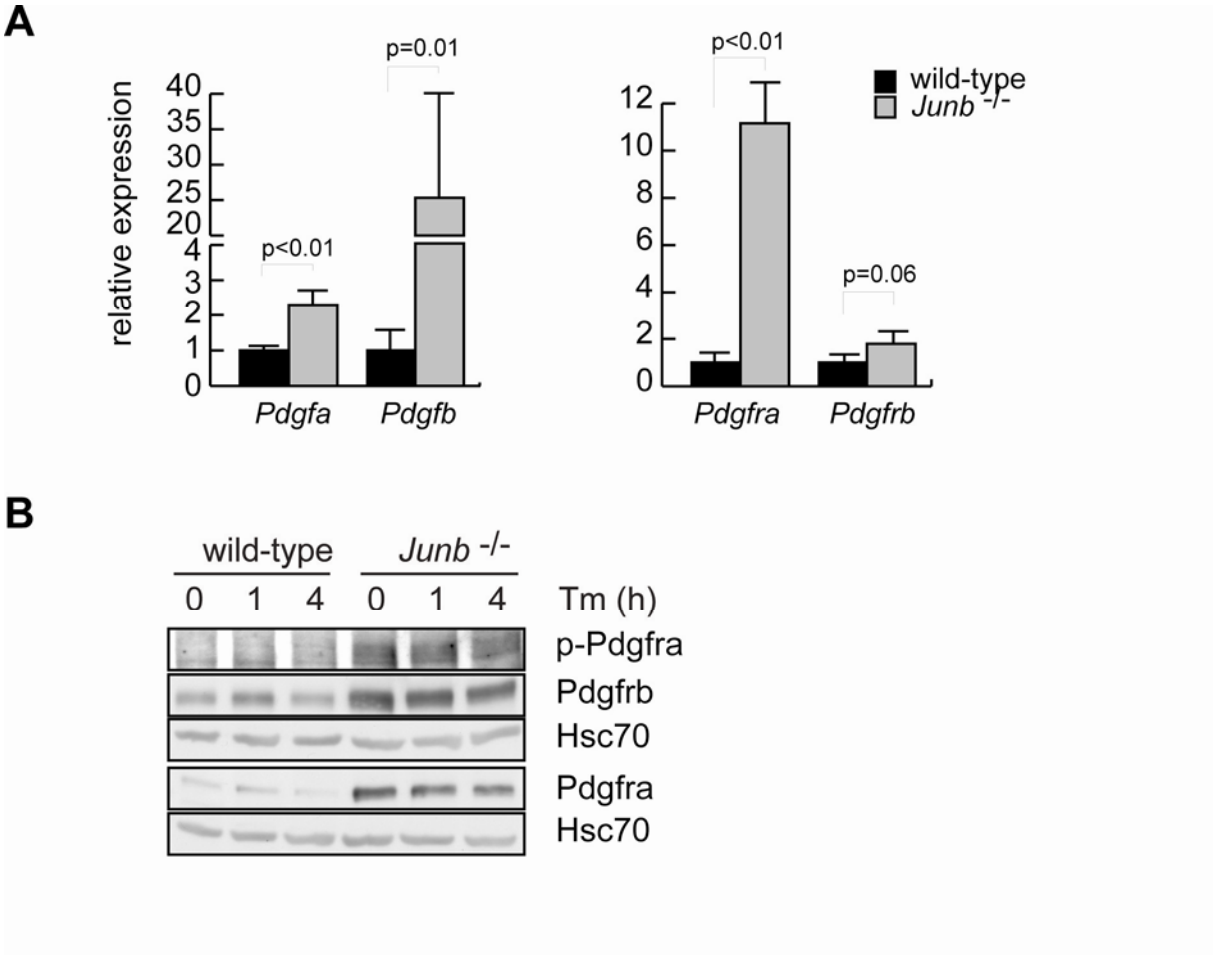

Figure 24: Enhanced Pdgf signaling in Junb-deficient MEFs. (A) qRT-PCR analysis revealed a significant increase in mRNA expression for *Pdgfa*, *Pdgfb* and *Pdgfra* in *Junb* $^{-/-}$ MEFs. Relative expression determined from three independent experiments is given. *Hprt* was used as housekeeping gene. p-value were calculated according to Student's t-test. (B) Immunoblot analysis of whole cell extracts shows an increased protein expression of Pdgfrb and Pdgfra as well as enhanced phosphorylation of Pdgfrb in Junb-null MEFs. Hsc70 was used as control for equal protein quality and loading.

Increased levels of *Pdgfb* mRNA in *Junb*$^{-/-}$ MEFs could be due to either increased transcription or enhanced mRNA stability. In order to discriminate between these two possibilities, wild-type and Junb-deficient MEFs were treated with the transcription inhibitor Actinomycin D (ActD) and levels of mRNA transcripts were quantified by qRT-PCR. Actinomycin D, a polypeptide antibiotic, binds to DNA at the transcription initiation complex

and prevents elongation by RNA polymerase (Sobell, 1985). Treatment of MEFs with ActD for 4 h induced a 10-fold decrease in *Pdgfb* transcript levels in both wild-type and Junb-deficient cells (Fig. 25). Thus, mRNA stability is not affected in Junb-deficient MEFs and increased levels of *Pdgfb* mRNA in *Junb*$^{-/-}$ most likely results of increased transcription.

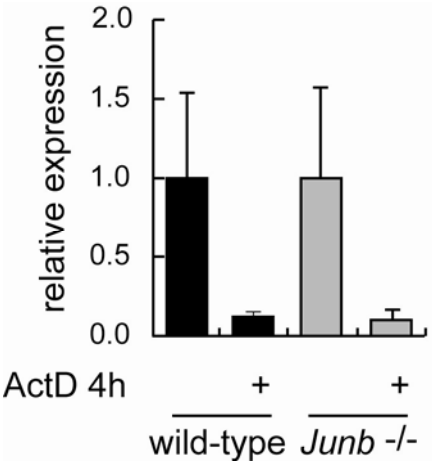

Figure 25: No difference in *Pdgfb* mRNA stability between wild-type and Junb-deficient MEFs. Cells were treated with the transcription inhibitor Actinomycin D (ActD) for 4h and levels of *Pdgfb* were measured by qRT-PCR. Relative expression versus untreated wild-type and *Junb*$^{-/-}$ cells, respectively, is given. *Hprt* was used as housekeeping gene.

In *silico* promoter analysis of *Pdgfb* highlighted the presence of two putative AP-1/TRE, one NF-κB, one Ets1 and one Sp1 transcription factor binding sites (Fig. 26A). In order to verify the ability of AP-1 and other transcription factors to bind to these putative sites *in vitro*, Electromobility Shift Assays (EMSA) were performed by incubation of biotin-labeled oligonucleotides with wild-type and Junb-deficient extracts and subsequent separation on a non-denaturing PAGE. The localization of transcription factor binding sites and oligonucleotides used for EMSA are given in figure legend 26A. EMSA analysis of the AP-1/TRE binding site (-388) revealed the binding of a complex which was diminished in Junb-deficient nuclear extracts (Fig. 26B left panel). Since the binding was competed by non-biotinylated oligonucleotides encompassing the previously described consensus TRE of MMP13 promoter (Angel et al., 1987), this complex appears to contain AP-1. EMSA with the NF-κB site produced only a very weak complex and no difference in binding was observed between wild-type and Junb-deficient extracts (data not shown). When oligonucleotides encompassing the TRE and Ets1 binding sites (TRE/Ets1 -70/-87) were analyzed, the binding of a complex was observed with nuclear extracts of wild-type but not of Junb-deficient MEFs. Competition experiments using unlabelled oligonucleotides comprising the stromyelosin Ets1, and the consensus TRE sites were unsuccessful, suggesting that this complex was neither composed of AP-1 nor Ets1. Yet, this complex was competed with an oligonucleotide containing a mutated AP-1 site but the original Ets1 site plus flanking sequences, meaning that this unidentified factor binds to a sequence site located 3' of the AP-

1 recognition sequence within the oligonucleotide (Fig. 26B, middle panel). Sp1 interacted strongly with its binding site located at position -53 in wild-type MEFs, while its binding activity was reduced in nuclear extracts from *Junb*$^{-/-}$ MEFs (Fig. 26B, right panel).

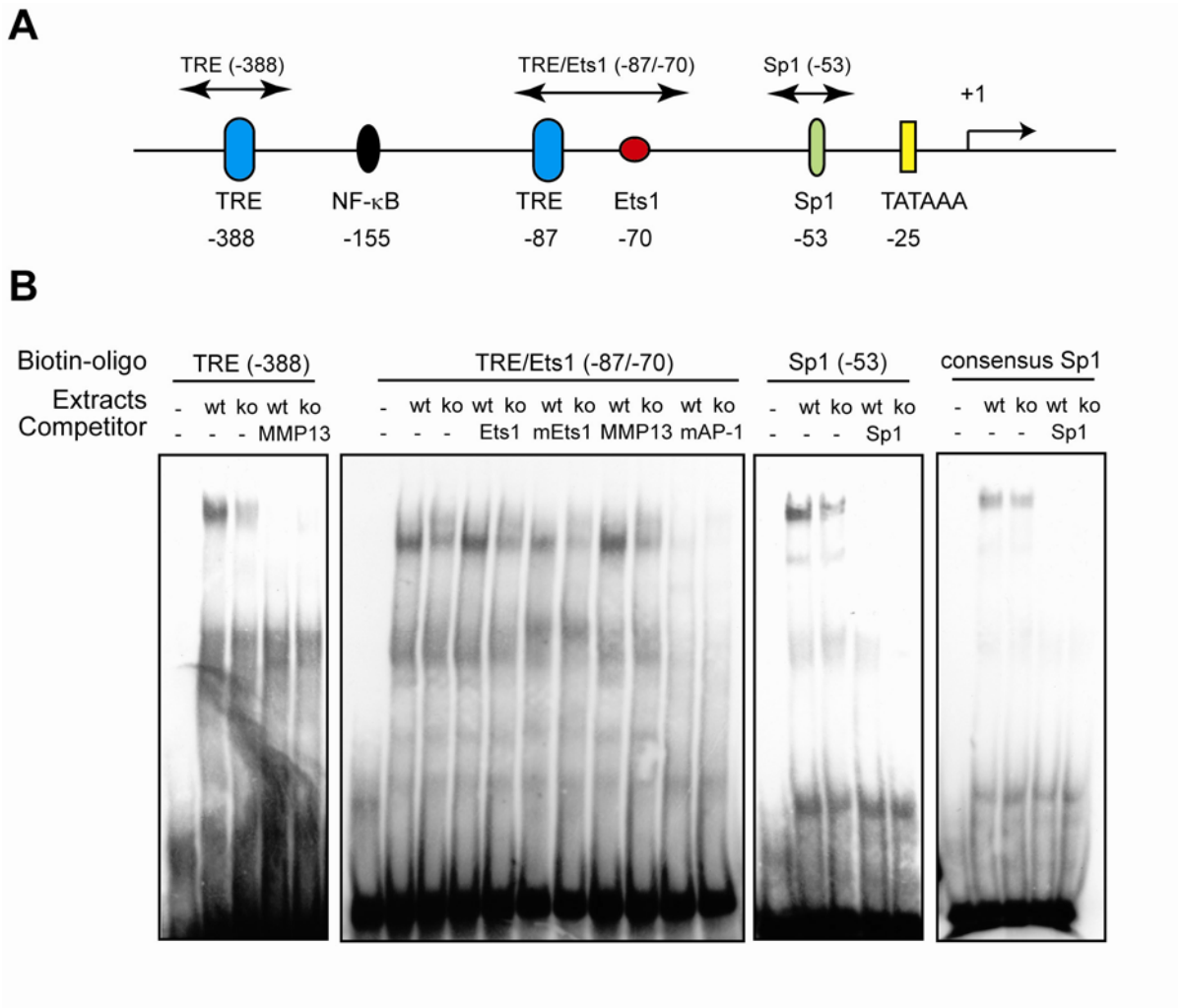

Figure 26: The promoter of Pdgfb harbors multiple transcription factor binding sites including a TRE recognized by AP-1. (A) Schematic representation of the Pdgfb promoter with its putative binding sites. Oligonucleotides used for EMSA are represented by two-headed arrows. (B) EMSA analysis of the Pdgfb promoter. Wild-type extracts exhibit strong binding activity forming complexes with the oligonucleotides covering the TRE, the TRE/Ets1 and the Sp1 sites. Transcription factors forming binding complexes were identified by competition experiments with consensus binding sites and confirmed binding of AP-1 to the -388 TRE, the presence of an unknown factor at the -87/-70 TRE/Ets1 sites and binding of Sp1 to the -53 Sp1 element. For Junb-deficient nuclear extracts, in general, a decreased binding activity is observed. Most interestingly, strongest binding activity of extracts from Junb-deficient cells is seen at a yet unidentified site within the -87/-70 TRE/Ets1 element. Binding to this element persists upon competition with a -87/-70 TRE/Ets1 element containing a mutated Ets1 site and also with a consensus TRE. These findings suggest that a yet unidentified factor more present in wild-type extracts than Junb-deficient extracts binds to this element. Consensus Sp1 oligonucleotide was used to ensure equal quantity and integrity of nuclear extracts used.

Taken together, the results identified in the *Pdgfb* promoter an AP-1/TRE binding site at position -388, an unidentified factor binding site at around -70 and a Sp1 binding site at -53, which were all less efficiently bound in absence of Junb.

In order to study the impact of the identified factors on the promoter activity, luciferase reporter assays were performed. Therefore, three different Pdgfb promoter regions were cloned in front of the luciferase gene: one comprised the Sp1 site, the unidentified binding site and the NF-κB site (named short construct); the two other reporter constructs encompassed a wild-type or a mutated AP-1/TRE as well as the Sp1, the yet unidentified binding site and the NF-κB sites (wtTRE, mutTRE; Fig. 27A). Wild-type and Junb-deficient MEFs were transfected with these luciferase constructs and promoter activity was measured 48 h post transfection. All three constructs displayed a 45-fold induction of luciferase activity compared to the empty vector in wild-type MEFs (Fig. 27B), indicating that the promoter activity was not affected by the mutation of the AP-1/TRE (-388) site. In Junb-deficient MEFs the luciferase reporter was only 15-fold induced when compared to empty vector and, in line with the findings received in wild-type cells, the promoter activity was not impaired upon mutation of the AP-1/TRE (-388) site (Fig. 27B).

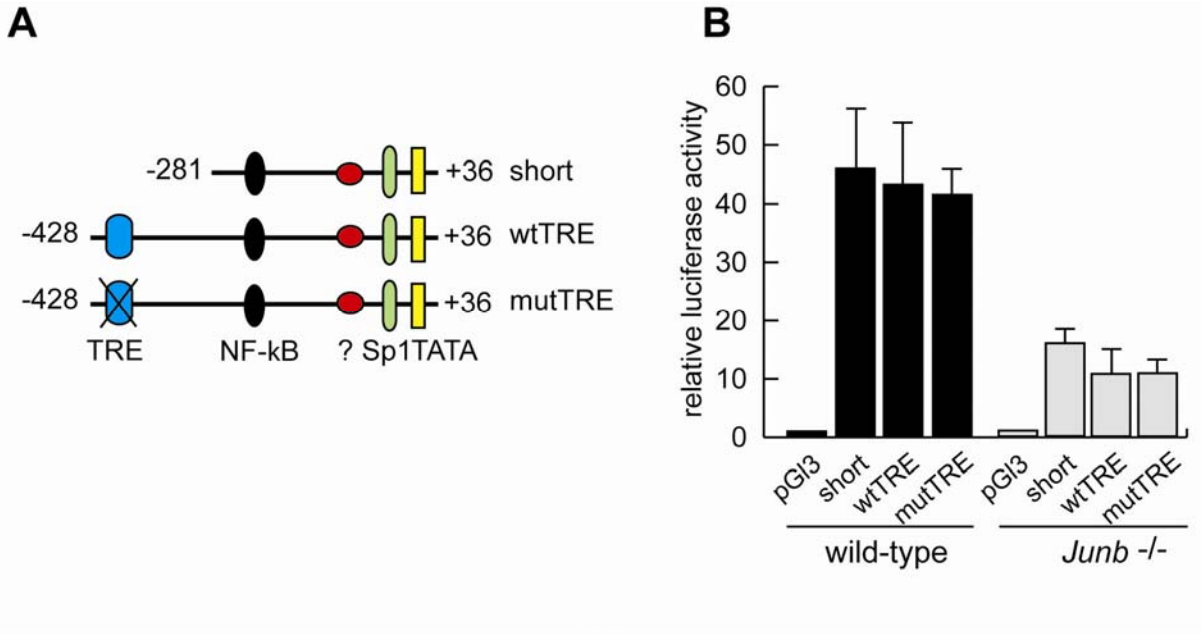

Figure 27: The identified TRE does not influence the activity of the *Pdgfb* promoter as measured by luciferase reporter assay. (A) Schematic representation of the reporter plasmids used. (B) High activity of the promoter in wild-type cells is not affected upon mutation of the TRE site in the promoter of *Pdgfb* while activity is low in Junb-deficient MEFs irrespective of the construct analyzed. 1μg of reporter were transfected in 25 000 MEFs, 48 h later cells were harvested and luciferase activity was measured. Relative luciferase activity is given. A cotransfected Renilla luciferase reference gene was used for normalization. The experiments were done in 6-plicates. Error bars show s.d.

Altogether, these results identified an AP-1/TRE binding site located at -388 of the Pdgfb promoter, but luciferase analyses showed that this binding site do not regulate the promoter activity.

6.2.9 Re-expression of Junb rescues the apoptosis failure of Junb-deficient MEFs

In order to ensure that solely the loss of Junb is responsible for the observed apoptosis resistance and to exclude that potential secondary mutations probably acquired during the immortalization process may account for the observed phenotype, Junb expression was restored in Junb-deficient MEFs. Therefore, wild-type and Junb-null MEFs were infected in parallel with retrovirus containing either an empty vector (+pMX) or a Junb expression vector (+pMX-Jb) both coexpressing GFP that facilitated the monitoring of transduction efficiency. Subsequently to retroviral infection, cells were selected with puromycin to obtain more than 95% cells transduced, as monitored by FACS analysis for GFP expression (data not shown). Re-expression of Junb in Junb-deficient MEFs resulted in a very high expression of Junb on protein level (Fig. 28A). Since the levels of Junb are very critical for the cells,

wild-type cells were as well infected with retrovirus containing Junb. Thus, wild-type MEFs could be obtained that express similar level of Junb as the Junb-transduced *Junb*$^{-/-}$ MEFs (Fig. 28A). *Pdgfb* mRNA levels were measured by qRT-PCR. While retroviral infection resulted in a further mild non significant increase of *Pdgfb* transcripts in *Junb*$^{-/-}$ MEFs, *Pdgfb* mRNA transcripts were robustly suppressed in *Junb*$^{-/-}$ MEFs rescued with Junb (Fig. 28B). Furthermore, levels of p-Akt, p-ERK and p-Bad in Junb-rescued *Junb*$^{-/-}$ MEFs were normalized to wild-type levels (Fig. 28C).

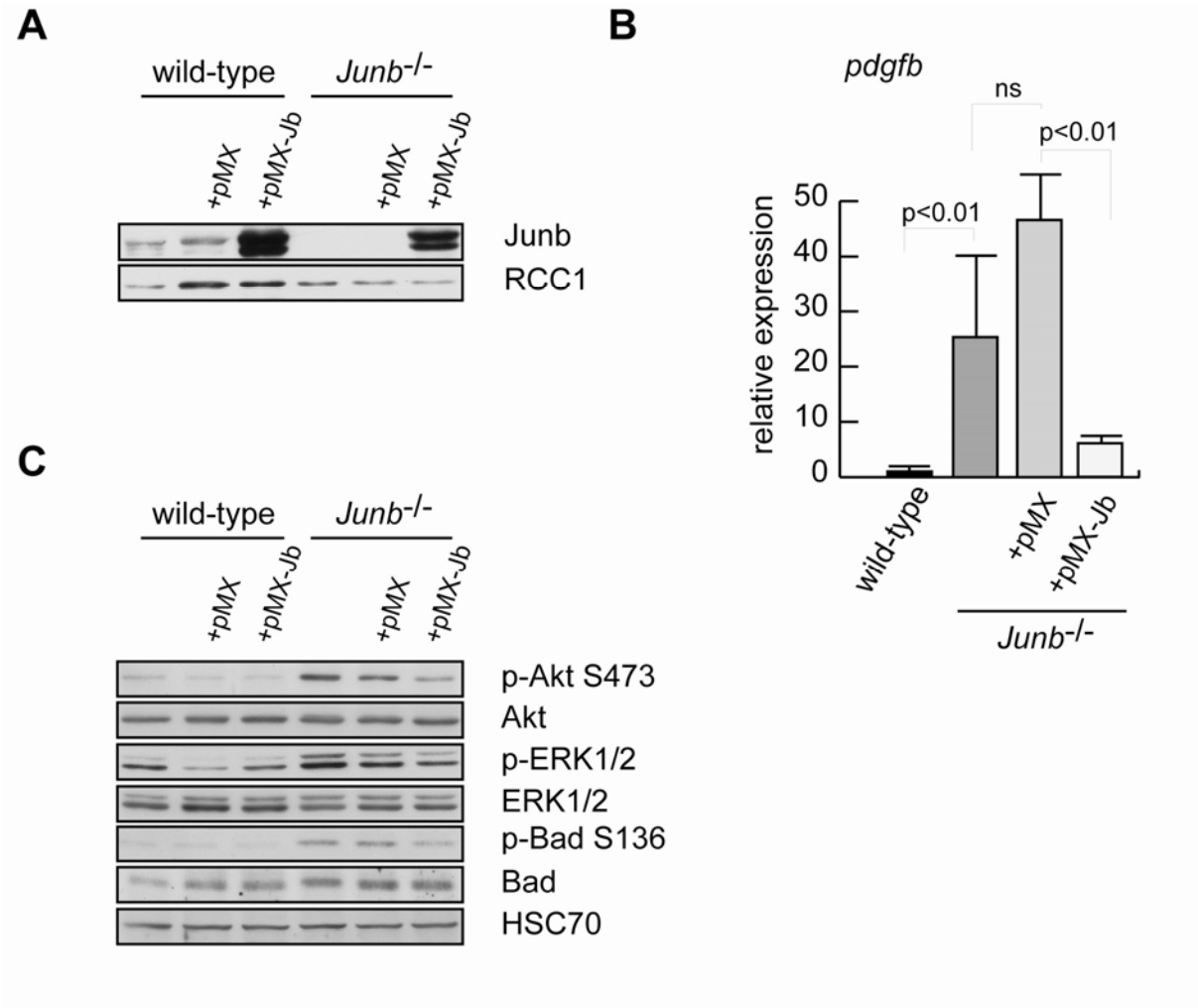

Figure 28: Re-expression of Junb in Junb-deficient MEFs suppresses *Pdgfb* expression as well as phosphorylation of Akt, ERK and Bad. Wild-type and *Junb*$^{-/-}$ MEFs were transduced with retrovirus containing the empty vector (pMX) or Junb (pMX-Jb) and further selected with puromycin to obtain more than 95% transduced cells. (A) Expression of Junb was analyzed by immunoblot of nuclear extracts. RCC1 was used as control for equal quality and loading of nuclear extracts. (B) *Pdgfb* levels in Junb rescue cells are reduced to wild-type levels as shown by qRT-PCR. Relative expression is given and *hprt* was used as housekeeping gene. p-value were calculated by Student's t-test. (C) Levels of phosphorylated Akt, ERK and Bad in Junb rescue cells are similar to those observed in wild-type cells. Immunoblot analyses were performed on whole cell extracts with specific antibodies. HSC70 was used as control for equal quality and loading of protein extracts.

Rescued cells were then treated with Tm and apoptosis was monitored by AnnexinV staining and subsequent FACS analysis (Fig. 29). No obvious differences in the rate of spontaneous apoptosis could be observed in cells left untreated (Fig. 29, left bars). While 45% wild-type cells were AnnexinV-positive upon 24 h treatment with Tm, only 35% of infected wild-type cells were stained with AnnexinV, meaning that infection of cells with retrovirus slightly impaired induction of cell death. Junb-rescued *Junb*$^{-/-}$ cells showed a minor increase in AnnexinV positive cell numbers 24h post Tm treatment while Junb-deficient cells did not undergo apoptosis (20% AnnexinV positive), Importantly, when the analysis was performed 32h post Tm application, 35% of all Junb-rescued *Junb*$^{-/-}$cells were AnnexinV positive. This number of apoptotic cells was similar to the one monitored for Junb over-expressing wild-type MEFs (Fig. 29). At this time point, Junb-null MEFs infected with the empty retrovirus displayed only 22% AnnexinV positive cells and, thus, exhibited similar number as uninfected Junb-deficient cells. Importantly, treatment of all cell lines with vehicle (DMSO) did not induce any significant cell death (Fig. 29, right bars).

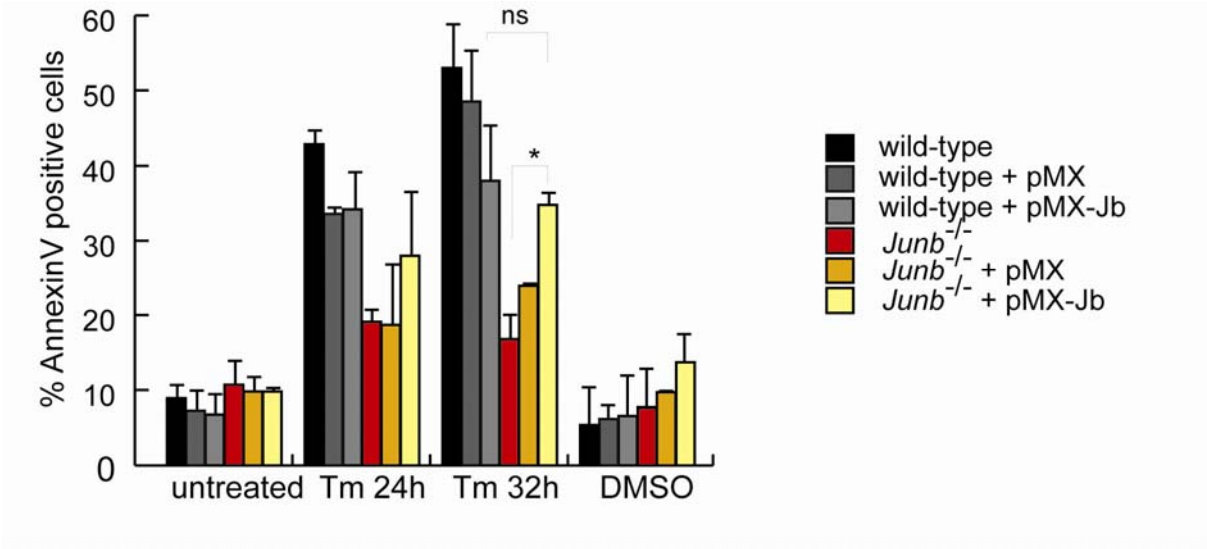

Figure 29: Re-expression of Junb in *Junb*$^{-/-}$ MEFs rescue the apoptosis phenotype. Wild-type and *Junb*$^{-/-}$ MEFs were transduced with retrovirus containing the empty vector (pMX) or Junb (pMX-Jb) and further selected with puromycin to obtain more than 95% transduced cells. Junb rescue MEFs were treated with Tm for 24 h and 32 h or vehicle (DMSO, 24h) and apoptosis was measured by AnnexinV staining and subsequent flow cytometry analysis. % AnnexinV positive cells is given. Error bars of at least 3 different measurements show s.d. values. *: $p<0.05$ according to Student's t-test.

Altogether, this experiment showed that re-expression of Junb in *Junb*$^{-/-}$ MEFs brings *Pdgfb*, p-Akt, p-ERK and p-Bad back to wild-type levels, and furthermore restores the ability of the MEFs to undergo apoptosis upon prolonged ER stress elicited by Tm treatment, meaning that solely the loss of Junb is responsible for the observed apoptosis resistance.

7 Discussion

7.1 Junb as positive and negative transcription regulator

Previous *in vitro* and *in vivo* experiments clearly defined Junb as both an activating and repressing transcription factor (Florin et al., 2004; Florin et al., 2006; Licht et al., 2006; Meixner et al., 2008; Schmidt et al., 2007; Szabowski et al., 2000). While the molecular mechanisms regulating AP-1 transcription activation were intensively studied, the mechanisms underlying transcription repression are so far poorly understood. In general, different mechanisms of gene repression have been proposed, involving inhibition of transcription initiation, inhibition or competition for activating factors as well as epigenetic mechanisms. For Junb, it has been claimed that it acts as a repressor on its own by forming heterodimers with other AP-1 subunits that, as a result, exhibit a much weaker transactivation potential. It is still a mystery how Junb is able to discriminate among target gene to repress and to activate. The understanding of this selectivity process and the underlying molecular mechanism may help to design specific drugs that could interfere with Junb function and thus interfere with the evil features of Junb. Therefore, I investigated in the present work additional mechanisms by which Junb may represses genes, and I could identify Junb target genes which are epigenetically regulated through two different mechanisms: HDAC-dependent deacetylation and DNA methylation.

Although no apparent difference in acetylation of histones and expression of HDACs could be observed between wild-type and Junb-deficient MEFs, the analysis of gene expression following treatment by two independent HDAC inhibitors revealed a few genes that are regulated by HDAC-dependent mechanisms. Four different classes of genes were identified depending on their expression following HDAC inhibitor treatment.

The first class of genes, which comprises *lipoprotein lipase (lpl)*, *clusterin (clu)*, *mapk phosphatase 1 (mkp1)* as well as others, had their expression induced by HDAC inhibitor both in wild-type and Junb-deficient MEFs. This suggests that these genes have the potential to be induced by HDAC inhibitors in a similar way in wild-type and Junb-deficient cells and excludes that the difference in basal expression may be due to increased acetylation levels of histones located on their promoter region in Junb-deficient cells.

The second class of genes is of particular interest since expression of these genes is enhanced by HDAC inhibitors only in wild-type cells. It includes *glutathione S-transferase alpha 4 (gsta4)*, *erythrocyte protein band 4.1 like 4b (epb4.1l4b) and inhibitor of DNA binding 1*

(id1). The fact that the gene expression cannot be further induced upon HDAC inhibition in absence of Junb suggests that the repression mechanisms involve HDACs and that they are impaired in Junb-null MEFs. Possible mechanisms will be discussed in more details in a subsequent paragraph.

The third identified class of genes shows no modification in their expression pattern upon treatment with HDAC inhibitors, suggesting that some other mechanisms may be involved. For instance, another transcription factor or co-activator may be super activated in Junb-deficient cells and be responsible for the enhanced expression. Novel experimental approaches, such as reverse genetic screens by RNA interference on a genome-wide scale in Junb-deficient cells or a recently describes break-through technology that quantitatively evaluates within a cell activities of dozens of transcription factors simultaneously (Romanov et al., 2008) would be required to address this issue.

The last and fourth class of genes finally comprises *inhibitor of DNA binding 3(id3)* and *keratinocyte growth factor (kgf)*, that display decreased expression upon treatment with HDAC inhibitors. HDAC inhibitors are reported to affect cell cycle progression and induce cell death (Marks et al., 2001). Since the two identified genes are involved in cell growth, proliferation and differentiation (Benharroch and Birnbaum, 1990; Lasorella et al., 2001; Zebedee and Hara, 2001), it is highly probable that the toxicity of such compounds is the major cause of their down-regulation.

Different mechanisms could be causative of the observed HDAC-dependent de-repression phenotype of the second class of genes. First, one could postulate that Junb may interact with a yet-to-be-identified HDAC and recruit it to the promoter of target genes. Indeed, several transcription factors recruit HDACs to promoters and thereby repress transcription in the absence of appropriate signals (Glass and Rosenfeld, 2000). For instance, HDAC3 binds to the N terminal region of unphosphorylated Jun and represses Jun activity. When Jun becomes phosphorylated by JNK in response to the activation of upstream signaling pathways, HDAC3 dissociates from Jun, thus, allowing Jun to transactivate genes (Weiss et al., 2003). It has been recently shown that such a de-repression mechanism occurs during inflammation for the very tightly controlled expression of the cytokine ccl2 following Interleukin-1 treatment (Wolter et al., 2008). If an HDAC-dependent mechanism is responsible for the de-repression of the described genes, one could expect endogenously increased levels of histone acetylation in the promoter region of derepressed target genes in Junb-deficient MEFs. Further

experiments, such as chromatin immunoprecipitation, are required to analyze acetylation levels of histones in the promoter region of those genes and to confirm the hypothesis.

Secondly, lysine acetylation may be implicated in the repression mechanism. Lysine acetylation has been originally identified in histones, but occurs also in a significant number of non-histone proteins including transcription factors, nuclear regulators and various cytoplasmic proteins. Thus, lysine acetylation is not only crucial in nucleus and transcriptional regulation, but also appears to be essential for regulating the activity of proteins involved in different processes, such as cytoskeleton dynamics, energy metabolism, endocytosis, autophagy and even signaling from the plasma membrane (Yang and Seto, 2008a). More than 80 transcription factors, including p53, Forkhead box transcription factors (FoxO) and STAT, are known to be modified by acetylation. Acetylation of p53 was intensively investigated and studies revealed that acetylation can enhance p53 DNA binding, binding to transcriptional co-activator such as CBP, as well as protein stability by precluding ubiquitination and subsequent degradation (Yang and Seto, 2008a). Further studies should show whether Junb is modified by acetylation and, if so, whether such post-translational modification might regulate Junb transactivation activity and transcription of *gsta4*, *id1* and *epb4.1l4b*. Finally, for the case that no difference in the acetylation of the promoter of the previously described genes or no acetylation modification of Junb will be observed, a global comparative analysis of the acetylome may help to explain the differences in gene expression observed in Junb-deficient MEFs.

Taken together, these data suggest that Junb regulates gene expression through a yet-to-be identified HDAC-triggered mechanism (Fig. 30B panel 1). Although Junb does neither regulate the histone H3 acetylation status nor the expression levels of HDACs, the data from the HDAC inhibitor experiment nevertheless state that some of the Junb target genes must be regulated by HDACs. Further studies will be required to underline the molecular mechanisms responsible and to decipher whether Junb represses the identified genes by recruiting an HDAC to their promoter, or whether Junb activity by itself is regulated via acetylation or whether absence of Junb results in abnormal post-translational modifications of another regulator or transcription factor.

With regard to gene repression by DNA methylation, my work revealed an essential role for Junb in the setting and/or maintenance of the imprinting of the non-coding RNA *H19*. *H19* was identified as the most deregulated transcript in Junb-deficient MEFs by previous global

gene expression analysis (Florin et al., 2004). Most importantly, I could confirm that solely the loss of Junb is responsible for the impaired expression of *H19* since re-expression of Junb in Junb-deficient MEFs suppressed *H19* expression. Although *H19* is one of the first imprinted genes discovered, its function has not yet been fully unraveled but much effort has been invested to understand its transcription regulation. While the expression of key regulators of *H19* transcription, such as CTCF, DNMT1 and DNMT3b, is unaffected in Junb-deficient MEFs, analyses of methylation by using two different techniques revealed a loss of methylation of the imprinting control region in absence of Junb. Surprisingly, the results obtained for wild-type cells by the two techniques used were not consistent. While the COBRA assay revealed an expected 50:50 ratio for unmethylated and methylated DNA, being consistent with one maternally imprinted allele, bisulfite sequencing analyses revealed almost 100% of methylation of all sites analyzed. Different reasons, which have been previously described, could be responsible for this difference. It has been reported that a bias could emerge in bisulfite sequencing from PCR amplification, sub-cloning into sequencing vector and transformation into bacteria due to a higher affinity of primers or ligase for DNA comprising cytosine residues (reminiscent of DNA methylation before the bisulfite conversion) versus DNA with uracil/thymidine residues (reminiscent of absence of DNA methylation before the bisulfite conversion) (Grunau et al., 2001; Warnecke et al., 1997). In the present work, both approaches have been carried out from the same PCR amplification products, therefore, I conclude that the bias, most likely, arose from a preferential sub-cloning or transformation of the PCR amplicons derived from previously methylated DNA rather than from a differential PCR amplification per se. Despite the presence of this bias, both methods revealed a loss of methylation of all four CTCF binding sites in Junb-deficient MEFs. In addition, bisulfite sequencing allows the determination of the methylation status of each cytosine residue in the region of interest. Interestingly, while the region encompassing the second CTCF binding site showed a loss of methylation of only the residues encompassing the consensus sequence, the fourth CTCF site displayed a loss of methylation for the whole region surrounding this binding site. This suggests that the molecular mechanisms responsible for the methylation regulation of both sites may be different.

Although Junb does regulate neither the expression of CTCF nor of DNA methyltransferases, it may regulate the targeting of these enzymes to the DNA and/or their activity. *In silico* analysis of the insulator revealed the presence of a TRE site (5'-TGA C TCA-3') located between the third and fourth CTCF consensus binding site. It will be crucial to determine

whether this site is required and essential for the regulation of imprinting by Junb. For this purpose, it will be important to confirm in future experiments *in vitro* and *in vivo* binding of Junb and, if a binding is confirmed, to test its impact by reporter assay and mutagenesis.

It is feasible to postulate that Junb may interact with a DNA methyltransferase and may even recruit DNA methylation activity to the insulator via the identified AP-1 binding site. Indeed, there is increasing evidence that transcription factors can directly bind to DNA methyltransferases and recruit the enzyme specifically to some promoters, in a similar way as described above for HDACs. For instance, the transcription factor Myc associates with DNMT3a and, through the DNA-binding protein Miz-1, targets DNA methylation and silencing of p21Cip1 gene (Brenner et al., 2005).

Moreover, *H19* is located in an imprinted cluster with *Igf2* and the expression of the two genes is differentially regulated by the same molecular determinant, namely the insulator. If the insulator is unmethylated, CTCF binds to its DNA sequence and creates a boundary which restricts the activity of the common downstream enhancer on *H19* gene. Due to the fact that, in absence of Junb, the insulator undergoes demethylation, the expression of *Igf2* should be reduced. However, preliminary analyses revealed that *Igf2* expression is rather enhanced in Junb-deficient MEFs. This suggests that, in addition to its impact on imprinting, Junb may regulate *Igf2* and/or *H19* expression directly through their promoters and further experiments shall address those questions.

The data obtained in the present work revealed for the first time an implication of Junb and AP-1 in imprinting and DNA methylation (Fig. 30B panel 2). Thus, it will be challenging to determine whether Junb and AP-1 regulate the DNA methylation of other imprinting clusters or promoters. For this purpose, further experiments such as analyses of DNA methylation pattern on a genome-wide level by methyl-DNA immunoprecipitation or genome-wide bisulfite sequencing are required.

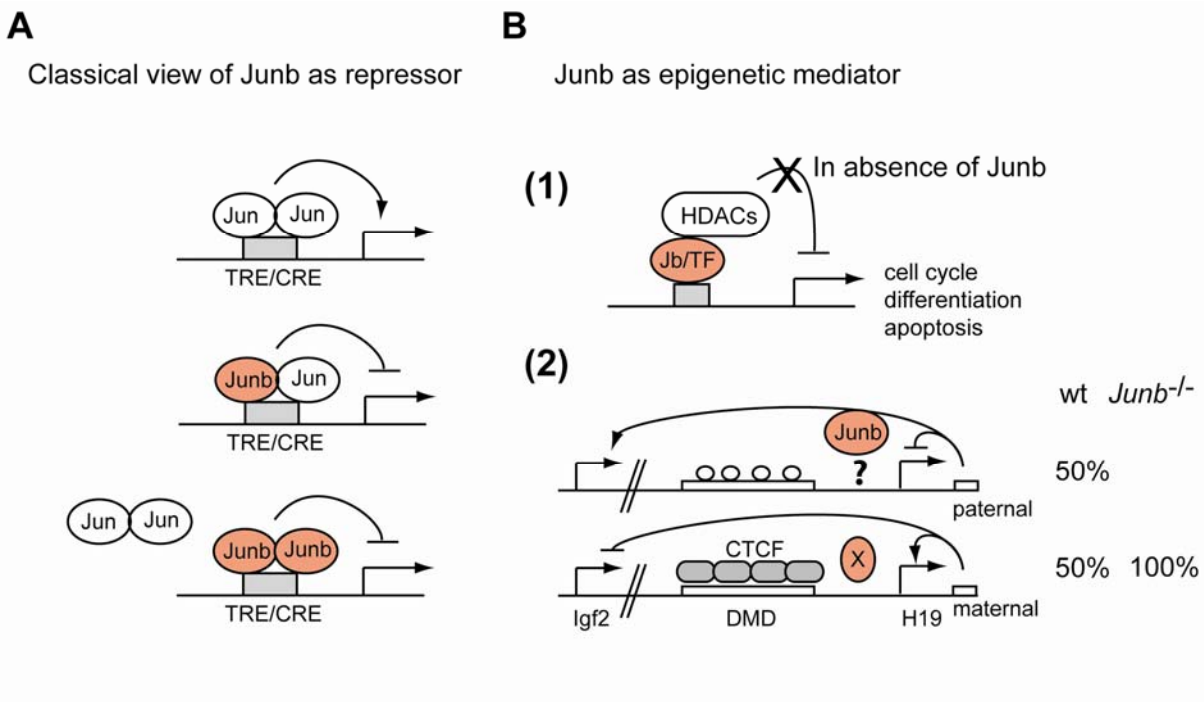

Figure 30 Model of Junb as transcriptional repressor. (A) Classical view of repression mechanisms orchestrated by Junb. Due to its weak transactivation domain, Junb can form inactive heterodimer with Jun or can compete with Jun homodimers for an AP-1 binding site within the promoter region of the target gene. (B) In addition, Junb acts as epigenetic mediator by (1) modulating HDAC-dependent mechanisms and by (2) regulating the DNA methylation of the Igf2/H19 imprinting control region via a yet unknown mechanism which may involve Junb-mediated methylation or demethylation in absence of Junb via an unknown factor X.

Altogether, this work confirms that Junb can repress genes by other mechanisms than absorbing the transcriptional activity of Jun and other AP-1 members (Fig. 30). Apparently, the molecular mechanisms involved in such a regulation are novel and very unusual for an AP-1 member, thus, they could not be fully deciphered during the course of this work. Many different possible mechanisms have been proposed and further experiments are required to confirm or exclude the hypotheses described above. Since impaired epigenetic modifications of the genome, including aberrant DNA methylation pattern and loss of imprinting, are observed in many tumors, the understanding of how Junb and AP-1 influence such processes will be of great importance in order to develop new possible therapies against cancer.

7.2 Junb is a novel decision maker for death or survival

The implication of AP-1 in stress response is very complex since it can have opposite function, being either pro-apoptotic or anti-apoptotic. Indeed, the net function depends on the relative abundance of AP-1 subunits, the composition of AP-1 dimers, the cell type, the cellular environment and the stimulus. Previous work based on *in vivo* mouse models and *in vitro* cell culture models defined a crucial role for one AP-1 member, Junb, in cellular

hypoxia and hypoglycemia responses. In the present work, I investigated the role of Junb in ER stress, a condition that has been described to contribute to hypoxia tolerance and tumor progression. Loss of Junb resulted in minor change in UPR, but most intriguingly Junb-ablated MEFs were unable to undergo apoptosis upon prolonged ER stress albeit they were able to sense ER stress. Remarkably, Junb-deficient MEFs were also resistant towards apoptosis in response to DNA damaging agents or proteasome inhibitors suggesting a general defect in stress-induced apoptosis due to very high levels of activated pro-survival kinases elicited by an autocrine loop and resulting in failure in mitochondria permeabilization and subsequent caspases activation. Very importantly, apoptosis resistance could be solely attributed to the absence of Junb and not to additional mutations acquired during spontaneous immortalization of the MEFs.

First, I found that Junb participates in the ER stress response as it is strongly induced on both mRNA and protein levels in response to Tunicamycin, which promotes ER stress by blocking protein glycosylation. Surprisingly, although Junb is described as an immediate early gene, whose expression is induced very fast after stress and rapidly returns to basal levels, Junb protein levels stayed high until 8 to 12 h post Tm application. Interestingly, such prolonged Junb induction was never observed so far for any kind of stress stimulus. At least two different causes could account for this observation: the specific requirement of Junb for the ER stress response or as a consequence of a cell cycle arrest. In an attempt to re-establish cellular homeostasis, the UPR will eventually results in cell cycle arrest. eIF2α, phosphorylated by PERK, has been proposed to block cyclin D1 protein translation, thus, causing cyclin D1 degradation and G1 phase arrest (Brewer and Cadman, 2000; Brewer and Diehl, 2000). In the past, it has been reported that the Junb is regulated during cell cycle progression with a peak at S/early G2 phase and a breakdown at M phase (Bakiri et al., 2000). Besides, Junb regulates cell cycle via its target genes p16/Ink4a, cyclin A, cyclin A2 and cyclin D1 (Andrecht et al., 2002; Bakiri et al., 2000; Farras et al., 2008; Passegue and Wagner, 2000). Moreover, the degradation of Junb at the M phase by the proteasome is absolutely required for proper cell cycle progression, since constitutive Junb expression results in cell cycle arrest at late G2/early M phase (Farras et al., 2008). Thus, it is feasible that the prolonged Junb induction is a consequence of cell cycle arrest. However, Junb could equally well be required for a proper late ER stress response. For instance, Junb-activated target genes may be involved in late UPR or may contribute to UPR induced cell cycle arrest. It will be a challenge to dissect cause and consequence as well as Junb direct and indirect

functions in this respect. Future experiments, incorporating cell cycle analysis along with UPR studies with synchronized wild-type and Junb-deficient MEFs, may be helpful in addressing these questions.

Since Junb was induced upon ER stress, I investigated whether it is involved in UPR by monitoring key UPR factors in wild-type and Junb-deficient MEFs. Only minor differences were observed in ER stress sensing and induction. Untreated as well as Tm-treated Junb-deficient MEFs harbored increased mRNA levels of the ER-located chaperones *grp78* and *grp94* and of the oxidoreductase and protein disulfide isomerase cofactor *oxidoreductin-like 1*. It appears unlikely that Junb, on its own, transcriptionally regulates all these three chaperones, moreover because differences in expression were only minor although significant, between 1.5 and 2.5 fold. Thus, increased levels of these factors may rather be a consequence of an increased requirement for ER folding capacity in absence of Junb. Indeed, while Junb-deficient MEFs produce about 50% less protein (Textor B and Schorpp-Kistner M, unpublished data), they express much more mRNA coding for cytokines and growth factors. Assuming that these factors once being translated have to transit through the ER, then, *Junb*$^{-/-}$ MEFs would require a much higher capacity of the ER chaperone machinery than wild-type cells. This could be reflected by the enhanced chaperone expression levels but also by different kinetics in the UPR. Indeed, minor differences were observed in the kinetics of Grp78 and CHOP protein induction and of XBP1 splicing, while eIF2α was already endogenously phosphorylated in Junb-deficient MEFs. Furthermore, increased Grp78 and Grp94 protein expression has been extensively correlated to resistance towards apoptosis and tumorigenesis (Moenner et al., 2007). eIF2α phosphorylation by PERK prevents as well ER stress-induced cell death as it was shown that PERK-deficient cells are more susceptible to apoptosis in response to ER stress (Harding et al., 2000b). However, due to the fact that apoptosis induction was as well impaired upon proteasomal inhibition and DNA damage, both endogenous increased Grp78 expression and phosphorylation of eIF2α are presumably not responsible for the apoptosis phenotype observed in absence of Junb.

Interestingly, Junb-deficient MEFs had the capacity to undergo apoptosis upon death receptor activation elicited by low concentrations of ectopically applied CD95L/FasL and were even more sensitive than wild-type cells. This is presumably due to increased levels of the receptor CD95/Fas on the surface of Junb-deficient MEFs (Bierbaum H, 2002). Thus, these data corroborate previous observations that AP-1 plays a dual role in cell survival and apoptosis depending on the type of stress stimulus.

Resistance towards apoptosis and absence of caspase activation in cells lacking Junb could be ascribed to an in impairment in Bax expression and oligomerization, in mitochondria membrane permeabilization and in cytochrome c release into the cytosol. Bax protein but not mRNA levels were diminished in Junb-deficient MEFs, suggesting that Bax is not a transcriptional Junb target. However, Junb loss may influence Bax translation or protein stability. Indeed, various reports highlighted the fact that some factors may regulate apoptosis through modulation of Bax stability. For instance, the E6 protein from human papillomavirus 16 and the glucosidase inhibitor pentagalloylglucose regulate the proteasomal degradation and protein stability of Bax (Chen and Lin, 2004; Magal et al., 2005).

Both, Bax oligomerization and mitochondria pore formation is tightly orchestrated by Bcl-2 protein family members and other proteins such as clusterin. Intracellular clusterin has been reported to interact with activated Bax, thus impeding Bax oligomerization and subsequent cytochrome c release (Zhang et al., 2005). Clusterin, first identified as Junb target gene upon global gene expression profiling (Florin et al., 2004), was indeed highly expressed in Junb-deficient MEFs both on protein and mRNA level. However, increased levels of clusterin were not responsible for the block of apoptosis since knock-down of clusterin in Junb-deficient MEFs by siRNA technology did not rescue the apoptosis phenotype.

Further analyses revealed aberrant post-translational modifications of the Bcl-2 family members Bim and Bad and enhanced upstream pro-survival signaling in absence of Junb. Functional regulation of Bim-dependent apoptosis is achieved via the regulation of its expression and via post-translational modification of the Bim protein by phosphorylation. Bim is phosphorylated on multiple residues by members of the MAPK family, including ERK, JNK and p38. While many studies have shown that ERK-dependent phosphorylation of Bim on the serine residues S-55,-65 and -73 targets Bim for proteasomal degradation, two reports provided evidence that ERK-dependent phosphorylation of BimEL attenuated its apoptotic activity independently of effects on protein stability (Collins et al., 2005; Wang et al., 2004). Bim is also phosphorylated on threonine 112 that is a target of both ERK and JNK signaling pathways. While JNK phosphorylates T-112 in response to UV radiation, ERK mediates phosphorylation at this site upon serum stimulation. Analysis of mice with germline mutations for the major Bim phosphorylation sites revealed furthermore that phosphorylation on S-55/65/73 negatively regulates BimEL expression and function, while JNK-triggered phosphorylation of Thr-112 increases the apoptotic activity of Bim (Hubner et al., 2008).

Due to the lack of antibodies recognizing specifically the phosphorylated residues, I investigated phosphorylation of Bim by the appearance of a slower migrating band on a denaturing polyacrylamide gel. In contrast to wild-type MEFs, unchallenged Junb-deficient MEFs harbored already increased levels of phosphorylated Bim while the late Tm-induced Bim phosphorylation that in wild-type cells coincides with JNK activation, was missing. One can speculate that the basal Bim phosphorylation is mediated by abundant p-ERK observed in *Junb*$^{-/-}$ cells. Intriguingly, this pro-survival signaling results at least in our cell culture model not in a phosphorylation-triggered proteasomal degradation of Bim but at least in an attenuation of its pro-apoptotic activity. Most importantly, Junb-deficiency leads to increased phosphorylation of a second pro-apoptotic BH3-only protein Bad. Both, ERK-mediated phosphorylation of Bad on serine residue S-112 as well as Akt-triggered phosphorylation on serine residue S-136 were robustly increased in logarithmically growing Junb-deficient MEFs. Bad has been shown to link survival signals to the mitochondrial cell death machinery. Growth factor-triggered Bad phosphorylation by Akt and its subsequent sequestration into the cytoplasm by 14-3-3zeta is considered as a major mechanism for survival factor-mediated block of apoptosis (Youle and Strasser, 2008). Concordantly, analyses of the upstream signaling pathways revealed enhanced PI3K activity and abundant p-ERK and p-Akt levels in unchallenged MEFs lacking Junb. Interestingly, JNK activation was completely abolished in Junb-deficient MEFs and most likely due to the imbalance between life and death cues in favor for pro-survival signaling. Indeed, there is evidence that Akt phosphorylates the JNK kinase ASK1 on S-83 and, thereby, inhibits JNK activation (Aikin et al., 2004).

With regard to the present knowledge on the BH3-only proteins Bad and Bim as upstream initiators of the intrinsic apoptotic pathway, it is obvious that survival factor-induced ERK and Akt-mediated phosphorylation of Bim and Bad, respectively, and the subsequent inhibition of their pro-apoptotic activity is finally causative of the apoptosis resistance of Junb-deficient cells.

Co-culture experiments clearly pointed out that one or multiple soluble factor(s) must be highly expressed in the absence of Junb and be responsible for autocrine pro-survival feed-forward loop (Fig. 31). Previous studies showed that Junb negatively regulates the transcription of multiple growth factors and cytokines, including Kgf, Lipocalin-2, Csf2 (Florin et al., 2006; Szabowski et al., 2000), and G-CSF (Meixner et al., 2008). In line with that, *in vivo* and *in vitro* phenotypes observed in absence of Junb have been associated to

alterations in expression levels and kinetics of cytokines. For instance, while impaired expression of Csf2 and Kgf are causative of skin abnormalities (Florin et al., 2006), increased levels of G-CSF obtained upon epidermal Junb-deficiency causes skin ulcerations, myeloproliferative disease and low bone mass (Meixner et al., 2008).

Among the factors described here above, Csf2 appeared as potential candidate since it has been reported to induce phosphorylation of Akt and ERK in myeloid cells (Klein et al., 2000). However, Csf2 could be excluded as the factor being responsible for increased phosphorylated Akt and ERK since Junb-deficient MEFs did not express the two subunits composing the Csf2 receptor.

Further candidate factors included Pdgf, which is very potent mitogenic growth factor acting on mesenchymal cells such as fibroblasts and induces Akt and ERK activation (Heldin and Westermark, 1999). The expression of the ligands Pdgfa and Pdgfb as well as their respective receptors Pdgfra and Pdgfrb were elevated in absence of Junb; in particular, mRNA levels of Pdgfb and protein levels of Pdgfrb were highly up-regulated (Fig. 31).

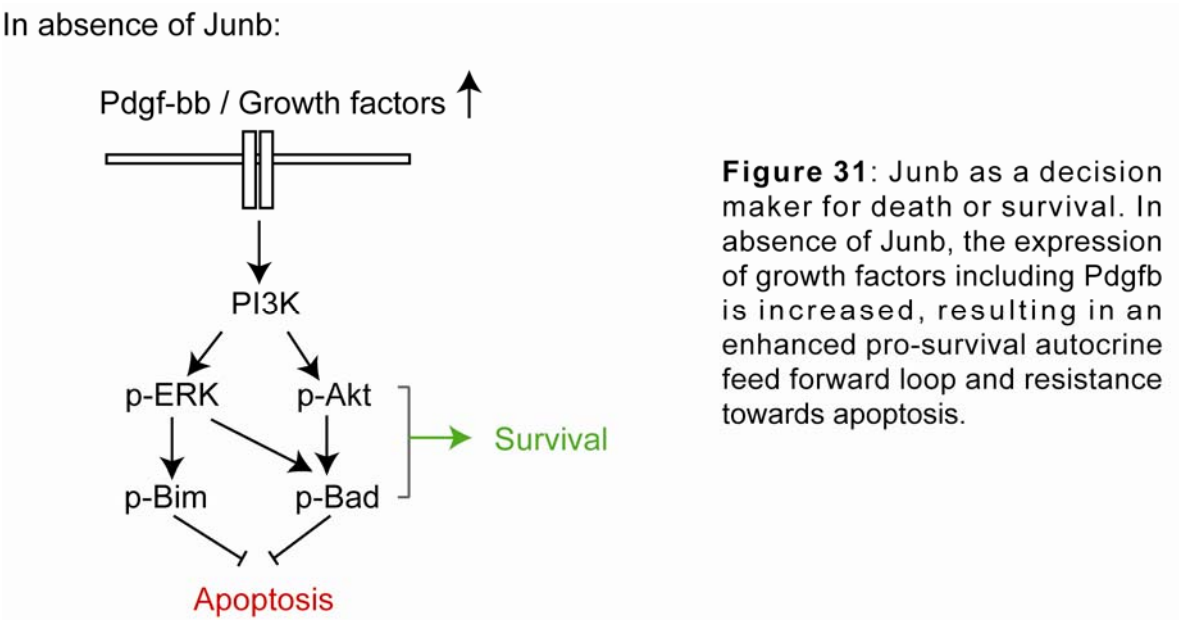

Figure 31: Junb as a decision maker for death or survival. In absence of Junb, the expression of growth factors including Pdgfb is increased, resulting in an enhanced pro-survival autocrine feed forward loop and resistance towards apoptosis.

Pdgfb, discovered more than 30 years ago, is the cellular homologue of the product of the retroviral oncogene v-sis of simian sarcoma virus (SSV). v-sis is sufficient to confer the transforming activity of SSV and SSV transformation involves autocrine growth stimulation by the PDGF-like molecule v-sis, thus, demonstrating for the first time the importance of autocrine growth stimulation in neoplastic transformation and cancer (Doolittle et al., 1983). Since then, three additional Pdgf genes have been characterized: Pdgfa, Pdgfc and Pdgfd. All

Pdgfs form dimers of disulfide-linked polypeptide chains and act via the receptor tyrosine kinase Pdgfra and Pdgfrb. The possible Pdgf-Pdgfr interactions are multiple and complex and include the formation of receptor heterodimers (Andrae et al., 2008; Heldin and Westermark, 1999). However, *in vivo* there is functional evidence only for a few interactions. For instance, Pdgf-aa interacts with Pdgfr-aa and Pdgf-bb with Pdgfr-bb (Andrae et al., 2008). Pdgfs have crucial roles during development and increased Pdgf activity has been linked with several diseases and pathological conditions, such as cancer. Numerous studies demonstrated that autocrine Pdgfb signaling confers self-sufficiency in growth signals but per se does not cause malignant cell behavior. Thus, Pdgfb signaling contributes to tumorigenesis by driving the proliferative expansion of pre-neoplastic and/or genetically unstable cell clones, which will eventually become fully malignant through further genetic alteration (Andrae et al., 2008). Moreover, a multifaceted role of Pdgf in cancer biology is now emerging as Pdgf signaling plays, in addition to providing a cell-autonomous proliferative stimulus, a role in invasion and in metastasis.

Among all Pdgf members, Pdgfb appeared as the best candidate responsible for the enhanced pro-survival signaling observed in Junb-deficient cells due to its strong overexpression and due to the observed enhanced phosphorylation of Pdgfrb in Junb-deficient MEFs. However, further experiments, including siRNA-mediated knock-down of Pdgfb in Junb-ablated MEFs, are needed to corroborate the impact of Pdgfb on the pro-survival phenotype and concomitant apoptosis resistance.

In this work, I identified Pdgfb as novel negatively regulated Junb-target gene. A promising TRE/AP-1 binding site was identified in the proximal promoter of Pdgfb. Although, I could confirm *in vitro* binding of AP-1 to this consensus site, reporter gene assay and mutagenesis analyses revealed that this TRE element was not the site through which repression of Pdgfb was achieved. Besides, other transcription factor binding sites, including a Sp1 and a yet-to-be identified site, have been characterized, but none of these sites was responsible for the repression of Pdgfb by Junb. Further analyses revealed three distal TRE-related CRE elements located at around -4000 relative to transcription initiation site. Preliminary results suggest that two of these sites are bound by AP-1 *in vitro* and further experiments will address the impact of these two distal CRE sites on Pdgfb transcription regulation by reporter gene assays and mutagenesis. One could hypothesize that an intrachromosomal loop involving the CRE and/or TRE binding sites could bring multiple transcription factors together and, thus, tightly regulate Pdgfb transcription. Such regulatory loop has been

reported for the transcriptional regulation of the Jun promoter, where phosphorylated Jun interacts with TCF4 and beta-catenin and form a ternary complex on the promoter, thus, regulating intestinal tumorigenesis (Nateri et al., 2005).

In addition to its impact on tumorigenesis, Pdgfb has important tasks in embryonic development. Endothelial expressed Pdgfb plays a crucial role in the recruitment of vascular smooth muscle cells (vSMC) and pericytes during embryogenesis (Hellstrom et al., 1999). Indeed, Pdgfb and Pdgfrb null embryos display pericyte and vSMC deficiency already at the onset of angiogenic sprouting. In spite of mural cell hypoplasia, the embryos continue to develop until embryonic day E16-E19 when finally widespread hemorrhage and edema cause embryonic lethality (Leveen et al., 1994). In addition, paracrine Pdgfb signaling plays a role in tumorigenesis by recruiting stromal cells, thereby inducing tumor angiogenesis and facilitating metastasis and drug resistance (see for review Andrae et al., 2008). Other studies reported that overexpression of Pdgfb even decreased colorectal and pancreatic cancer growth by increasing tumor pericyte content (McCarty et al., 2007). With regard to the numerous roles of Pdgfb signaling in fibrotic diseases, cancer and vascular disorders, it will be very important to prove that the negative regulation of this growth factor by Junb is also of relevance *in vivo*. It will be of high interest to investigate whether mice with conditionally ablated Junb display striking differences in Pdgfb signaling and whether some of the observed phenotypes can be attributed to aberrant Pdgfb signaling.

Altogether, our results identified Junb as tumor suppressor since its absence in mouse embryonic fibroblasts results in resistance towards apoptosis due to an enhanced autocrine loop (Fig. 32). However, many studies, including the present one, which addressed the impact of Junb on apoptosis and cancer, suggest diverse even contradictory functions of Junb. For instance, previous work has suggested a tumor suppressor role of Junb in myeloid cells. Absence of Junb in myeloid cells in mice results in CML due to an uncontrolled expansion of LT-HSC and GMP. Increased Csf2 expression in Junb-deficient myeloid precursor cells initiates an autocrine loop favoring increased proliferation and decreased apoptosis (Passegue and Wagner, 2000). Additionally, high systemic levels of G-CSF resulting from the absence of Junb in epidermis cause as well myeloproliferative disease by favoring myeloid cell proliferation (Meixner et al., 2008). By contrast, Junb acts as tumor promoter in beta cells. Knock-down of Junb by siRNA in pancreas beta cells results in higher sensitivity towards the chemical ER stress inducer cyclopiazonic acid, while overexpression of Junb protects beta

cells from cytokine-induced cell death due to diminished iNOS levels (Gurzov et al., 2008b). Moreover, partial reduction of Junb levels by siRNA in wild-type murine fibroblasts causes increased proliferation and tumorigenicity, whereas in Jun-deficient cells it induces p53-independent cell cycle arrest and apoptosis. Finally, Junb knock-down combined with JNK inhibition in melanoma B16 cancer cells results in cell cycle arrest and apoptosis-inducing factor-dependant apoptosis (Gurzov et al., 2008a). Altogether, these findings suggest that the role of Junb in apoptosis regulation is very complex and may depend on many parameters such as the cell type, transformation of the cells, the amount of Junb, as well as the balance between all AP-1 members.

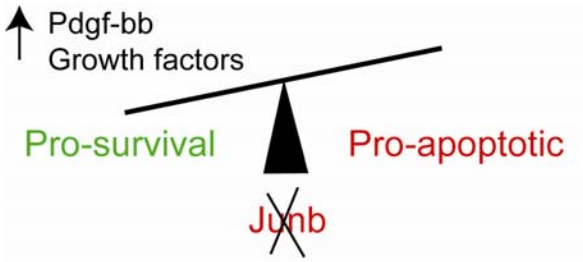

Figure 32: Loss of Junb results in an imbalance between pro-survival and pro-apoptotic cues due to increased levels of growth factors such as Pdgfb. This suggests that Junb acts as a tumor suppressor in mouse embryonic fibroblasts.

In conclusion, negative regulation of cytokines by Junb is of unequivocal importance to suppress pro-inflammatory and pro-tumorigenic phenotypes. Due to the fact that Junb has double-faced functions, it cannot be a rational therapeutical target. However, understanding how Junb represses gene and, most importantly, specific targeting this mechanism would represent a promising therapeutic approach in the future in order to treat inflammatory disease and cancer.

8 References

Ahringer, J. (2000). NuRD and SIN3 histone deacetylase complexes in development. Trends Genet *16*, 351-356.

Aikin, R., Maysinger, D., and Rosenberg, L. (2004). Cross-talk between phosphatidylinositol 3-kinase/AKT and c-jun NH2-terminal kinase mediates survival of isolated human islets. Endocrinology *145*, 4522-4531.

Andrae, J., Gallini, R., and Betsholtz, C. (2008). Role of platelet-derived growth factors in physiology and medicine. Genes Dev *22*, 1276-1312.

Andrecht, S., Kolbus, A., Hartenstein, B., Angel, P., and Schorpp-Kistner, M. (2002). Cell cycle promoting activity of JunB through cyclin A activation. J Biol Chem *277*, 35961-35968.

Andreucci, J.J., Grant, D., Cox, D.M., Tomc, L.K., Prywes, R., Goldhamer, D.J., Rodrigues, N., Bedard, P.A., and McDermott, J.C. (2002). Composition and function of AP-1 transcription complexes during muscle cell differentiation. J Biol Chem *277*, 16426-16432.

Angel, P., Imagawa, M., Chiu, R., Stein, B., Imbra, R.J., Rahmsdorf, H.J., Jonat, C., Herrlich, P., and Karin, M. (1987). Phorbol ester-inducible genes contain a common cis element recognized by a TPA-modulated trans-acting factor. Cell *49*, 729-739.

Angel, P., and Karin, M. (1991). The role of Jun, Fos and the AP-1 complex in cell-proliferation and transformation. Biochim Biophys Acta *1072*, 129-157.

Apel, I., Yu, C.L., Wang, T., Dobry, C., Van Antwerp, M.E., Jove, R., and Prochownik, E.V. (1992). Regulation of the junB gene by v-src. Mol Cell Biol *12*, 3356-3364.

Bakiri, L., Lallemand, D., Bossy-Wetzel, E., and Yaniv, M. (2000). Cell cycle-dependent variations in c-Jun and JunB phosphorylation: a role in the control of cyclin D1 expression. EMBO J *19*, 2056-2068.

Bannister, A.J., Zegerman, P., Partridge, J.F., Miska, E.A., Thomas, J.O., Allshire, R.C., and Kouzarides, T. (2001). Selective recognition of methylated lysine 9 on histone H3 by the HP1 chromo domain. Nature *410*, 120-124.

Behrens, A., Haigh, J., Mechta-Grigoriou, F., Nagy, A., Yaniv, M., and Wagner, E.F. (2003). Impaired intervertebral disc formation in the absence of Jun. Development *130*, 103-109.

Behrens, A., Sibilia, M., and Wagner, E.F. (1999). Amino-terminal phosphorylation of c-Jun regulates stress-induced apoptosis and cellular proliferation. Nat Genet *21*, 326-329.

Bell, A.C., and Felsenfeld, G. (2000). Methylation of a CTCF-dependent boundary controls imprinted expression of the Igf2 gene. Nature *405*, 482-485.

Benharroch, D., and Birnbaum, D. (1990). Biology of the fibroblast growth factor gene family. Isr J Med Sci *26*, 212-219.

Bernstein, B.E., Meissner, A., and Lander, E.S. (2007). The mammalian epigenome. Cell *128*, 669-681.

Bertolotti, A., Zhang, Y., Hendershot, L.M., Harding, H.P., and Ron, D. (2000). Dynamic interaction of BiP and ER stress transducers in the unfolded-protein response. Nat Cell Biol *2*, 326-332.

Bi, M., Naczki, C., Koritzinsky, M., Fels, D., Blais, J., Hu, N., Harding, H., Novoa, I., Varia, M., Raleigh, J., *et al.* (2005). ER stress-regulated translation increases tolerance to extreme hypoxia and promotes tumor growth. EMBO J *24*, 3470-3481.

Bierbaum, H., (2002), The function of the transcription factor AP-1 in the regulation of apoptosis, PhD thesis, University of Bonn, Germany

Bird, A. (2002). DNA methylation patterns and epigenetic memory. Genes Dev *16*, 6-21.

Brannan, C.I., and Bartolomei, M.S. (1999). Mechanisms of genomic imprinting. Curr Opin Genet Dev *9*, 164-170.

Brenner, C., Deplus, R., Didelot, C., Loriot, A., Vire, E., De Smet, C., Gutierrez, A., Danovi, D., Bernard, D., Boon, T., *et al.* (2005). Myc represses transcription through recruitment of DNA methyltransferase corepressor. EMBO J *24*, 336-346.

Brewer, J., and Cadman, C. (2000). Emotional intelligence: enhancing student effectiveness and patient outcomes. Nurse Educ *25*, 264-266.

Brewer, J.W., and Diehl, J.A. (2000). PERK mediates cell-cycle exit during the mammalian unfolded protein response. Proc Natl Acad Sci U S A *97*, 12625-12630.

Brown, J.R., Ye, H., Bronson, R.T., Dikkes, P., and Greenberg, M.E. (1996). A defect in nurturing in mice lacking the immediate early gene fosB. Cell *86*, 297-309.

Cai, X., and Cullen, B.R. (2007). The imprinted H19 noncoding RNA is a primary microRNA precursor. RNA *13*, 313-316.

Calfon, M., Zeng, H., Urano, F., Till, J.H., Hubbard, S.R., Harding, H.P., Clark, S.G., and Ron, D. (2002). IRE1 couples endoplasmic reticulum load to secretory capacity by processing the XBP-1 mRNA. Nature *415*, 92-96.

Chan, S.W., Henderson, I.R., and Jacobsen, S.E. (2005). Gardening the genome: DNA methylation in Arabidopsis thaliana. Nat Rev Genet *6*, 351-360.

Chen, W.J., and Lin, J.K. (2004). Induction of G1 arrest and apoptosis in human jurkat T cells by pentagalloylglucose through inhibiting proteasome activity and elevating p27Kip1, p21Cip1/WAF1, and Bax proteins. J Biol Chem *279*, 13496-13505.

Chiu, R., Angel, P., and Karin, M. (1989). Jun-B differs in its biological properties from, and is a negative regulator of, c-Jun. Cell *59*, 979-986.

Coffer, P., de Jonge, M., Mettouchi, A., Binetruy, B., Ghysdael, J., and Kruijer, W. (1994). junB promoter regulation: Ras mediated transactivation by c-Ets-1 and c-Ets-2. Oncogene *9*, 911-921.

Collins, N.L., Reginato, M.J., Paulus, J.K., Sgroi, D.C., Labaer, J., and Brugge, J.S. (2005). G1/S cell cycle arrest provides anoikis resistance through Erk-mediated Bim suppression. Mol Cell Biol *25*, 5282-5291.

Courey, A.J., and Jia, S. (2001). Transcriptional repression: the long and the short of it. Genes Dev *15*, 2786-2796.

Cowell, I.G. (1994). Repression versus activation in the control of gene transcription. Trends Biochem Sci *19*, 38-42.

Cress, W.D., and Seto, E. (2000). Histone deacetylases, transcriptional control, and cancer. J Cell Physiol *184*, 1-16.

Doolittle, R.F., Hunkapiller, M.W., Hood, L.E., Devare, S.G., Robbins, K.C., Aaronson, S.A., and Antoniades, H.N. (1983). Simian sarcoma virus onc gene, v-sis, is derived from the gene (or genes) encoding a platelet-derived growth factor. Science *221*, 275-277.

Eferl, R., Sibilia, M., Hilberg, F., Fuchsbichler, A., Kufferath, I., Guertl, B., Zenz, R., Wagner, E.F., and Zatloukal, K. (1999). Functions of c-Jun in liver and heart development. J Cell Biol *145*, 1049-1061.

Eferl, R., and Wagner, E.F. (2003). AP-1: a double-edged sword in tumorigenesis. Nat Rev Cancer *3*, 859-868.

Eferl, R., Zenz, R., Theussl, H.C., and Wagner, E.F. (2007). Simultaneous generation of fra-2 conditional and fra-2 knock-out mice. Genesis *45*, 447-451.

Farras, R., Baldin, V., Gallach, S., Acquaviva, C., Bossis, G., Jariel-Encontre, I., and Piechaczyk, M. (2008). JunB breakdown in mid-/late G2 is required for down-regulation of cyclin A2 levels and proper mitosis. Mol Cell Biol *28*, 4173-4187.

Fedoriw, A.M., Stein, P., Svoboda, P., Schultz, R.M., and Bartolomei, M.S. (2004). Transgenic RNAi reveals essential function for CTCF in H19 gene imprinting. Science *303*, 238-240.

Florin, L., Hummerich, L., Dittrich, B.T., Kokocinski, F., Wrobel, G., Gack, S., Schorpp-Kistner, M., Werner, S., Hahn, M., Lichter, P.*, et al.* (2004). Identification of novel AP-1 target genes in fibroblasts regulated during cutaneous wound healing. Oncogene *23*, 7005-7017.

Florin, L., Knebel, J., Zigrino, P., Vonderstrass, B., Mauch, C., Schorpp-Kistner, M., Szabowski, A., and Angel, P. (2006). Delayed wound healing and epidermal hyperproliferation in mice lacking JunB in the skin. J Invest Dermatol *126*, 902-911.

Garaude, J., Farras, R., Bossis, G., Charni, S., Piechaczyk, M., Hipskind, R.A., and Villalba, M. (2008). SUMOylation regulates the transcriptional activity of JunB in T lymphocytes. J Immunol *180*, 5983-5990.

Geijsen, N., Koenderman, L., and Coffer, P.J. (2001). Specificity in cytokine signal transduction: lessons learned from the IL-3/IL-5/GM-CSF receptor family. Cytokine Growth Factor Rev *12*, 19-25.

Glass, C.K., and Rosenfeld, M.G. (2000). The coregulator exchange in transcriptional functions of nuclear receptors. Genes Dev *14*, 121-141.

Gruda, M.C., van Amsterdam, J., Rizzo, C.A., Durham, S.K., Lira, S., and Bravo, R. (1996). Expression of FosB during mouse development: normal development of FosB knockout mice. Oncogene *12*, 2177-2185.

Grunau, C., Clark, S.J., and Rosenthal, A. (2001). Bisulfite genomic sequencing: systematic investigation of critical experimental parameters. Nucleic Acids Res *29*, E65-65.

Gurzov, E.N., Bakiri, L., Alfaro, J.M., Wagner, E.F., and Izquierdo, M. (2008a). Targeting c-Jun and JunB proteins as potential anticancer cell therapy. Oncogene *27*, 641-652.

Gurzov, E.N., Ortis, F., Bakiri, L., Wagner, E.F., and Eizirik, D.L. (2008b). JunB Inhibits ER Stress and Apoptosis in Pancreatic Beta Cells. PLoS ONE *3*, e3030.

Hakem, R., Hakem, A., Duncan, G.S., Henderson, J.T., Woo, M., Soengas, M.S., Elia, A., de la Pompa, J.L., Kagi, D., Khoo, W.*, et al.* (1998). Differential requirement for caspase 9 in apoptotic pathways in vivo. Cell *94*, 339-352.

Harding, H.P., Novoa, I., Zhang, Y., Zeng, H., Wek, R., Schapira, M., and Ron, D. (2000a). Regulated translation initiation controls stress-induced gene expression in mammalian cells. Mol Cell *6*, 1099-1108.

Harding, H.P., Zhang, Y., Bertolotti, A., Zeng, H., and Ron, D. (2000b). Perk is essential for translational regulation and cell survival during the unfolded protein response. Mol Cell *5*, 897-904.

Hark, A.T., Schoenherr, C.J., Katz, D.J., Ingram, R.S., Levorse, J.M., and Tilghman, S.M. (2000). CTCF mediates methylation-sensitive enhancer-blocking activity at the H19/Igf2 locus. Nature *405*, 486-489.

Hartenstein, B., Teurich, S., Hess, J., Schenkel, J., Schorpp-Kistner, M., and Angel, P. (2002). Th2 cell-specific cytokine expression and allergen-induced airway inflammation depend on JunB. EMBO J *21*, 6321-6329.

Hassa, P.O., Haenni, S.S., Elser, M., and Hottiger, M.O. (2006). Nuclear ADP-ribosylation reactions in mammalian cells: where are we today and where are we going? Microbiol Mol Biol Rev *70*, 789-829.

Heldin, C.H., and Westermark, B. (1999). Mechanism of action and in vivo role of platelet-derived growth factor. Physiol Rev *79*, 1283-1316.

Hellstrom, M., Kalen, M., Lindahl, P., Abramsson, A., and Betsholtz, C. (1999). Role of PDGF-B and PDGFR-beta in recruitment of vascular smooth muscle cells and

pericytes during embryonic blood vessel formation in the mouse. Development *126*, 3047-3055.

Hess, J., Angel, P., and Schorpp-Kistner, M. (2004). AP-1 subunits: quarrel and harmony among siblings. J Cell Sci *117*, 5965-5973.

Hess, J., Hartenstein, B., Teurich, S., Schmidt, D., Schorpp-Kistner, M., and Angel, P. (2003). Defective endochondral ossification in mice with strongly compromised expression of JunB. J Cell Sci *116*, 4587-4596.

Hilberg, F., Aguzzi, A., Howells, N., and Wagner, E.F. (1993). c-jun is essential for normal mouse development and hepatogenesis. Nature *365*, 179-181.

Hubner, A., Barrett, T., Flavell, R.A., and Davis, R.J. (2008). Multisite phosphorylation regulates Bim stability and apoptotic activity. Mol Cell *30*, 415-425.

Jackson-Grusby, L., Beard, C., Possemato, R., Tudor, M., Fambrough, D., Csankovszki, G., Dausman, J., Lee, P., Wilson, C., Lander, E., and Jaenisch, R. (2001). Loss of genomic methylation causes p53-dependent apoptosis and epigenetic deregulation. Nat Genet *27*, 31-39.

Jochum, W., Passegue, E., and Wagner, E.F. (2001). AP-1 in mouse development and tumorigenesis. Oncogene *20*, 2401-2412.

Johnson, R.S., Spiegelman, B.M., and Papaioannou, V. (1992). Pleiotropic effects of a null mutation in the c-fos proto-oncogene. Cell *71*, 577-586.

Johnson, R.S., van Lingen, B., Papaioannou, V.E., and Spiegelman, B.M. (1993). A null mutation at the c-jun locus causes embryonic lethality and retarded cell growth in culture. Genes Dev *7*, 1309-1317.

Jones, P.A., and Baylin, S.B. (2002). The fundamental role of epigenetic events in cancer. Nat Rev Genet *3*, 415-428.

Jones, P.A., and Baylin, S.B. (2007). The epigenomics of cancer. Cell *128*, 683-692.

Karin, M., Liu, Z., and Zandi, E. (1997). AP-1 function and regulation. Curr Opin Cell Biol *9*, 240-246.

Kenner, L., Hoebertz, A., Beil, T., Keon, N., Karreth, F., Eferl, R., Scheuch, H., Szremska, A., Amling, M., Schorpp-Kistner, M., *et al.* (2004). Mice lacking JunB are osteopenic due to cell-autonomous osteoblast and osteoclast defects. J Cell Biol *164*, 613-623.

Klein, J.B., Rane, M.J., Scherzer, J.A., Coxon, P.Y., Kettritz, R., Mathiesen, J.M., Buridi, A., and McLeish, K.R. (2000). Granulocyte-macrophage colony-stimulating factor delays neutrophil constitutive apoptosis through phosphoinositide 3-kinase and extracellular signal-regulated kinase pathways. J Immunol *164*, 4286-4291.

Koumenis, C. (2006). ER stress, hypoxia tolerance and tumor progression. Curr Mol Med *6*, 55-69.

Kouzarides, T. (2007). Chromatin modifications and their function. Cell *128*, 693-705.

Kovacs, J.J., Murphy, P.J., Gaillard, S., Zhao, X., Wu, J.T., Nicchitta, C.V., Yoshida, M., Toft, D.O., Pratt, W.B., and Yao, T.P. (2005). HDAC6 regulates Hsp90 acetylation and chaperone-dependent activation of glucocorticoid receptor. Mol Cell *18*, 601-607.

Kuroda, K.O., Meaney, M.J., Uetani, N., and Kato, T. (2008). Neurobehavioral basis of the impaired nurturing in mice lacking the immediate early gene FosB. Brain Res *1211*, 57-71.

Lamb, J.A., Ventura, J.J., Hess, P., Flavell, R.A., and Davis, R.J. (2003). JunD mediates survival signaling by the JNK signal transduction pathway. Mol Cell *11*, 1479-1489.

Lasorella, A., Uo, T., and Iavarone, A. (2001). Id proteins at the cross-road of development and cancer. Oncogene *20*, 8326-8333.

Lei, K., and Davis, R.J. (2003). JNK phosphorylation of Bim-related members of the Bcl2 family induces Bax-dependent apoptosis. Proc Natl Acad Sci U S A *100*, 2432-2437.

Leveen, P., Pekny, M., Gebre-Medhin, S., Swolin, B., Larsson, E., and Betsholtz, C. (1994). Mice deficient for PDGF B show renal, cardiovascular, and hematological abnormalities. Genes Dev *8*, 1875-1887.

Li, B., Tournier, C., Davis, R.J., and Flavell, R.A. (1999). Regulation of IL-4 expression by the transcription factor JunB during T helper cell differentiation. EMBO J *18*, 420-432.

Li, E., Bestor, T.H., and Jaenisch, R. (1992). Targeted mutation of the DNA methyltransferase gene results in embryonic lethality. Cell *69*, 915-926.

Licht, A.H., Pein, O.T., Florin, L., Hartenstein, B., Reuter, H., Arnold, B., Lichter, P., Angel, P., and Schorpp-Kistner, M. (2006). JunB is required for endothelial cell morphogenesis by regulating core-binding factor beta. J Cell Biol *175*, 981-991.

Loeffler, M., and Kroemer, G. (2000). The mitochondrion in cell death control: certainties and incognita. Exp Cell Res *256*, 19-26.

Luger, K., Mader, A.W., Richmond, R.K., Sargent, D.F., and Richmond, T.J. (1997). Crystal structure of the nucleosome core particle at 2.8 A resolution. Nature *389*, 251-260.

Magal, S.S., Jackman, A., Ish-Shalom, S., Botzer, L.E., Gonen, P., Schlegel, R., and Sherman, L. (2005). Downregulation of Bax mRNA expression and protein stability by the E6 protein of human papillomavirus 16. J Gen Virol *86*, 611-621.

Marks, P.A., Richon, V.M., Breslow, R., and Rifkind, R.A. (2001). Histone deacetylase inhibitors as new cancer drugs. Curr Opin Oncol *13*, 477-483.

Marushige, K. (1976). Activation of chromatin by acetylation of histone side chains. Proc Natl Acad Sci U S A *73*, 3937-3941.

Masud, A., Mohapatra, A., Lakhani, S.A., Ferrandino, A., Hakem, R., and Flavell, R.A. (2007). Endoplasmic reticulum stress-induced death of mouse embryonic fibroblasts requires the intrinsic pathway of apoptosis. J Biol Chem *282*, 14132-14139.

McCarty, M.F., Somcio, R.J., Stoeltzing, O., Wey, J., Fan, F., Liu, W., Bucana, C., and Ellis, L.M. (2007). Overexpression of PDGF-BB decreases colorectal and pancreatic cancer growth by increasing tumor pericyte content. J Clin Invest *117*, 2114-2122.

McCullough, K.D., Martindale, J.L., Klotz, L.O., Aw, T.Y., and Holbrook, N.J. (2001). Gadd153 sensitizes cells to endoplasmic reticulum stress by down-regulating Bcl2 and perturbing the cellular redox state. Mol Cell Biol *21*, 1249-1259.

Meixner, A., Karreth, F., Kenner, L., and Wagner, E.F. (2004). JunD regulates lymphocyte proliferation and T helper cell cytokine expression. EMBO J *23*, 1325-1335.

Meixner, A., Zenz, R., Schonthaler, H.B., Kenner, L., Scheuch, H., Penninger, J.M., and Wagner, E.F. (2008). Epidermal JunB represses G-CSF transcription and affects haematopoiesis and bone formation. Nat Cell Biol *10*, 1003-1011.

Minden, A., and Karin, M. (1997). Regulation and function of the JNK subgroup of MAP kinases. Biochim Biophys Acta *1333*, F85-104.

Moazed, D. (2001). Common themes in mechanisms of gene silencing. Mol Cell *8*, 489-498.

Moenner, M., Pluquet, O., Bouchecareilh, M., and Chevet, E. (2007). Integrated endoplasmic reticulum stress responses in cancer. Cancer Res *67*, 10631-10634.

Nakagawa, T., Zhu, H., Morishima, N., Li, E., Xu, J., Yankner, B.A., and Yuan, J. (2000). Caspase-12 mediates endoplasmic-reticulum-specific apoptosis and cytotoxicity by amyloid-beta. Nature *403*, 98-103.

Nakajima, K., Kusafuka, T., Takeda, T., Fujitani, Y., Nakae, K., and Hirano, T. (1993). Identification of a novel interleukin-6 response element containing an Ets-binding site and a CRE-like site in the junB promoter. Mol Cell Biol *13*, 3027-3041.

Nateri, A.S., Spencer-Dene, B., and Behrens, A. (2005). Interaction of phosphorylated c-Jun with TCF4 regulates intestinal cancer development. Nature *437*, 281-285.

Nathan, D., Ingvarsdottir, K., Sterner, D.E., Bylebyl, G.R., Dokmanovic, M., Dorsey, J.A., Whelan, K.A., Krsmanovic, M., Lane, W.S., Meluh, P.B., *et al.* (2006). Histone sumoylation is a negative regulator in Saccharomyces cerevisiae and shows dynamic interplay with positive-acting histone modifications. Genes Dev *20*, 966-976.

Nausch, N., Florin, L., Hartenstein, B., Angel, P., Schorpp-Kistner, M., and Cerwenka, A. (2006). Cutting edge: the AP-1 subunit JunB determines NK cell-mediated target cell killing by regulation of the NKG2D-ligand RAE-1epsilon. J Immunol *176*, 7-11.

Nicholls, R.D., and Knepper, J.L. (2001). Genome organization, function, and imprinting in Prader-Willi and Angelman syndromes. Annu Rev Genomics Hum Genet *2*, 153-175.

Nowak, S.J., and Corces, V.G. (2004). Phosphorylation of histone H3: a balancing act between chromosome condensation and transcriptional activation. Trends Genet *20*, 214-220.

Okada, S., Wang, Z.Q., Grigoriadis, A.E., Wagner, E.F., and von Ruden, T. (1994). Mice lacking c-fos have normal hematopoietic stem cells but exhibit altered B-cell differentiation due to an impaired bone marrow environment. Mol Cell Biol *14*, 382-390.

Okano, M., Bell, D.W., Haber, D.A., and Li, E. (1999). DNA methyltransferases Dnmt3a and Dnmt3b are essential for de novo methylation and mammalian development. Cell *99*, 247-257.

Ozcan, U., Cao, Q., Yilmaz, E., Lee, A.H., Iwakoshi, N.N., Ozdelen, E., Tuncman, G., Gorgun, C., Glimcher, L.H., and Hotamisligil, G.S. (2004). Endoplasmic reticulum stress links obesity, insulin action, and type 2 diabetes. Science *306*, 457-461.

Ozcan, U., Yilmaz, E., Ozcan, L., Furuhashi, M., Vaillancourt, E., Smith, R.O., Gorgun, C.Z., and Hotamisligil, G.S. (2006). Chemical chaperones reduce ER stress and restore glucose homeostasis in a mouse model of type 2 diabetes. Science *313*, 1137-1140.

Palmada, M., Kanwal, S., Rutkoski, N.J., Gustafson-Brown, C., Johnson, R.S., Wisdom, R., and Carter, B.D. (2002). c-jun is essential for sympathetic neuronal death induced by NGF withdrawal but not by p75 activation. J Cell Biol *158*, 453-461.

Pant, V., Mariano, P., Kanduri, C., Mattsson, A., Lobanenkov, V., Heuchel, R., and Ohlsson, R. (2003). The nucleotides responsible for the direct physical contact between the chromatin insulator protein CTCF and the H19 imprinting control region manifest parent of origin-specific long-distance insulation and methylation-free domains. Genes Dev *17*, 586-590.

Passegue, E., Jochum, W., Schorpp-Kistner, M., Mohle-Steinlein, U., and Wagner, E.F. (2001). Chronic myeloid leukemia with increased granulocyte progenitors in mice lacking junB expression in the myeloid lineage. Cell *104*, 21-32.

Passegue, E., and Wagner, E.F. (2000). JunB suppresses cell proliferation by transcriptional activation of p16(INK4a) expression. EMBO J *19*, 2969-2979.

Passegue, E., Wagner, E.F., and Weissman, I.L. (2004). JunB deficiency leads to a myeloproliferative disorder arising from hematopoietic stem cells. Cell *119*, 431-443.

Perez-Albuerne, E.D., Schatteman, G., Sanders, L.K., and Nathans, D. (1993). Transcriptional regulatory elements downstream of the JunB gene. Proc Natl Acad Sci U S A *90*, 11960-11964.

Phinney, D.G., Tseng, S.W., Hall, B., and Ryder, K. (1996). Chromosomal integration dependent induction of junB by growth factors requires multiple flanking evolutionarily conserved sequences. Oncogene *13*, 1875-1883.

Pray-Grant, M.G., Daniel, J.A., Schieltz, D., Yates, J.R., 3rd, and Grant, P.A. (2005). Chd1 chromodomain links histone H3 methylation with SAGA- and SLIK-dependent acetylation. Nature *433*, 434-438.

Pugh, B.F. (2000). Control of gene expression through regulation of the TATA-binding protein. Gene *255*, 1-14.

Rassidakis, G.Z., Thomaides, A., Atwell, C., Ford, R., Jones, D., Claret, F.X., and Medeiros, L.J. (2005). JunB expression is a common feature of CD30+ lymphomas and lymphomatoid papulosis. Mod Pathol *18*, 1365-1370.

Reik, W., Dean, W., and Walter, J. (2001). Epigenetic reprogramming in mammalian development. Science *293*, 1089-1093.

Ricci, R., Eriksson, U., Oudit, G.Y., Eferl, R., Akhmedov, A., Sumara, I., Sumara, G., Kassiri, Z., David, J.P., Bakiri, L., *et al.* (2005). Distinct functions of junD in cardiac hypertrophy and heart failure. Genes Dev *19*, 208-213.

Romanov, S., Medvedev, A., Gambarian, M., Poltoratskaya, N., Moeser, M., Medvedeva, L., Diatchenko, L., and Makarov, S. (2008). Homogeneous reporter system enables quantitative functional assessment of multiple transcription factors. Nat Methods *5*, 253-260.

Ron, D., and Walter, P. (2007). Signal integration in the endoplasmic reticulum unfolded protein response. Nat Rev Mol Cell Biol *8*, 519-529.

Ryu, E.J., Harding, H.P., Angelastro, J.M., Vitolo, O.V., Ron, D., and Greene, L.A. (2002). Endoplasmic reticulum stress and the unfolded protein response in cellular models of Parkinson's disease. J Neurosci *22*, 10690-10698.

Saito, M., Korsmeyer, S.J., and Schlesinger, P.H. (2000). BAX-dependent transport of cytochrome c reconstituted in pure liposomes. Nat Cell Biol *2*, 553-555.

Saleh, M., Mathison, J.C., Wolinski, M.K., Bensinger, S.J., Fitzgerald, P., Droin, N., Ulevitch, R.J., Green, D.R., and Nicholson, D.W. (2006). Enhanced bacterial clearance and sepsis resistance in caspase-12-deficient mice. Nature *440*, 1064-1068.

Sasaki, H., Ishihara, K., and Kato, R. (2000). Mechanisms of Igf2/H19 imprinting: DNA methylation, chromatin and long-distance gene regulation. J Biochem *127*, 711-715.

Saunders, L.R., and Verdin, E. (2007). Sirtuins: critical regulators at the crossroads between cancer and aging. Oncogene *26*, 5489-5504.

Schlesinger, P.H., Gross, A., Yin, X.M., Yamamoto, K., Saito, M., Waksman, G., and Korsmeyer, S.J. (1997). Comparison of the ion channel characteristics of proapoptotic BAX and antiapoptotic BCL-2. Proc Natl Acad Sci U S A *94*, 11357-11362.

Schmidt, D., Textor, B., Pein, O.T., Licht, A.H., Andrecht, S., Sator-Schmitt, M., Fusenig, N.E., Angel, P., and Schorpp-Kistner, M. (2007). Critical role for NF-kappaB-induced JunB in VEGF regulation and tumor angiogenesis. EMBO J *26*, 710-719.

Schoenherr, C.J., Levorse, J.M., and Tilghman, S.M. (2003). CTCF maintains differential methylation at the Igf2/H19 locus. Nat Genet *33*, 66-69.

Schorpp-Kistner, M., Wang, Z.Q., Angel, P., and Wagner, E.F. (1999). JunB is essential for mammalian placentation. EMBO J *18*, 934-948.

Schreiber, M., Kolbus, A., Piu, F., Szabowski, A., Mohle-Steinlein, U., Tian, J., Karin, M., Angel, P., and Wagner, E.F. (1999). Control of cell cycle progression by c-Jun is p53 dependent. Genes Dev *13*, 607-619.

Schreiber, M., Wang, Z.Q., Jochum, W., Fetka, I., Elliott, C., and Wagner, E.F. (2000). Placental vascularisation requires the AP-1 component fra1. Development *127*, 4937-4948.

Sedlak, T.W., Oltvai, Z.N., Yang, E., Wang, K., Boise, L.H., Thompson, C.B., and Korsmeyer, S.J. (1995). Multiple Bcl-2 family members demonstrate selective dimerizations with Bax. Proc Natl Acad Sci U S A *92*, 7834-7838.

Shi, Y. (2006). Mechanical aspects of apoptosome assembly. Curr Opin Cell Biol *18*, 677-684.

Shilatifard, A. (2006). Chromatin modifications by methylation and ubiquitination: implications in the regulation of gene expression. Annu Rev Biochem *75*, 243-269.

Sjin, R.M., Lord, K.A., Abdollahi, A., Hoffman, B., and Liebermann, D.A. (1999). Interleukin-6 and leukemia inhibitory factor induction of JunB is regulated by distinct cell type-specific cis-acting elements. J Biol Chem *274*, 28697-28707.

Sobell, H.M. (1985). Actinomycin and DNA transcription. Proc Natl Acad Sci U S A *82*, 5328-5331.

Solter, D. (1988). Differential imprinting and expression of maternal and paternal genomes. Annu Rev Genet *22*, 127-146.

Sterner, D.E., and Berger, S.L. (2000). Acetylation of histones and transcription-related factors. Microbiol Mol Biol Rev *64*, 435-459.

Stokoe, D. (2005). The phosphoinositide 3-kinase pathway and cancer. Expert Rev Mol Med *7*, 1-22.

Syntichaki, P., Topalidou, I., and Thireos, G. (2000). The Gcn5 bromodomain co-ordinates nucleosome remodelling. Nature *404*, 414-417.

Szabowski, A., Maas-Szabowski, N., Andrecht, S., Kolbus, A., Schorpp-Kistner, M., Fusenig, N.E., and Angel, P. (2000). c-Jun and JunB antagonistically control cytokine-regulated mesenchymal-epidermal interaction in skin. Cell *103*, 745-755.

Szegezdi, E., Logue, S.E., Gorman, A.M., and Samali, A. (2006). Mediators of endoplasmic reticulum stress-induced apoptosis. EMBO Rep *7*, 880-885.

Textor, B., Licht, A.H., Tuckermann, J.P., Jessberger, R., Razin, E., Angel, P., Schorpp-Kistner, M., and Hartenstein, B. (2007). JunB is required for IgE-mediated degranulation and cytokine release of mast cells. J Immunol *179*, 6873-6880.

Textor, B., Sator-Schmitt, M., Richter, K.H., Angel, P., and Schorpp-Kistner, M. (2006). c-Jun and JunB are essential for hypoglycemia-mediated VEGF induction. Ann N Y Acad Sci *1091*, 310-318.

Thepot, D., Weitzman, J.B., Barra, J., Segretain, D., Stinnakre, M.G., Babinet, C., and Yaniv, M. (2000). Targeted disruption of the murine junD gene results in multiple defects in male reproductive function. Development *127*, 143-153.

Thiel, G., Lietz, M., and Hohl, M. (2004). How mammalian transcriptional repressors work. Eur J Biochem *271*, 2855-2862.

Tsuruta, F., Sunayama, J., Mori, Y., Hattori, S., Shimizu, S., Tsujimoto, Y., Yoshioka, K., Masuyama, N., and Gotoh, Y. (2004). JNK promotes Bax translocation to mitochondria through phosphorylation of 14-3-3 proteins. EMBO J *23*, 1889-1899.

Urano, F., Wang, X., Bertolotti, A., Zhang, Y., Chung, P., Harding, H.P., and Ron, D. (2000). Coupling of stress in the ER to activation of JNK protein kinases by transmembrane protein kinase IRE1. Science *287*, 664-666.

Vanhaesebroeck, B., and Waterfield, M.D. (1999). Signaling by distinct classes of phosphoinositide 3-kinases. Exp Cell Res *253*, 239-254.

Vaquero, A., Sternglanz, R., and Reinberg, D. (2007). NAD+-dependent deacetylation of H4 lysine 16 by class III HDACs. Oncogene *26*, 5505-5520.

Verona, R.I., Mann, M.R., and Bartolomei, M.S. (2003). Genomic imprinting: intricacies of epigenetic regulation in clusters. Annu Rev Cell Dev Biol *19*, 237-259.

Wang, P., Gilmore, A.P., and Streuli, C.H. (2004). Bim is an apoptosis sensor that responds to loss of survival signals delivered by epidermal growth factor but not those provided by integrins. J Biol Chem *279*, 41280-41285.

Wang, Z.Q., Ovitt, C., Grigoriadis, A.E., Mohle-Steinlein, U., Ruther, U., and Wagner, E.F. (1992). Bone and haematopoietic defects in mice lacking c-fos. Nature *360*, 741-745.

Warnecke, P.M., Stirzaker, C., Melki, J.R., Millar, D.S., Paul, C.L., and Clark, S.J. (1997). Detection and measurement of PCR bias in quantitative methylation analysis of bisulphite-treated DNA. Nucleic Acids Res *25*, 4422-4426.

Wei, M.C., Zong, W.X., Cheng, E.H., Lindsten, T., Panoutsakopoulou, V., Ross, A.J., Roth, K.A., MacGregor, G.R., Thompson, C.B., and Korsmeyer, S.J. (2001). Proapoptotic BAX and BAK: a requisite gateway to mitochondrial dysfunction and death. Science *292*, 727-730.

Weiss, C., Schneider, S., Wagner, E.F., Zhang, X., Seto, E., and Bohmann, D. (2003). JNK phosphorylation relieves HDAC3-dependent suppression of the transcriptional activity of c-Jun. EMBO J *22*, 3686-3695.

Weksberg, R., Shuman, C., and Smith, A.C. (2005). Beckwith-Wiedemann syndrome. Am J Med Genet C Semin Med Genet *137C*, 12-23.

Whitfield, J., Neame, S.J., Paquet, L., Bernard, O., and Ham, J. (2001). Dominant-negative c-Jun promotes neuronal survival by reducing BIM expression and inhibiting mitochondrial cytochrome c release. Neuron *29*, 629-643.

Wolter, S., Doerrie, A., Weber, A., Schneider, H., Hoffmann, E., von der Ohe, J., Bakiri, L., Wagner, E.F., Resch, K., and Kracht, M. (2008). c-Jun controls histone modifications, NF-kappaB recruitment, and RNA polymerase II function to activate the ccl2 gene. Mol Cell Biol *28*, 4407-4423.

Yang, M.Y., Liu, T.C., Chang, J.G., Lin, P.M., and Lin, S.F. (2003). JunB gene expression is inactivated by methylation in chronic myeloid leukemia. Blood *101*, 3205-3211.

Yang, X.J., and Seto, E. (2008a). Lysine acetylation: codified crosstalk with other posttranslational modifications. Mol Cell *31*, 449-461.

Yang, X.J., and Seto, E. (2008b). The Rpd3/Hda1 family of lysine deacetylases: from bacteria and yeast to mice and men. Nat Rev Mol Cell Biol *9*, 206-218.

Ye, J., Rawson, R.B., Komuro, R., Chen, X., Dave, U.P., Prywes, R., Brown, M.S., and Goldstein, J.L. (2000). ER stress induces cleavage of membrane-bound ATF6 by the same proteases that process SREBPs. Mol Cell *6*, 1355-1364.

Yoo-Warren, H., Pachnis, V., Ingram, R.S., and Tilghman, S.M. (1988). Two regulatory domains flank the mouse H19 gene. Mol Cell Biol *8*, 4707-4715.

Youle, R.J., and Strasser, A. (2008). The BCL-2 protein family: opposing activities that mediate cell death. Nat Rev Mol Cell Biol *9*, 47-59.

Zebedee, Z., and Hara, E. (2001). Id proteins in cell cycle control and cellular senescence. Oncogene *20*, 8317-8325.

Zenz, R., Eferl, R., Kenner, L., Florin, L., Hummerich, L., Mehic, D., Scheuch, H., Angel, P., Tschachler, E., and Wagner, E.F. (2005). Psoriasis-like skin disease and arthritis caused by inducible epidermal deletion of Jun proteins. Nature *437*, 369-375.

Zenz, R., Scheuch, H., Martin, P., Frank, C., Eferl, R., Kenner, L., Sibilia, M., and Wagner, E.F. (2003). c-Jun regulates eyelid closure and skin tumor development through EGFR signaling. Dev Cell *4*, 879-889.

Zha, H., Aime-Sempe, C., Sato, T., and Reed, J.C. (1996). Proapoptotic protein Bax heterodimerizes with Bcl-2 and homodimerizes with Bax via a novel domain (BH3) distinct from BH1 and BH2. J Biol Chem *271*, 7440-7444.

Zhang, H., Kim, J.K., Edwards, C.A., Xu, Z., Taichman, R., and Wang, C.Y. (2005). Clusterin inhibits apoptosis by interacting with activated Bax. Nat Cell Biol *7*, 909-915.

Zhang, J., Zhang, D., McQuade, J.S., Behbehani, M., Tsien, J.Z., and Xu, M. (2002). c-fos regulates neuronal excitability and survival. Nat Genet *30*, 416-420.

Zhang, Y., Kwon, S., Yamaguchi, T., Cubizolles, F., Rousseaux, S., Kneissel, M., Cao, C., Li, N., Cheng, H.L., Chua, K., *et al.* (2008). Mice lacking histone deacetylase 6 have

hyperacetylated tubulin but are viable and develop normally. Mol Cell Biol *28*, 1688-1701.

Zhang, Y., Li, N., Caron, C., Matthias, G., Hess, D., Khochbin, S., and Matthias, P. (2003). HDAC-6 interacts with and deacetylates tubulin and microtubules in vivo. EMBO J *22*, 1168-1179.

Zhang, Y., and Reinberg, D. (2001). Transcription regulation by histone methylation: interplay between different covalent modifications of the core histone tails. Genes Dev *15*, 2343-2360.